HELSINGIN YLIOPISTO
HELSINGFORS UNIVERSITET
UNIVERSITY OF HELSINKI

Master's Thesis
Department of Geosciences and Geography
Economic Geology

GEOCHEMISTRY AND MINERALOGICAL CHARACTERISTICS OF METAMORPHOSED PALEOPROTEROZOIC VOLCANOGENIC MASSIVE SULFIDE DEPOSIT AT VIHANTI, CENTRAL FINLAND

Muhammad Mohsin Tahir

2019

University of Helsinki
Faculty of Science

PL 64 (Gustaf Hällströmin katu 2)
00014 Univesrity of Helsinki

HELSINGIN YLIOPISTO
HELSINGFORS UNIVERSITET
UNIVERSITY OF HELSINKI

Tiedekunta/Osasto Fakultet/Sektion – Faculty	Laitos/Institution– Department
Faculty of Science	Geosciences and Geography

Tekijä/Författare – Author
Muhammad Mohsin Tahir

Työn nimi / Arbetets Titel – Title
Geochemistry and mineralogical characteristics of metamorphosed paleoproterozoic VHMS deposit at Vihanti, Central Finland

Oppiaine /Läroämne – Subject
Geology

Työn laji/Arbetets art – Level	Aika/Datum – Month and year	Sivumäärä/ Sidoantal – Number of pages
MSc. project	12.2019	70

Tiivistelmä/Referat – Abstract

The Vihanti-Lampinsaari group in the Raahe-Ladoga belt, central Finland, hosts massive sulphide deposits. Host rocks are highly deformed and metamorphosed (amphibolite to granulite facies) felsic to intermediate volcanic rocks with minor mafic metavolcanics. Due to intense metamorphism, it is difficult to figure out the nature of the original protolith of hosts rocks and there is no systematic examination of the trace elements behaviour found in the literature for the rocks in the Lampinsaari region.

Two main topics were studied: (1) The trace elements behaviour of the rocks in the Vihanti (Lampinsaari) group, and (2) origin of the volcanic rocks and volcanic architecture of the Vihanti group. Better knowledge on the geochemistry of the immobile trace elements in these highly metamorphosed rocks led to the more accurate and precise determination of the origin of volcanic rocks and their volcanic architecture.

Igneous (Felsic-intermediate-mafic) metavolcanic rocks of the Vihanti-Lampinsaari region have all calc-alkaline magmatic affinity according to (Ross and Bedard; 2009) Zr vs Y and major elements classification by Miyashiro (1974). The chondrite normalized patterns of the trace elements having enriched concentrations of LREE relative to low HREE indicates island arc settings.

There is no significant hydrothermal material present in metasedimentary rocks of the Vihanti Lampinsaari area. Meta-sedimentary rocks of the Vihanti group are largely silica-rich with the presence of detrital components. Two calc-silicate bearing paragneisses have higher concentrations of Fe which are due to the pyrite while three distinct samples with higher P_2O_5 having higher concentrations of Mn represents phosphate minerals. Negative Eu anomaly due to Ca-replacement and enriched LREE with respect to HREE is an indication of evolved source areas. Sedimentary carbonates with one rock type of serpentinite-dolomite are mineralized ones have a higher concentration of Mn and are enriched in FeO which is due to the hydrothermal alteration in the sediments. Volcanic sedimentary rocks are highly evolved in composition but show depletion in Ba, Ti and Sr.

Investigated sulfide ore deposits of the Vihanti-Lampinsaari region have diverse REE behaviour in chondrite normalized patterns due to high fluid/rock ratios. Due to high fluid/rock ratios, it is more likely to lose parent texture of the rocks with dissimilar trends in primitive and chondritic normalized patterns. Positive anomalies of Eu represent ore mineralization and considered for better chances of ore-bearing rocks. While negative Eu anomalies indicate late-stage mineralization in these mineralized rocks of the Vihanti-Lampinsaari region.

Avainsanat – Nyckelord – Keywords
Metamorphism, Geochemistry, VMS deposits, Mineralogy, Trace elements, Rare Earth Element (REE), Sphalerite, Chlorite, Pyrite

Säilytyspaikka – Förvaringställe – Where deposited
University of Helsinki, Department of Geosciences and Geography, Kumpula Science Library

Muita tietoja – Övriga uppgifter – Additional information

Contents

1. INTRODUCTION

The most important volcanogenic massive sulfide (VMS) deposits of Finland are found in the Vihanti-Pyhäsalmi belt. The Vihanti-Pyhäsalmi belt belongs to the northwest-southeast trending Raahe-Ladoga zone (RLZ) which represents a border zone between Paleoproterozoic island arcs and Archean terranes. Raahe Ladoga zone is considered as the main sulfide ore belt in Finland (Kahma 1973). The Vihanti and Pyhäsalmi Volcanogenic Massive Sulfide (VMS) deposits linked with the Paleoproterozoic island arc (1.93-1.92 Ga ago) formed in an ocean located on the western side of the Archean basement complex (Mäki et al. 2015).

In the Vihanti-Pyhäsalmi ore zone, many small unexploited sulfide deposits, both VMS and SEDEX-type are known. However, only two large VMS Zn-Cu-Pb deposits have been exploited. Namely, the Pyhäsalmi mine and the Vihanti mine operated from 1954-1992. Zinc has been an important metal in the Vihanti mine, and the ore reserves of more than 75% were present in three main lodes: Lampinsaari, Ristonaho and Välisaari (Västi 2008). The Vihanti deposits and minor satellite mineralizations are hosted by the dominated intermediate and felsic metavolcanic rocks, with metamorphic grade ranging from lower amphibolite facies to upper amphibolite facies, producing 28Mt at 5.12% Zn, 0.48% Cu, 0.36% Pb, 25 ppm Ag and 0.49 ppm Au from 1954-1992 (Mäki et al. 2015).

The Vihanti Zn-Pb-Ag deposits are situated on the southwestern edge of the antiformal dome of the Lampinsaari-Alpua area (Figure 1.1)(Mäki et al. 2015). The volcanism in the area is mainly of felsic to intermediate metavolcanic rocks with minor mafic metavolcanics as well. The Vihanti (Lampinsaari) study area has been poorly investigated so the first objective is to improve the basic scientific geological knowledge on the area. The most recent research from the study area is from 2014 where the focus was to develop 3D model of the VMS structures of the area (Makkonen and Luukas 2014) and on 2008 when the focus was only the chemical composition of the black shales schist including carbonaceous metasedimentary rocks in the selected targets of Vihanti area (Västi 2008). The area is studied from 1999-2003 by Vihanti-Pyhäsalmi project (GTK) in collaboration with Geological Research Unit of James Cook University (Australia) and studies were focused on the mineralized areas and related volcanic rocks (Luukas et al. 2004). In a detailed investigation of the volcanic rocks was in the year

1968, when Pentti, Rouhunkoski intended to produce a paper on the ore deposits of Vihanti area as a salient feature of the study (Rouhunkoski 1968).

The aim of this Master's Thesis is to study samples from one of the ore deposits of Vihanti area i.e. Lampinsaari and provide their characterization for chemical and mineralogical composition. Due to intense metamorphism in the study area, stratigraphic interpretations are difficult to make. Geochemistry of the immobile trace elements is important in determining and reconstructing the tectonic settings of the ancient volcanic formations, especially when rocks have undergone intense metamorphism with deformed primary textures.

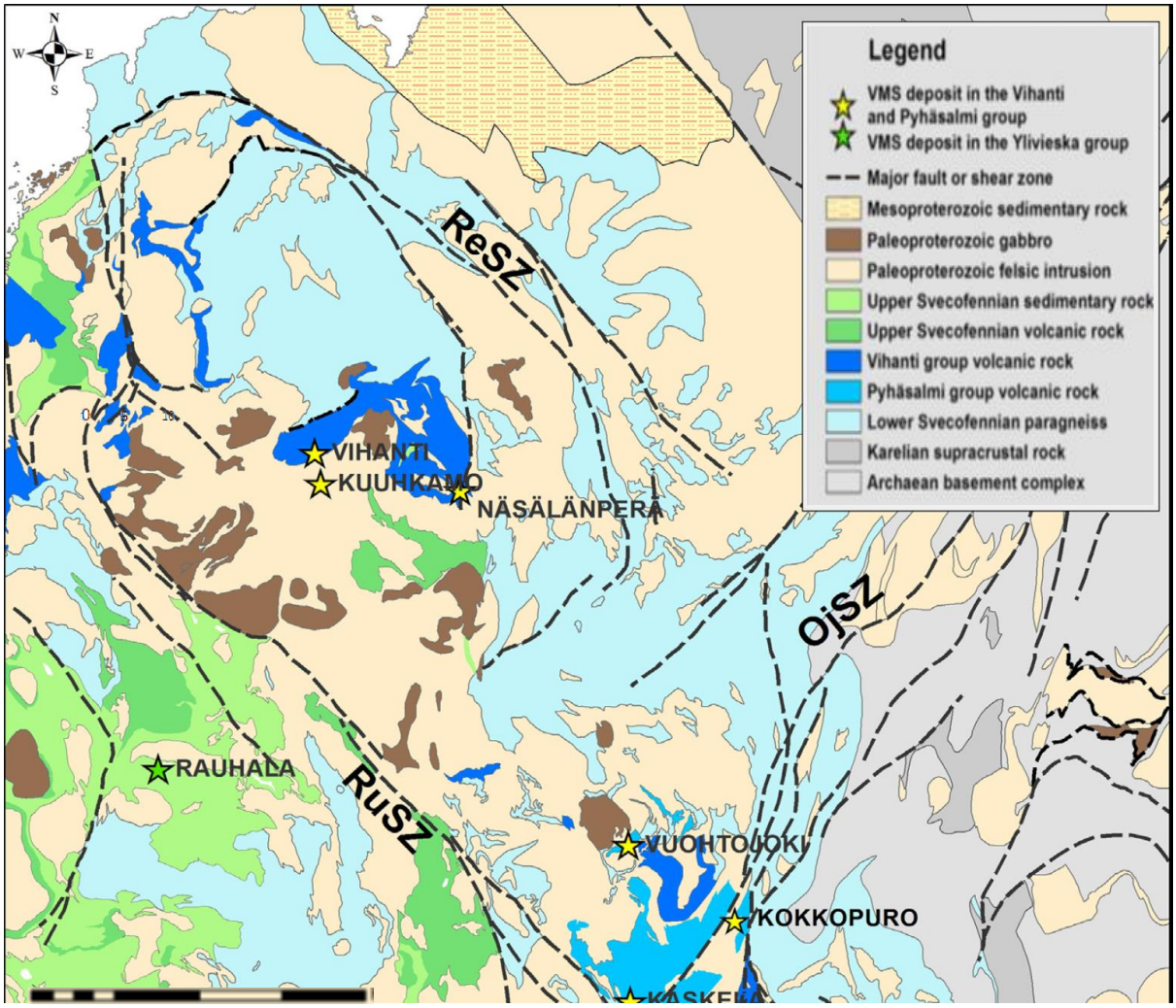

Figure 1.1 general geology of the north-western part of the Raahe-Ladoga zone. The most important Zn-Cu deposits of the Vihanti and Pyhäsalmi area are shown with stars. The main structural features are represented by black dashed lines (OjSZ= Oulujärvi shear zone, ReSZ = Revonneva shear zone, RuSZ = Ruhaperä shear zone). Source: (Mäki et al. 2015)

2. GEOLOGICAL SETTING

2.1. Regional Geology of the Vihanti-Pyhäsalmi Belt

The Vihanti-Pyhäsalmi belt is located at the border between the Archean basement complex (3.1-2.6 Ga) and the Paleoproterozoic Svecofennian domain in central Finland. The Vihanti-Pyhäsalmi belt belongs to the northwest-southeast trending Raahe-Ladoga zone, that characterize the collisional border between Paleoproterozoic island arcs and Archean terranes. The bedrock of the belt consists of the eastern part of Paleoproterozoic Svecofennian domain bordered by Archean basement complexes in the east, CFGC (Central Finland Granitoid Complex) and western supracrustal formations of the Svecofennian domain (Figure 1.1).
The volcanogenic massive sulfide (VMS) deposits of the Vihanti and Pyhäsalmi are related to Paleoproterozoic island arc formed in an ocean on the western side of the Archean basement complex 1.93-1.92 Ga ago (Mäki et al. 2015). (Figure 1.1 & Figure 2.1).

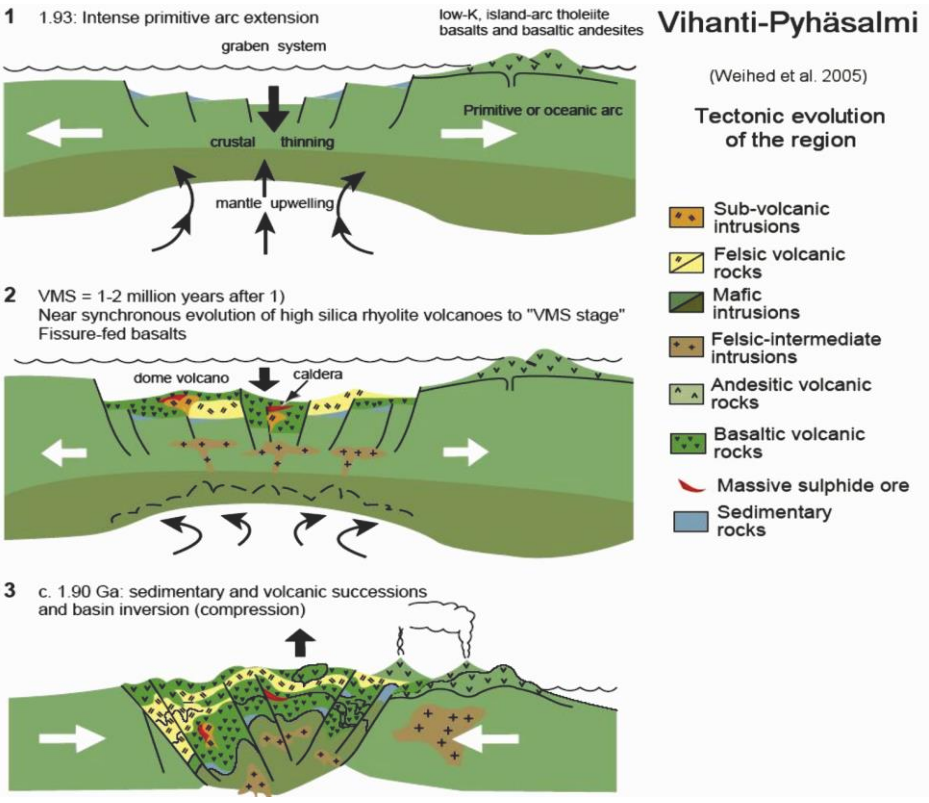

Figure 2.1 Schematic modelling (Weihed and Eilu 2005)

2.1.1. Supracrustal Rocks

Supracrustal rocks of the area along RLZ are chiefly of turbiditic metasedimentary rocks that have dominant graphite bearing schists and minor mafic metavolcanic interlayers. This sequence is defined as Näläntöjäarvi suite by (Laajoki 1988) and it is considered as a depositional basement for the volcanic rocks of the island arc (Mäki et al. 2015). In the western part of the Näläntöjärvi suite volcanic arc-related rocks of the Vihanti and Pyhäsalmi belts contain several separate volcanic centres (Figure 1.1). Regional metamorphic grade in the Vihanti-Pyhäsalmi belt ranges from lower amphibolite facies to upper amphibolite facies. While locally, in the Kiuruvesi area, it reaches much higher grades of granulite facies.

2.1.2. Shear Zones

There are two major blocks of the volcanic belt, one including southwest-northeast trending Oulujärvi shear zone and other southeast-northwest trending faults of Revonneva and Ruhapperä shear zones (Kärki et al. 1993). These blocks have distinct lithological features that define the Vihanti and Pyhäsalmi lithological associations.

2.1.3. Volcanic Groups

There is an informal schematic lithostratigraphic classification for the Vihanti and Pyhäsalmi group shown in Figure 1.1. Interpretation cannot be considered as final because of the poor outcrop relations along the belt and overlapping dating results of metamorphosed volcanic rocks of both groups (Mäki et al. 2015). The bimodal metavolcanic rocks of the Pyhäsalmi group can be separated from the Ylivieska-type (1.89-1.88) in the west through the distinct lithogeochemical signatures. Wide range of volcanic composition exists with a bimodal felsic-mafic metavolcanics. While in the Vihanti block, intermediate and felsic metavolcanics are dominant with minor mafic metavolcanic rocks (Mäki et al. 2015). Despite their broadly similar ages, both groups (1.93-1.92 Ga) represents two different volcanic environments. The Vihanti group overlying the lower bimodal felsic-mafic metavolcanic sequence of the Pyhäsalmi group, have a series of felsic and intermediate metavolcanic rocks with calc-silicate and graphite tuffite interlayers, deposited during continuous evolution of the arc.

2.1.4. Ore Deposits

Mineralization is typically found in specific lithological associations. Currently, there is one operating and four closed mines and several uneconomic deposits in Vihanti-Pyhäsalmi belt. The Pyhäsalmi Cu-Zn deposits are the largest VMS deposits of Finland, with total reserves of 58.3 Mt @Cu 0.9%, Zn 2.4%, S 37.8%, Au 0.4 g/t and Ag 14 g/t. Vihanti Zn-mine operational time period was from 1954 to 1992. It produces in a total of 28 Mt ore (1.447 Mt Zn, 131000 t Cu, 103 000 t Pb, 190 t Ag, 3038 kg Au) (Mäki et al. 2015).

2.2. Regional Geology of the Vihanti area

Vihanti area itself belongs to the Vilminko formation of the Vihanti group (Figure 2.2). The composition of the Vilminko formation is of intermediate and felsic metavolcanic rocks and minor mafic metavolcanic rocks. There is a continuous layer of distinct calc-silicate horizon intercalated with dolomites and graphite bearing metatuffs, known as U-P horizon due to the presence of Uranium and phosphorous components (Rehtijarvi et al. 1979). Due to the presence of graphite and sulfide components these horizons are easy to follow on geophysical maps. Uppermost lithological part of the Vilminko formation comprises a massive greywacke sequence.

The Vihanti area has magmatic history from approximately 1.93-1.87 Ga. Two separate porphyry sills have been dated. A quartz-plagioclase porphyry sill (Kokkoneva porphyry) yielded an age of 1926 Ma and is, completely or partly altered with disseminated pyrite. Another younger quartz porphyry sill (1874 Ma) intruded in the Vilminko area. Altered rocks are mostly quartz or cordierite-sillimanite-sericite rocks. Metavolcanic rocks of the Vilminko formation has an anticline in the Vihanti mine area and syncline in the Näsälänperä area (Figure 2.2).

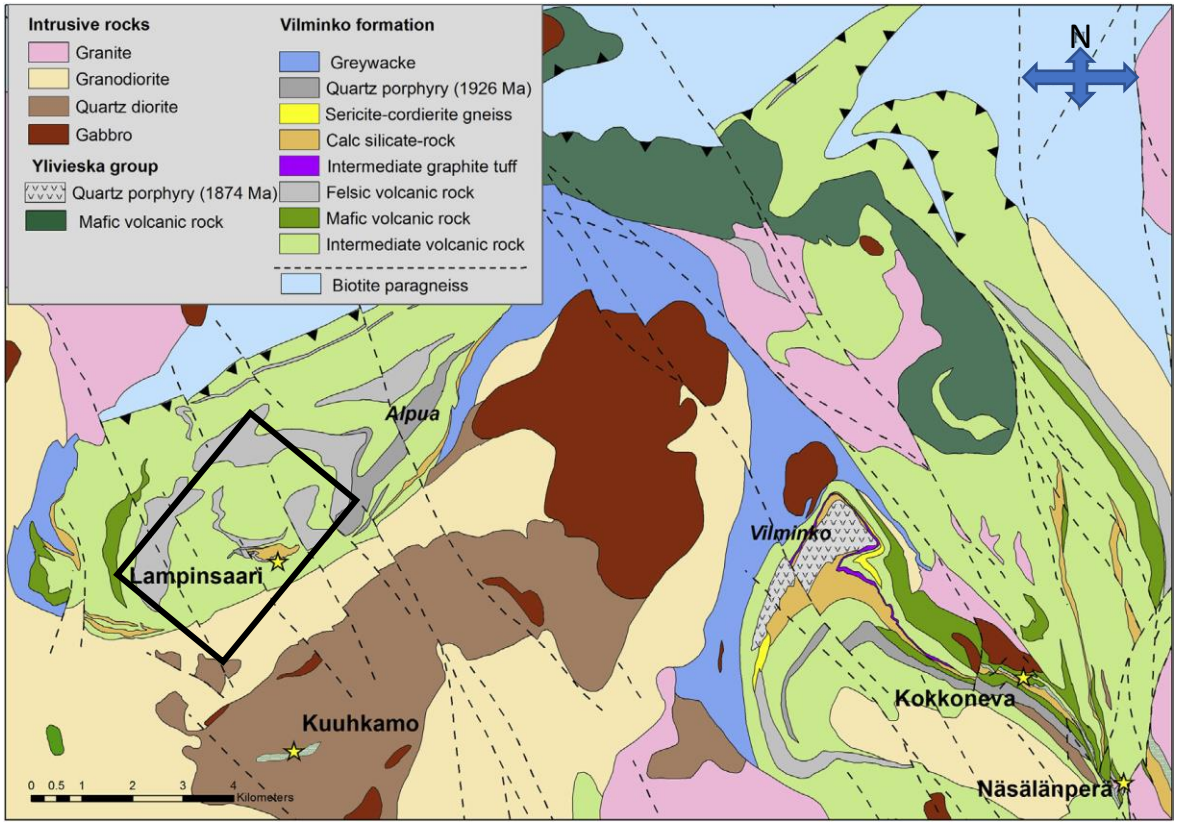

Figure 2.2 Geology of the Vihanti area. Source. The map is modified after Bedrock of Finland-DigiKP (2013). Source: Minerals deposits of Finland.

3. MATERIAL AND METHODS

The research material for the study was provided by the Geological Survey of Finland (GTK). There are four drilling profiles and several single drill cores from the Vihanti Lampinsaari Zn-mine in the GTK Loppi drill core depot. In October 2009 working group Raimo Lahtinen, Pasi Heino and Jukka Kousa logged 12 drill cores from the profiles PL106 and PL130. Altogether 95 samples were taken and later analyzed by XRF and ICP-MS (REE and trace elements) methods in Labtium Oy laboratories. Also, 94 polished thin sections were made in the GTK thin section laboratory in Kuopio (see Table 1 and appendix 1). Logging results were in Excel-format and low-resolution digital pictures have been provided. This study is mainly based on thin section and geochemical analysis of these samples. The major and trace element data are presented in Appendix 1. Mine profile PL106 includes drill cores R851, R1095, R667, R911 and R1640 and profile PL130 drill cores R1475, R644, R917, R1589, R1457, R768 and R2061 (Figure 3.1).

Table 1. The number of thin sections and analyses (columns named after Labtium method code) of the selected drill cores in profiles PL106 and PL130 (relogged 10/2009 by Pasi Heino, Raimo Lahtinen and Jukka Kousa).

Profile	Drill hole	Number of thin sections	Number of analyses, columns named after the laboratory method code by Labtium Oy					
			175X	308M	515M	515P	811L	816L
PL106	R667	3	3	3	3	3	3	3
PL106	R851	16	17	17	17	17	17	17
PL106	R911	4	4	4	4	4	4	4
PL106	R1095	13	13	13	13	13	13	13
PL106	R1640	8	8	8	8	8	8	8
PL130	R644	5	5	5	5	5	5	5
PL130	R768	4	4	4	4	4	4	4
PL130	R917	11	11	11	11	11	11	11
PL130	R1457	15	15	15	15	15	15	15
PL130	R1475	3	3	3	3	3	3	3
PL130	R1589	4	4	4	4	4	4	4
PL130	R2061	8	8	8	8	8	8	8

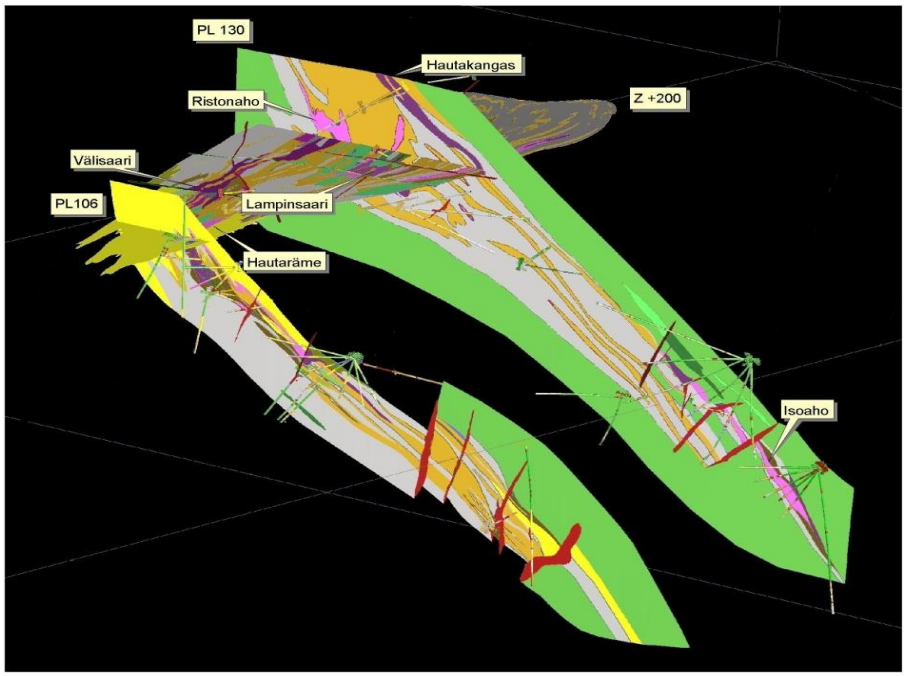

Figure 3.1 Vihanti Lampinsaari Zn-mine Profiles PL106 and PL130 on plan +200 map. Rock types: green = intermediate metavolcanic rocks, grey= felsic metavolcanic rocks, orange = calc-silicate rocks, dolomite, Lilac = ore, yellow = cordierite-sillimanite gneiss, red = younger dikes. Source:(Luukas et al. 2004).

3.1. Petrography

Overall 25 samples of thin sections were chosen in the study from two selected drill holes, R851 and R1457 (Figure 3 & 4) and were examined by using both transmitted and reflected light microscopy for determination of the textures of the mineralization, common mineral assemblages and their internal structures. Thin section study in relation to the geochemical whole rock data is essential in determining the rock types more precisely and accurately.

3.2. Geochemical Data

Trace elements (especially the Rare Earth Elements REE and immobile trace elements) study has become a vital part of the modern-day petrology and has proved to be capable of discriminating between petrological processes. Analysing the immobile trace elements data is the main topic of this thesis work. Rare earth elements (REE) and immobile trace elements are a powerful tool for the study of highly altered and metamorphosed rocks in determining their protoliths and primary magma compositions(Maclean and Barrett 1993, Janousek et al. 2006).

The 95 samples were collected to cover the whole study area and represent two profiles and 12 drill cores. (Appendix 1). The samples were analysed at the Labtium Oy, the former laboratory of GTK. The main oxides were analysed with +175 Multi-Assay XRF method including few trace elements given as approximate total concentrations in percentages (%) mentioned in Table 2. Only two trace elements, namely Ga and Cl were used from XRF data rests are excluded and taken from the other methods results. Different methods include ICP-MS (308M), Multivariate assay by ICP-MS (515M) and Multi-element assay with ICP-OES (515P) were used for trace elements data. ICP-MS (308M) used for the elements mentioned in Table 2. Concentrations of trace elements are in percentages (%), mg/kg and for few as µg/kg Table 2. For the determination of carbon, two methods, +811L (Carbon Analyzer) and 816L (Leco Analyzer) were used. Some of the samples have been analysed by two or more methods. However, priority is given to samples analysed first with ICP-MS (308M), then ICP-MS (515M) and in last to ICP-OES (515P).

The geochemical data has been analysed and edited to diagrams with Geochemical Data Toolkit (GCD-Kit) program (Janousek et al. 2006) and further editing in diagrams is done in thesis work.

Table 2 Major and trace elements of the whole rock data of the 95 rock samples from Vihanti region categorized by different methods mentioned in the heading as bold letters.

+175X *(%)*	308M *(mg/kg)*	515M *(mg/kg)*	515P *(mg/kg)*
Na_2O	Ce	Ag	Al
MgO	Co	As	B
Al_2O_3	Cu	Au *(µg/kg)*	Ba
SiO_2	Dy	Bi	Ca
P_2O_5	Er	Cd	Cr
K_2O	Eu	Co	Cu
CaO	Gd	Pd (µg/kg)	Fe
TiO_2	Hf	Pt (µg/kg)	K
MnO	Ho	Sb	La
Fe_2O_3	La	Se	Li
S	Lu	Sn	Mg
Cl	Nb	Te *(µg/kg)*	Mn
Cr	Nd	Tl	Mo
Ga	Ni		Na
As	Pr		Ni
Sr	Rb		P
Mo	Sc		Pb
Sn	Sm		S
Sb	Ta		Sc
Ba	Tb		Sr
Pb	Th		Th
Bi	Tm		Ti
	U		V
	V		Y
	Y		Zn
	Yb		Zr
	Zn		
	Zr		

4. RESULTS

4.1. Geochemistry of Sedimentary Rocks

Supracrustal rocks along the RLZ are mainly turbiditic metasedimentary rocks that locally contain abundant graphite bearing schists and minor mafic metavolcanic interlayers. This sequence is defined as the Näläntöjärvi suite by Laajoki and Luukas (1988) and it has been proposed that it is a depositional basement for the volcanic rocks of the island arc (Kousa 1997). These rocks (34 samples) are highly metamorphosed and sub-grouped further by the different composition into several rock types. They include graphite-pyrrhotite bearing paragneiss, pyrrhotite paragneiss, calc-silicate bearing paragneiss, biotite paragneiss, quartz-feldspar gneiss, graphite bearing paragneiss, magnetite bearing biotite paragneiss, pyrite-pyrrhotite paragneiss and quartzite. The regional metamorphic grade in the Vihanti-Pyhäsalmi belt is mainly from lower amphibolite facies to upper amphibolite facies. Locally, for example, in the Kiuruvesi area, the metamorphic grade is higher and reaches granulite facies (Korsman et al. 1997).

Sedimentary rocks in the Vihanti (Lampinsaari) group do not show evidence of significant mineralization, however, with few exceptions, some samples have wide variability in iron content (Figure 4.1 & Figure 4.2). Main components of the meta-sediments are Si, Fe and Ca.

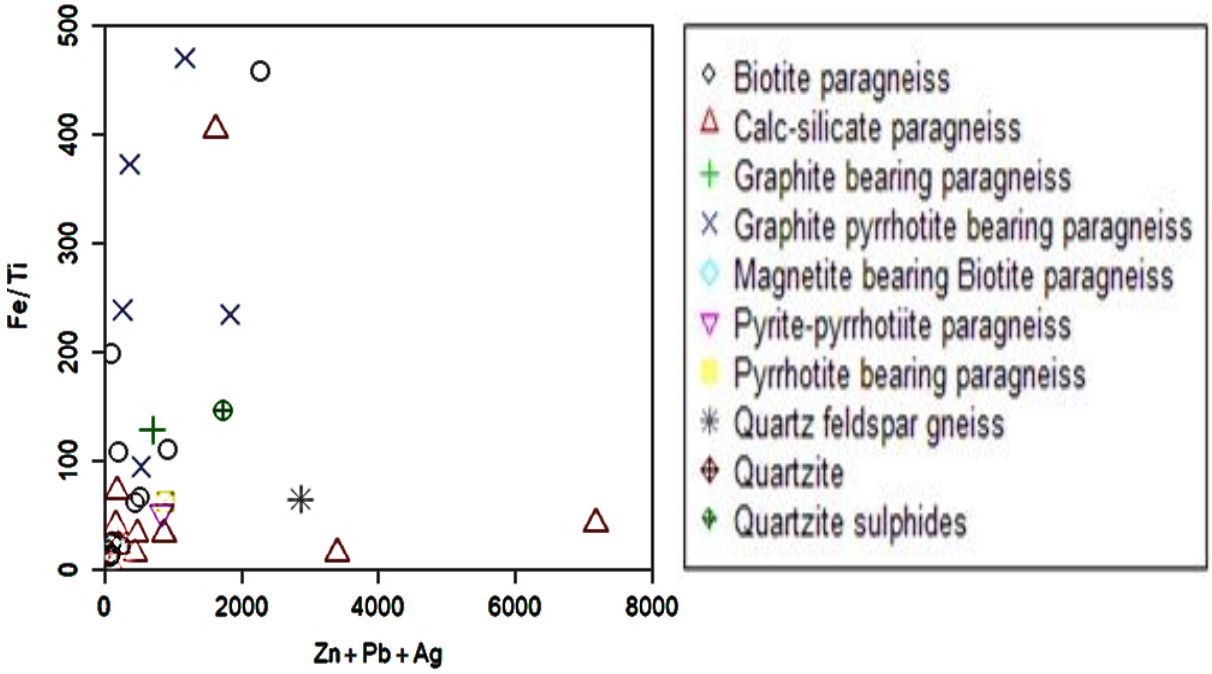

Figure 4.1 Bivariate geochemical plots of the metamorphosed sedimentary rocks from the Vihanti group (Lampinsaari). Fe/Ti vs. Zn+Pb+Ag plot. Most samples are characterized by low Zn+Pb+Ag and low Fe/Ti with few samples in exception.

Silica occurs as quartz, while Fe is mostly present in pyrrhotite, pyrite and to a lesser extent magnetite. Calcium (Ca) content in calc-silicate bearing paragneiss's. SiO_2 and FeO_2 contents of the most metalliferous sediments are quite high. SiO_2 contents range from 44.46% in calc-silicates to 86.359% in one sample of quartzite. FeO^t content varies from 1.5% to 21.6%. Most of the samples studied have a typical low grade of MnO (<0.2%). Correlation between MnO and CaO is not clear anymore which could be due to high-grade metasomatism in specifically calc-silicates of paragneiss. The MgO content of the samples varies from 0.9% in graphite-pyrrhotite bearing paragneiss to highest 16.4% in calc-silicate paragneiss. Na_2O, K_2O, P_2O_5 and TiO_2 values are either very low or generally does not display strong variations Figure 4.3.

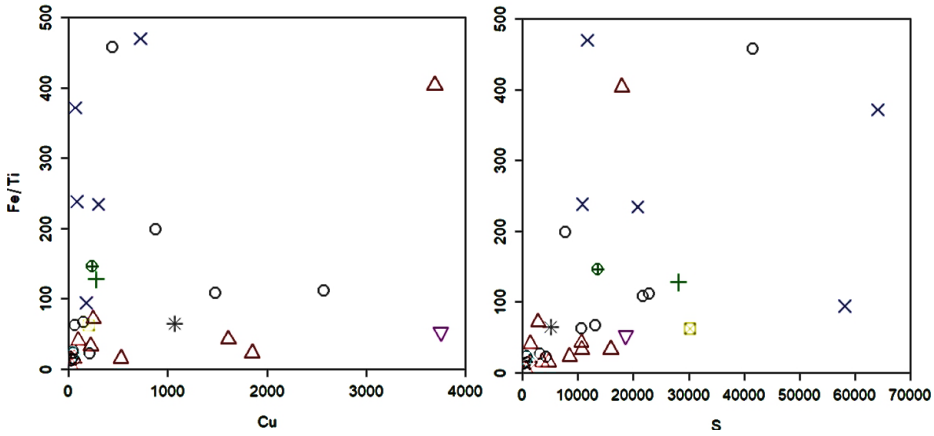

Figure 4.2 Harker plot of meta-sedimentary rocks from the Vihanti Lampinsaari area. Fe/Ti vs Cu & S plot. Legends as in Figure 4.1

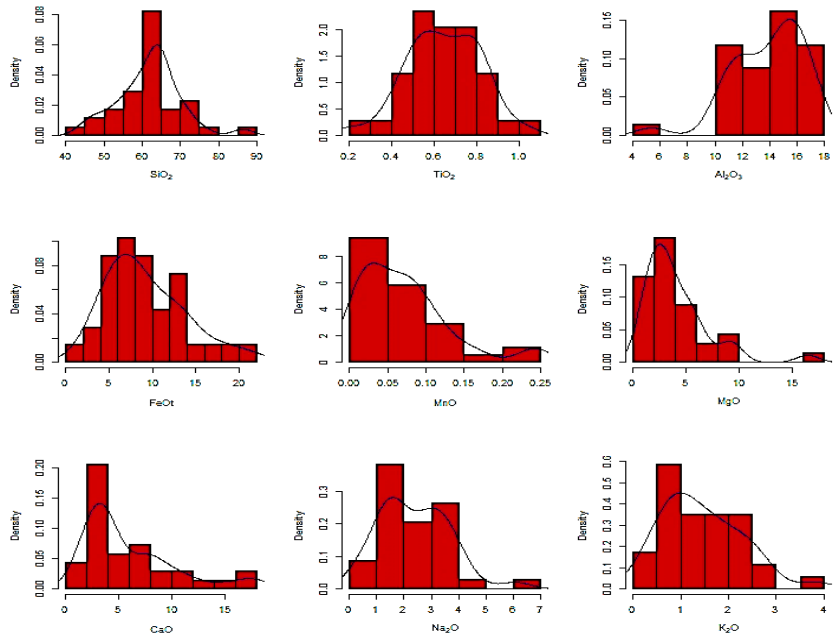

Figure 4.3 Histogram of the major elements of all the samples of Meta-Sedimentary rocks of the Lampinsaari area. Software used GCD-Kit 4.1.

Higher the CaO content in samples, the lower SiO_2 and FeO^t gets. Loss on ignition in these samples is very low. As Sr easily substitutes for Ca in carbonates, samples with high CaO also contains the highest Sr contents. Mostly SiO_2 is high in all the samples except three calc-silicates bearing paragneiss, having as low as 44% SiO_2. This decrease in SiO_2 of these samples results in higher concentrations of FeO^t, Al_2O_3 and CaO. The difference occurs because higher concentrations of Fe_2O_3, Al_2O_3 and CaO will reduce the amounts of other major elements (SiO_2) due to dilution. (Hollis et al., 2015). Another dominant component of meta-sediments is SiO_2, which is likely to be found as a result of excess quartz saturation (Kalogeropoulos and Scott, 1983). Figure 4.5 is displaying Fe_2O_3-Al_2O_3-SiO_2 ternary diagram, according to which the meta-sedimentary rocks in the Vihanti group are largely silica-rich. While the Al_2O_3 component of the rocks is also notable in Figure 4.4.

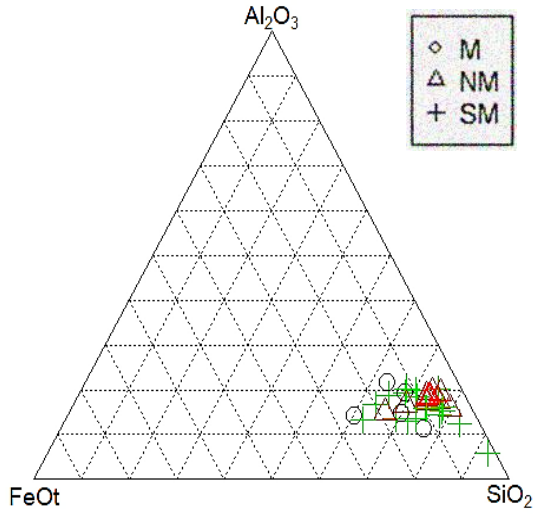

Figure 4.5 Ternary FeO^t-Al_2O_3-SiO_2 discriminant plot for the meta-sedimentary rocks form the Vihanti (Lampinsaari) group. Legends M=Mineralized, NM= Not Mineralized and SM= Slightly Mineralized.

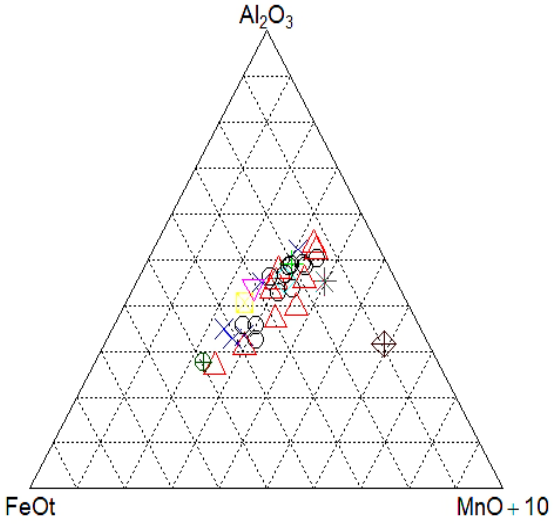

Figure 4.4 Ternary Al_2O_3-FeO^t-MnO+10 discriminant plot for the meta-sedimentary rocks from the Vihanti Lampinsaari area. Legends as in Figure 4.1 by rock types.

Large variations in concentrations exist for Al_2O_3 (5.3-17.1 wt%), TiO_2 (0.2-1.01 wt%), Sc (5-32 ppm), Zr (34-340 ppm), Th (0.6-20 ppm), Nb (2.2-12 ppm) and Rb (1.9-291 ppm). Higher concentrations of these elements reflect the presence of detrital components (Kalogeropoulos and Scott 1983, Spry et al. 2000, Slack et al. 2009). A ternary plot of Fe-Al-Mn+10, Figure 4.4 is used to distinguish between hydrothermal and detrital inputs to these meta-sedimentary rocks (Boström 1973, Spry et al. 2000, Slack et al. 2009). Such plots have been developed by collecting samples of hydrothermal and non-hydrothermal iron formations from a variety of worldwide sites. The reasoning behind this distinction is that Fe and Mn are chiefly due to

hydrothermal origin, while Al is essential of detrital origin. Almost all the samples restricted to Al-rich apex of the Ternary diagram (Figure 4.4) representing the presence of detrital materials and an almost negligible amount of hydrothermal material in the sediments.

Metal concentrations in sediments are rather low. However, some sediments referred in figures as mineralized contain base metal contents to some extent. In Figure 4.1 two samples of calc-

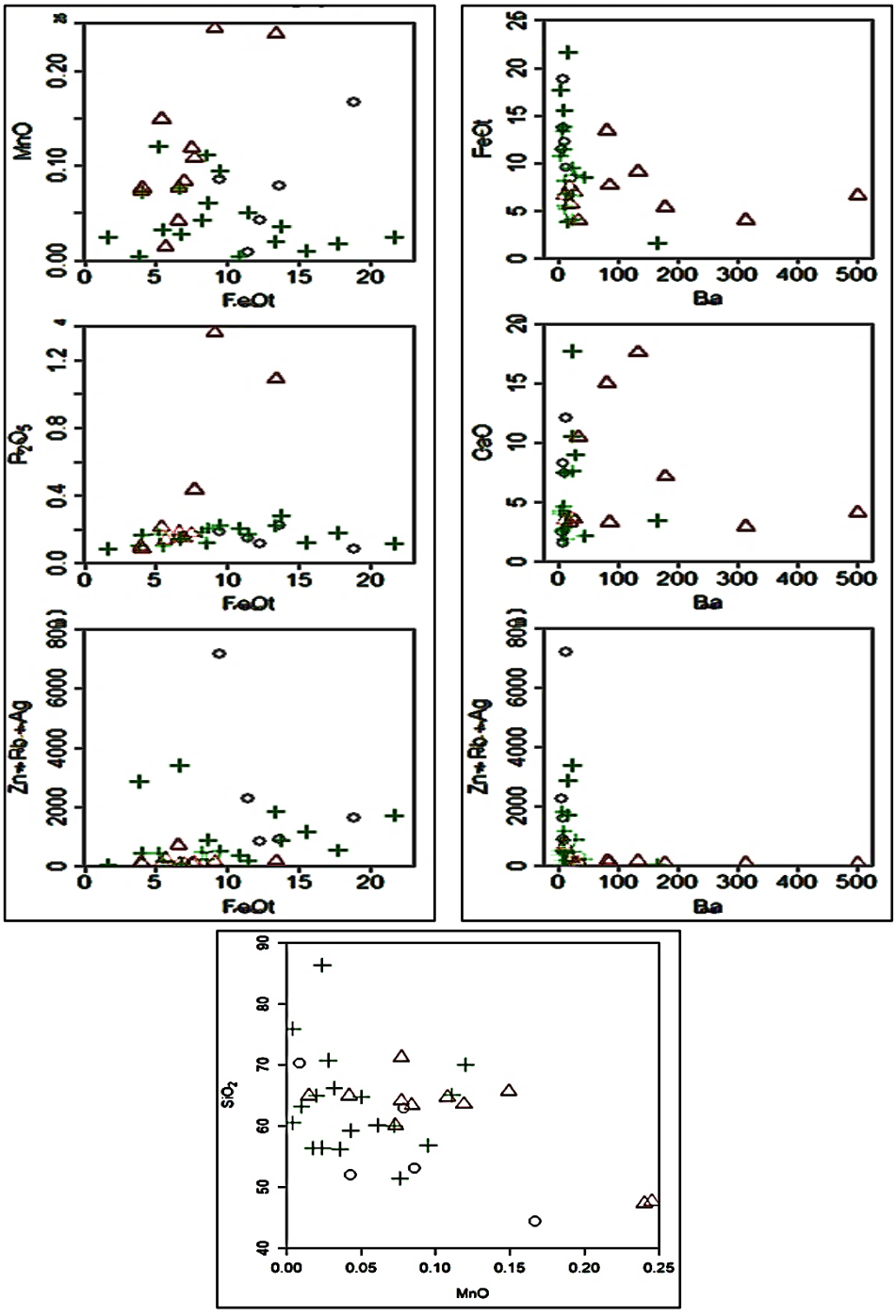

Figure 4.6 Bivariant geochemical plot of meta-sedimentary rocks of Vihanti (Lampinsaari) group. (a) Plots of FeO^t vs. MnO, P_2O_5 and Zn+Pb+Ag. (b) Plots of Ba vs. Fe_2O_3, CaO and Zn+Pb+Ag. (c) SiO_2 vs MnO discrimination of M=mineralized, SM= slightly mineralized samples from NM= Not mineralized samples. Symbols as in figure 4.5.

silicate bearing paragneiss deviate abnormally from the rest, one having the highest Fe/Ti ratios with Zn+Pb+Ag of approx. 2000 ppm, while the other calc-silicate bearing paragneiss having Zn+Pb+Ag greater than 7000 ppm with Fe/Ti ratios less than 50 ppm. Slightly mineralized samples grouped in graphite-pyrrhotite bearing paragneiss in Figure 4.1 and Figure 4.2 are consistent in containing high Fe/Ti ratios relatively. Au values have elevated to 297 ppb in slightly mineralized calc-silicate paragneiss rock. Two highest values of gold are both representing mineralized samples of pyrite-pyrrhotite and calc-silicate paragneiss with concentrations of 108 ppb and 189 ppb respectively. Cu content is <3750 ppm and Ba and Bi values are low. Increase in Ni and Co concentrations are notable in the Fe-rich samples. Elevated content of V (19.9-1370 ppm) is quite noticeable while U and Sr do not show elevated values. There are three distinct samples with high P_2O_5 vs FeO^t (Figure 4.6). Same samples are high in Mn content. These samples contain phosphate minerals.

The rare earth elements (REE) data that are chondrite and primitive mantle normalized for all the 34 metasedimentary rock samples show broad variations in their patterns. (Figure 4.7 & Figure 4.8). So, for the sake of clarity, their classification is done for mineralized, slightly mineralized and non-mineralized samples (Figure 4.7) and then by rock types (Figure 4.8).

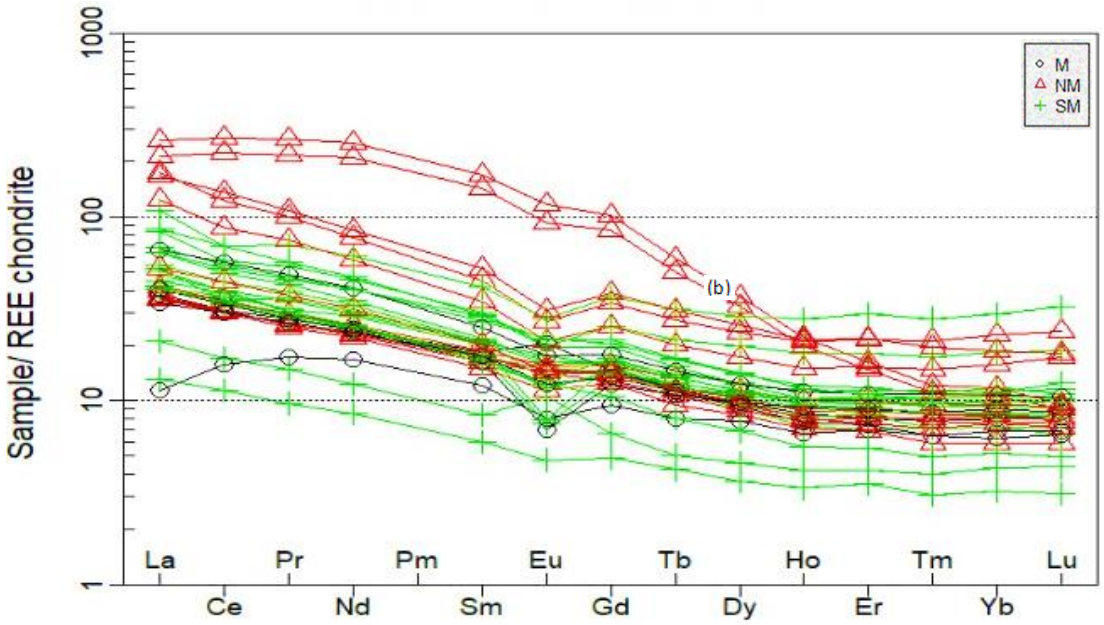

Figure 4.7 Chondrite-normalized REE patterns of the meta-sedimentary rocks from the Lampinsaari mine of the profile logs PL130 and PL106. Legends M=Mineralized, NM=Not Mineralized and SM= Slightly mineralized samples. Chondrite normalization after (Boynton 1984).

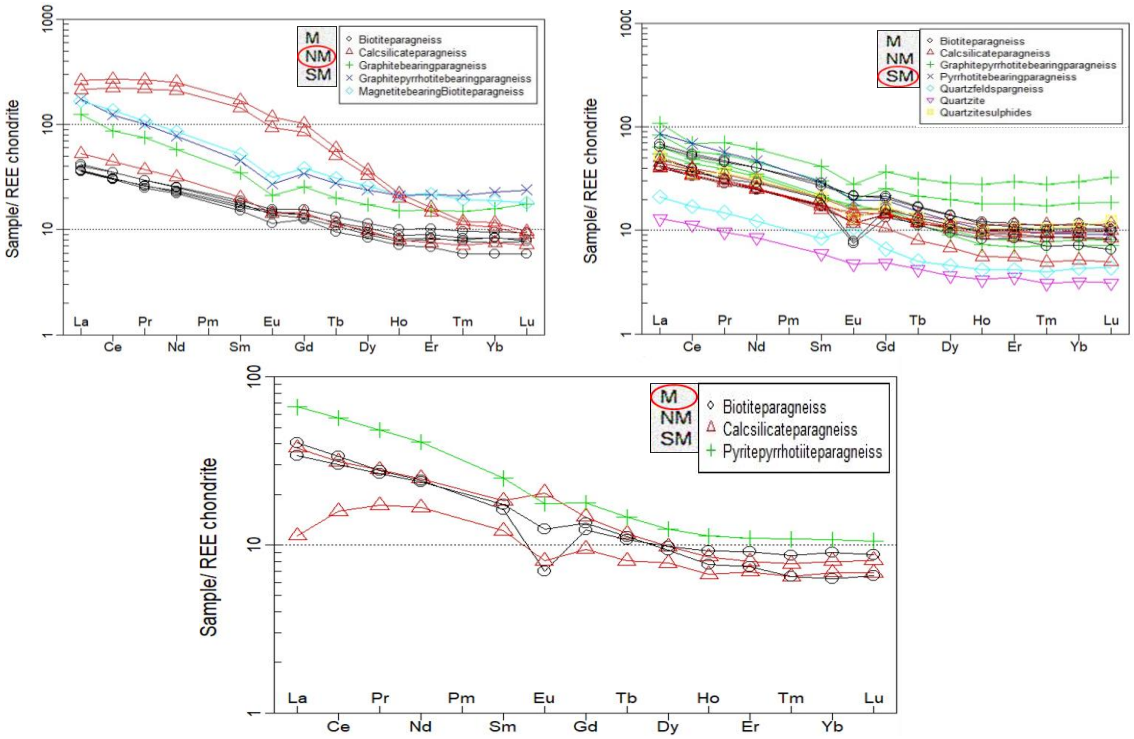

Figure 4.8 Chondrite-normalized (Boynton 1984) REE patterns of the (a) NM=Not Mineralized, (b) SM=Slightly Mineralized and (c) M=Mineralized samples of the meta-sedimentary rocks referred in Figure 4.7. Samples further sub-categorized to the rock types in legends.

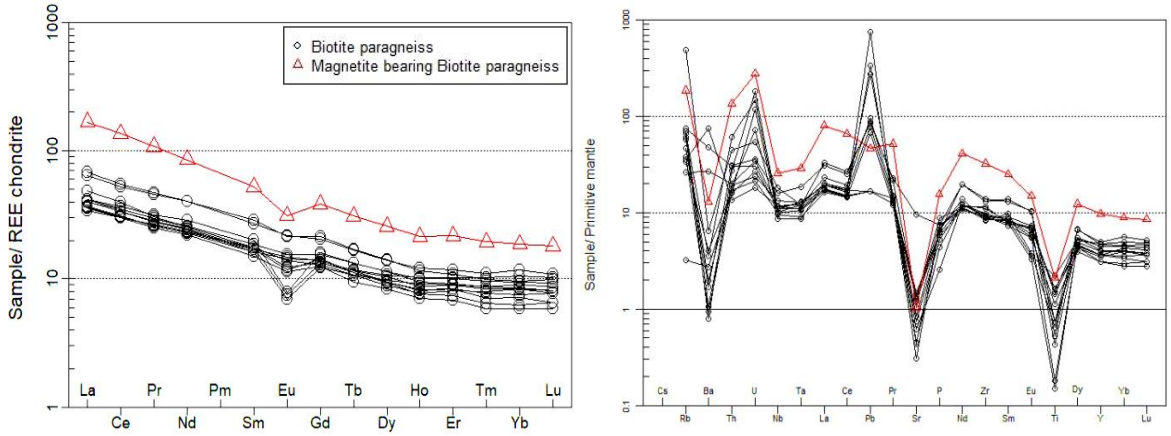

Figure 4.09 Chondrite-normalized (Boynton 1984) and primitive mantle-normalized (McDonough and Sun 1995) REE patterns of the biotite paragneiss and magnetite bearing biotite paragneiss.

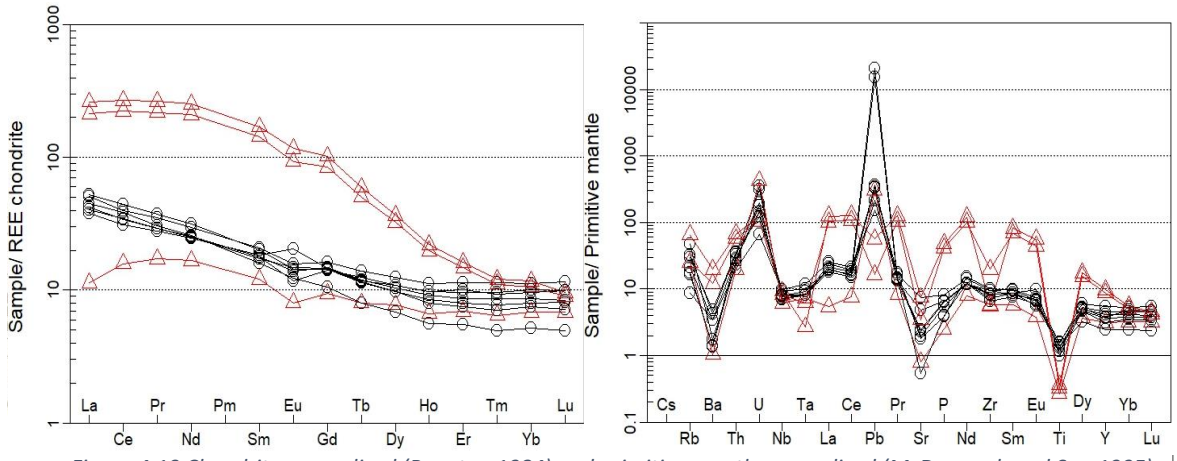

Figure 4.10 Chondrite-normalized (Boynton 1984) and primitive mantle-normalized (McDonough and Sun 1995) REE patterns of the calc-silicate paragneiss.

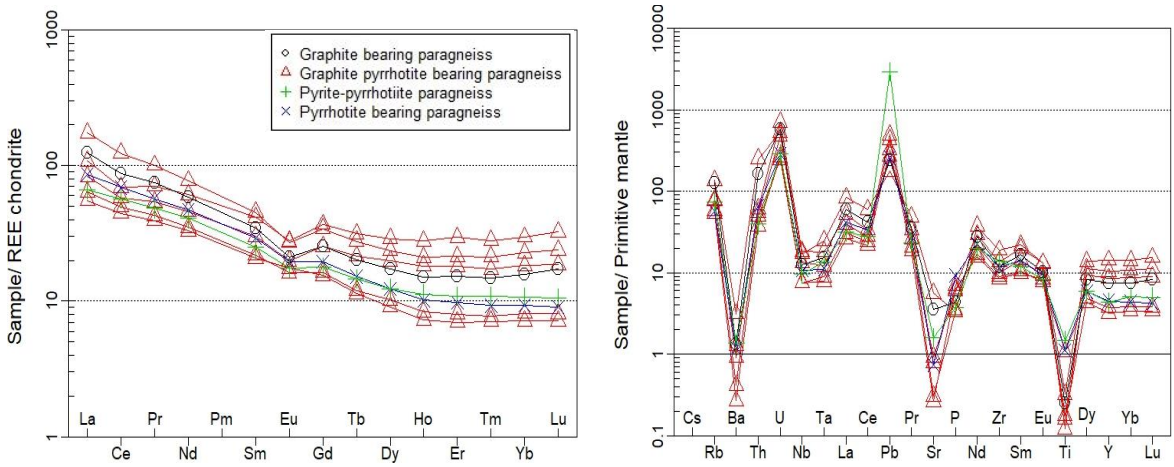

Figure 4.11 Chondrite-normalized (Boynton 1984) and primitive mantle-normalized (McDonough and Sun 1995) REE patterns of the graphite-pyrrhotite bearing paragneiss, graphite bearing paragneiss, pyrite-pyrrhotite paragneiss and pyrrhotite bearing paragneiss.

Figures from Figure 4.7 to 4.1 have been classified according to the rock types of all 34 samples of meta-sedimentary rocks. Each group with rock types is further normalized both with chondrites (Boynton 1984) and primitive mantle spider plot (McDonough and sun 1995).

Analysed samples in Figure 4.8 have a clear decrease in LREE to HREE content in the order of non-mineralized (NM), slightly mineralized (SM) to mineralized (M) samples of the meta-sedimentary rocks. Samples are slightly enriched in light rare earth elements (LREEs) than the relatively flat heavy-REE slopes. It is noteworthy that samples exhibit pronounced negative europium (Eu) anomalies. Usually, it is the result of Ca replacement. However, negative Eu anomaly in metal-containing rocks could be explained by the detrital material contribution (Spry et al. 2000, Davidson et al. 2001). Significant enrichment of LREE relative to HREE is the indication of evolved source areas.

The lack of high Y/Ho ratios can be interpreted as the absence of significant seawater contribution (Bau 1996). The Y/Ho ratios of all the samples lie close to chondrite values as in Figure 4.9.

Due to complex structure of VMS ore deposits forming on the seafloor it is very difficult to recognize a wide variety of ore facies after the metamorphism and deformation, which is a very

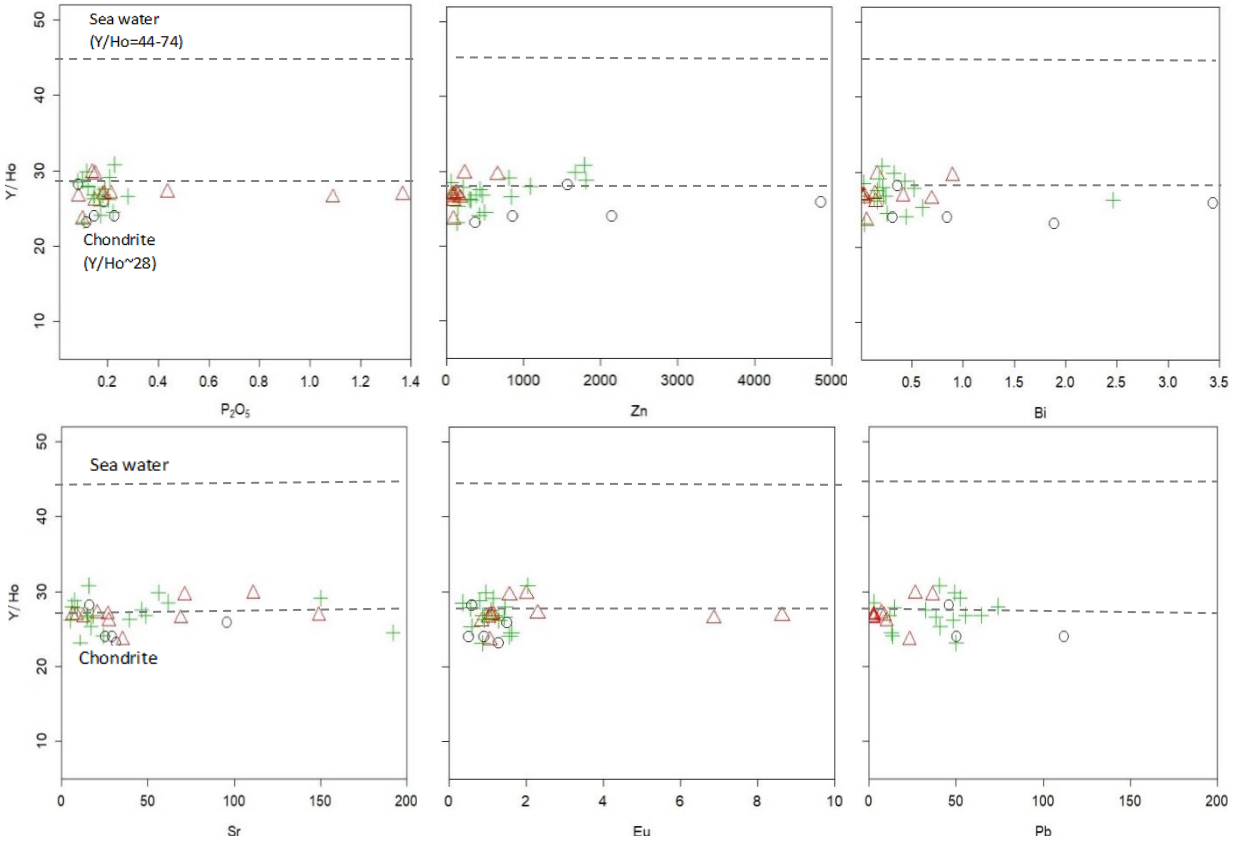

Figure 4.9 Bivariate plots of Y/Ho versus selected trace elements in the meta-sedimentary rock samples from the Lampinsaari region.

common problem in VMS districts (Kalogeropoulos and Scott 1983, Allen et al. 2002). There are diverse views on the metamorphosed sedimentary rocks associated with VMS deposits on a global scale. For distinguishing between these different types having textural and mineralogical variety, the geochemical method is the best tool (Maslennikov et al. 2012, Hollis et al. 2015).

Low Fe/Ti and high Al/(Al+Fe+Mn), Rb, Th, Zr, Sc and Nb in most of the meta-sedimentary rocks of the Lampinsaari mine is the indication of the significant detrital components of volcanic and volcaniclastic rocks. Negative Eu anomalies also support the contribution of clastic material. Supracrustal rocks along the Raahe Ladoga zone RLZ are mainly turbiditic metasedimentary rocks (Laajoki and Luukas 1988). Since they form the depositional basement

for the volcanic rocks of the island arc (Kousa 1997), these meta-sedimentary rocks of the Lampinsaari region can be classified as sedimentary rocks with detrital volcanic material.

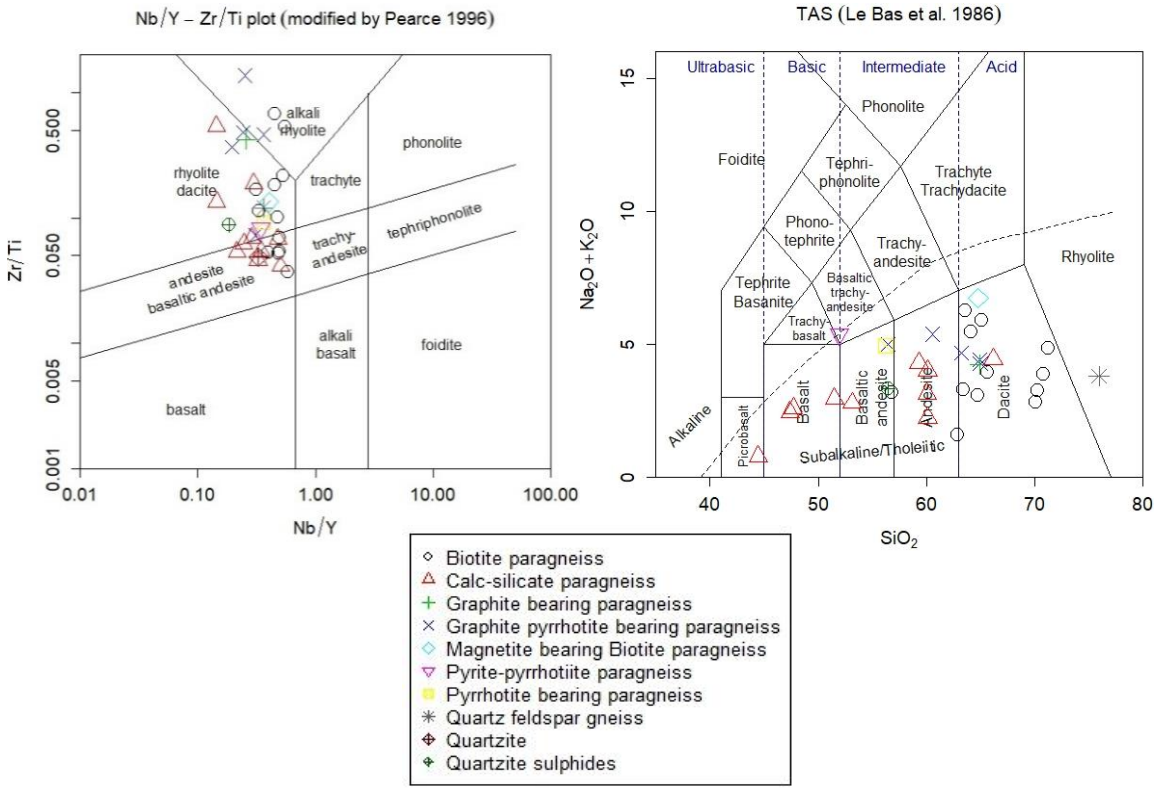

Figure 4.10 Classification of rock types of the 34 samples of metasedimentary rocks of the Lampinsaari-Viahti area by using TAS (le Bas et al. 1986) and Nb/Y vs Zr/Ti plot (modified by Pearce 1996).

For general classification of these 34 metasedimentary rocks, TAS (Le Bas et al. 1985) major elements and Nb/Y vs Zr/Ti (modified by Pearce 1996) trace elements plots are used (Figure 4.10). Large variations in metasedimentary rocks composition can be seen in both major and trace elements classifications diagrams. They range from rhyolitic to basaltic, alkali-rhyolitic to andesite-basaltic andesitic in composition. Almost all biotite paragneiss are acidic except for one sample being in the basaltic-andesitic field. Calc-silicates have composition ranging from andesitic to basaltic with one sample in the field of Picro-basalt (Figure 4.10).

4.2. Geochemistry of Felsic Intermediate and Mafic Meta-Volcanics

The Vihanti Lampinsaari volcanic sequence is composed of felsic to intermediate metavolcanic rocks with minor mafic metavolcanics (Rehtijärvi et al. 1979). In the Vihanti block, the dominant protoliths are intermediate and felsic metavolcanic rocks while mafic metavolcanic

rocks are rare and sparsely distributed (Mäki et al. 2015). There are 10 samples for Felsic metavolcanics, 3 for mafic and 8 for intermediate metavolcanic rocks.

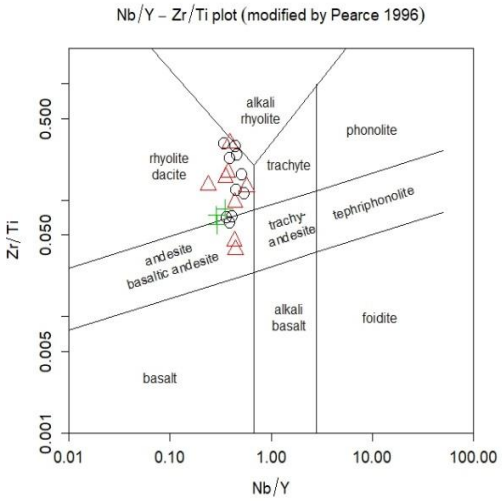

Figure 4.11 Plot of Zr/Ti versus Nb/Y (Pearce, 1996) showing variation in composition of igneous rocks in the Lampinsaari region. Legends as in fig.12

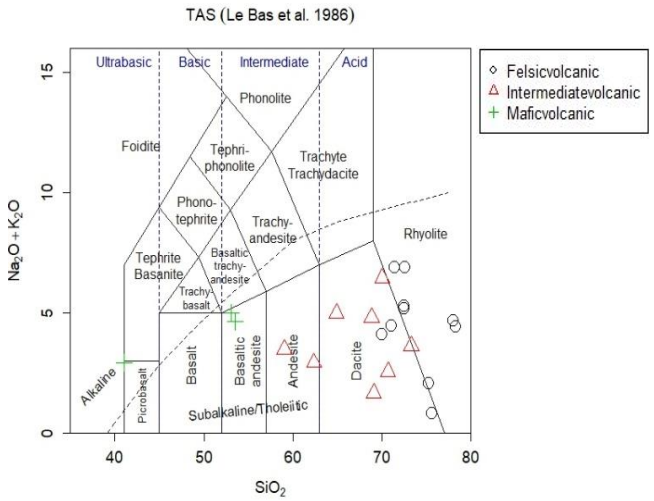

Figure 4.12 Total Alkali Silica (TAS) diagram (Le Bas et al. 1986) for felsic, intermediate and mafic meta-volcanic.

Compositionally the Lampinsaari felsic and intermediate volcanic rocks are categorized in the basaltic-andesite (mafic metavolcanics) to andesite-dacite (intermediate) and rhyolites (felsic meta-volcanic) according to the major elements TAS classification Figure 4.12. However, potassium being mobile (Figure 4.12) behave irregularly in these elements, it does not follow the general differentiation as other immobile trace elements do in Figure 4.11 (i.e. Zr/TiO_2 vs Nb/Y). The overall calc-silicate character is postulated for these rocks. By analysing the immobile trace elements in Figure 4.11. Zr/Ti vs Nb/Y we can observe different behaviour of these rocks. Majority of the samples including mafic metavolcanics plot in the field of evolved rhyolitic dacitic subalkaline. Intermediate rocks show gradational features from andesite to basaltic andesite to rhyolitic dacite. There is no distinct break in these cluster of rocks instead of a gradational feature

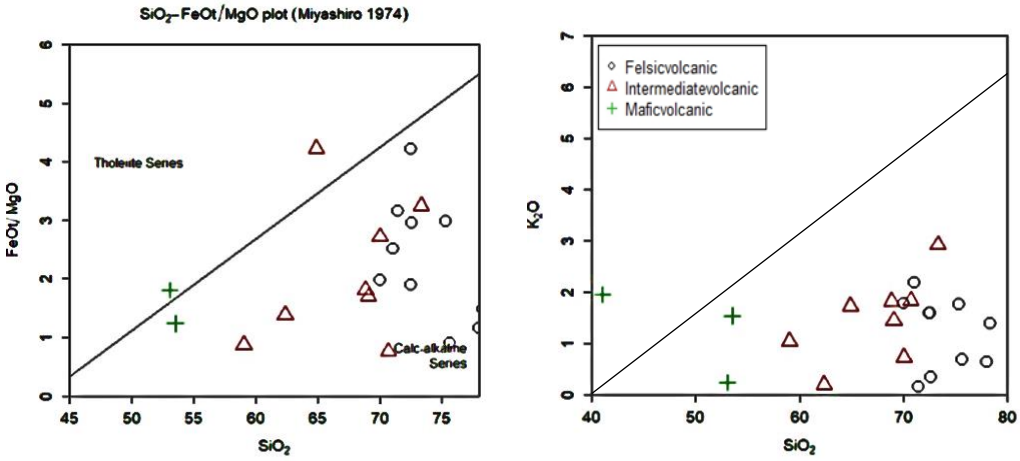

Figure 4.14 K_2O vs SiO_2 and FeO/MgO vs SiO_2 diagrams for felsic, intermediate and mafic metavolcanic rocks in Lampinsaari region. The division between tholeiitic and calc-alkaline fields on the FeO/MgO vs SiO_2 diagrams is from Miyashiro (1974).

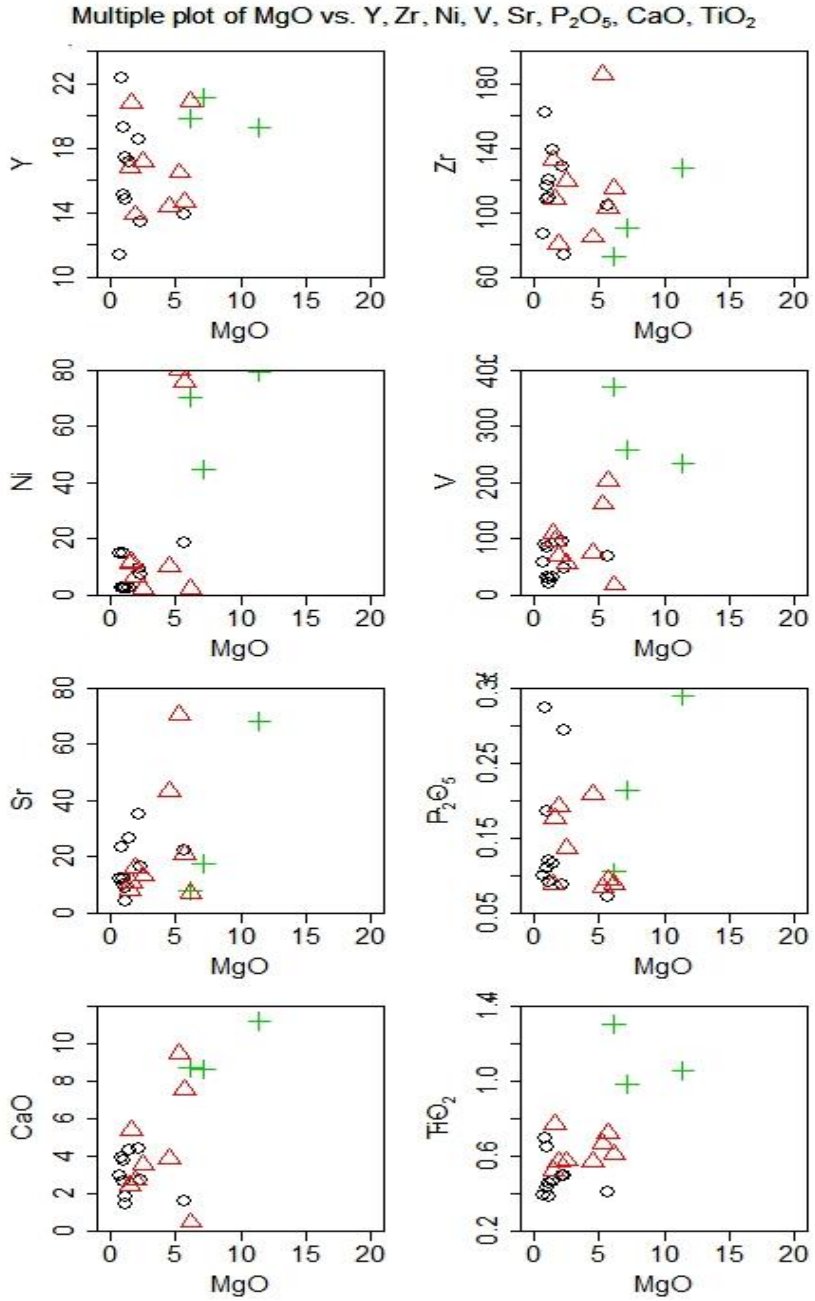

Figure 4.13 Harker diagrams for the selected major elements (%) and trace elements in (ppm) variation diagrams for felsic, intermediate and mafic meta volcanics in Lampinsaari mine area. Oxides are normalized. Figure 4.12 for legends.

especially due to intermediate rocks. However, this cluster of the igneous rocks of the region indicates these host rocks are of either felsic-siliciclastic or bimodal-felsic group according to the classification of Barrie & Hannington (1999) and; Franklin *et al*. (2005). A plot of the Zr versus Y (Figure 4.15) (Ross and Bedard, 2009) agrees with the major element's ratios in Figure 4.12 from Miyashiro 1974 and strongly differentiate them all in the calc-alkaline magmatic affinity with enriched Zr relative to Y.

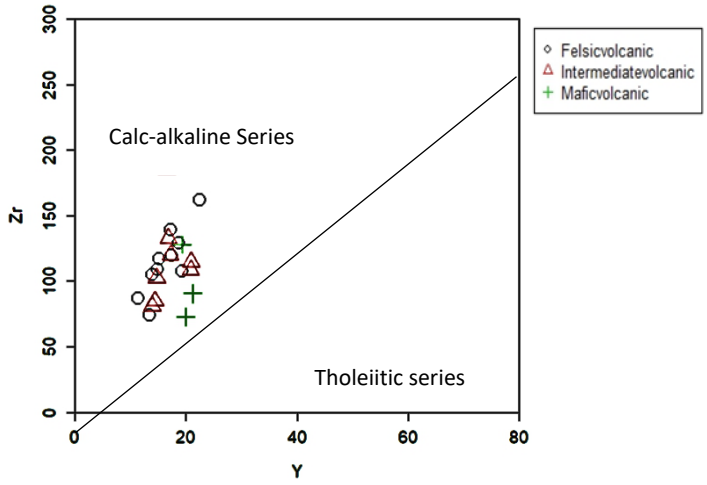

Figure 4.15 Zr versus Y plot of felsic, intermediate and mafic metavolcanic to differentiate magma series by Ross and Bedard, 2009.

4.2.1. Felsic Meta-volcanic rocks

Felsic meta-volcanic rocks are further subcategorized into rock types of major quartz-feldspar schist and cordierite gneiss with one sample of quartz-feldspar porphyry. Rocks have more

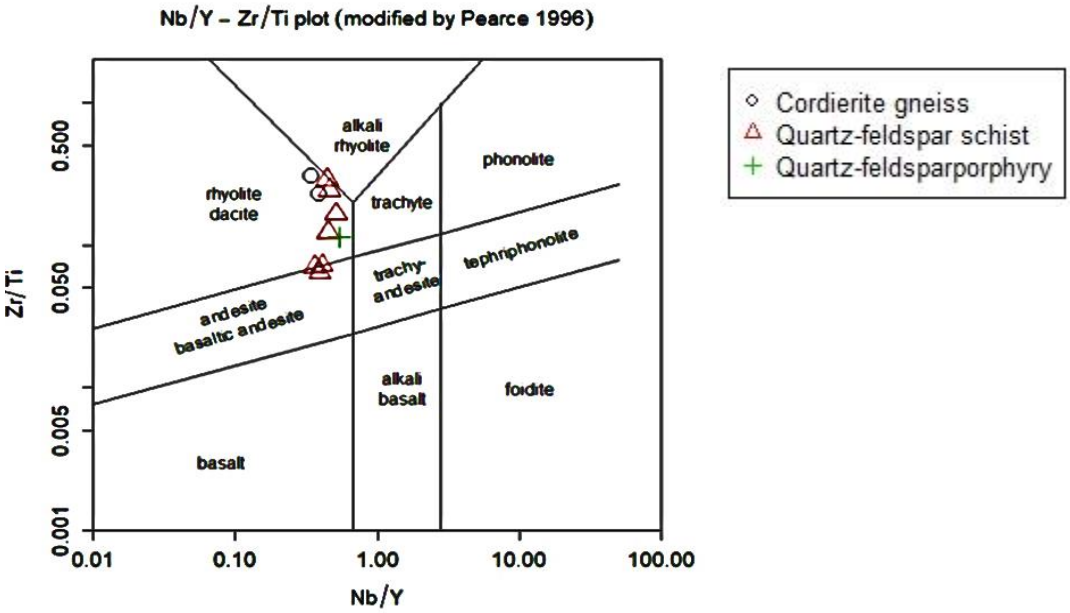

Figure 4.16 Plot of Zr/Ti versus Nb/Y (Pearce, 1996) showing variation in composition in Felsic metavolcanics rocks in the Lampinsaari region. Legends subcategorized from felsic group to rock types.

evolved composition relative to the other two intermediate and mafic metavolcanic groups based on their relative Zr/Ti ratios (Figure 4.16). Samples occur more in gradational sequence than in cluster form. This difference occurs due to the variation of the TiO_2 content. Rocks with lower Zr/Ti, dominantly three quartz feldspar schists have higher TiO_2 contents than those of the high Zr/Ti samples.

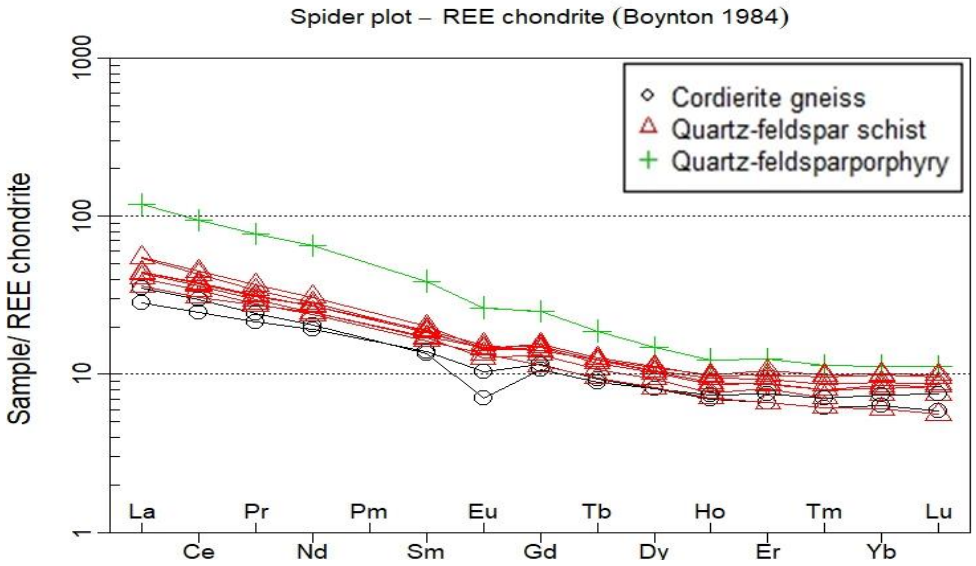

Figure 4.17 Chondrite normalized rare earth element patterns. Legends given as rock types.

Despite the variation in TiO_2 contents, the chondrite normalized REE patterns of the samples are remarkably similar except for one distinct quartz-feldspar porphyry sample (Figure 4.17). Enriched LREE relative to HREE and negative Eu anomalies is of almost similar magnitude.

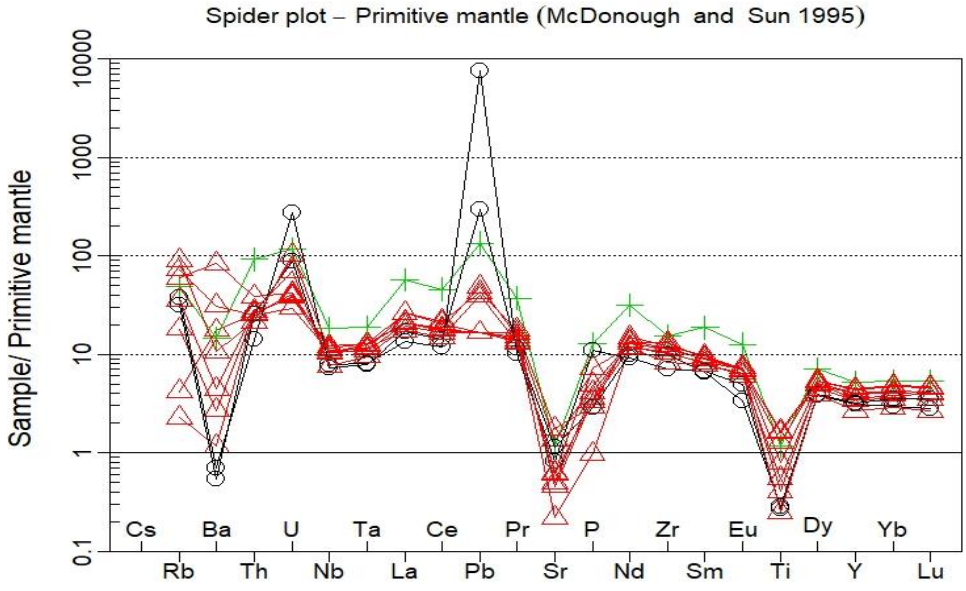

Figure 4.18 Primitive mantle normalized extended trace elements pattern for Lampinsaari felsic metavolcanics. Legends same as in Figure 4.17.

In the primitive mantle normalized extended REE patterns (Figure 4.18) Ba, Sr and Ti exhibit strong negative anomalies.

4.2.2. Mafic Meta-Volcanic Rocks

Minor mafic metavolcanics are considered separately with three rock samples and subcategorized into two samples of amphibolites and one sample of altered mafic rock.

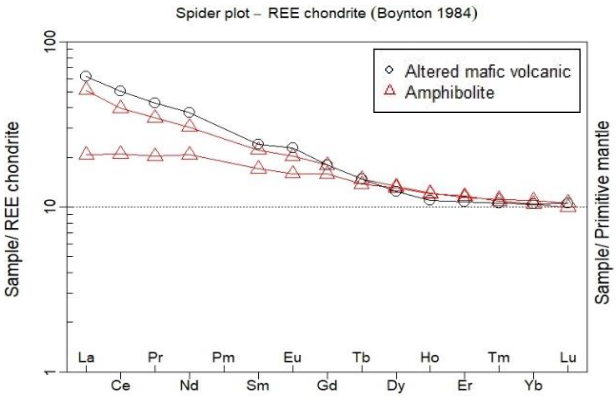

Figure 4.20 Chondrite normalized (Boynton 1984) rare earth element patterns of mafic meta volcanics of the Lampinsaari region. Legends given.

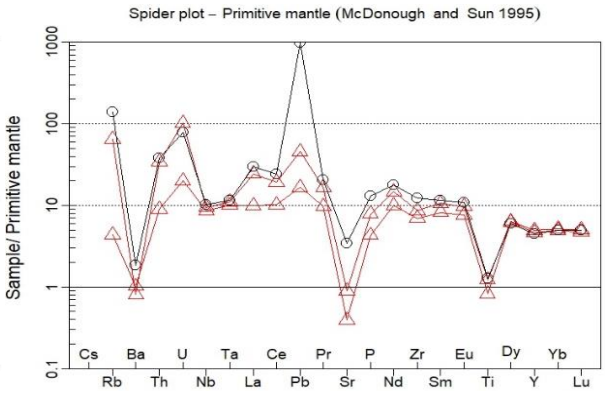

Figure 4.19 Primitive mantle normalized extended trace element pattern for mafic meta volcanics of Lampinsaari region (McDonough and Sun 1995).

The analysis of the chondrite normalized REE patterns (Figure 4.20) show that the light rare earth elements (LREE) are slightly enriched relative to heavy REE (HREE). Almost no distinct Eu anomaly observed probably reflecting no plagioclase fractionation during magmatic evolution. On the extended trace element plots (Figure 4.19) normalized to a primitive-mantle, these rocks generally exhibit slight to an intense increase of Pb, U and Rb relative to the

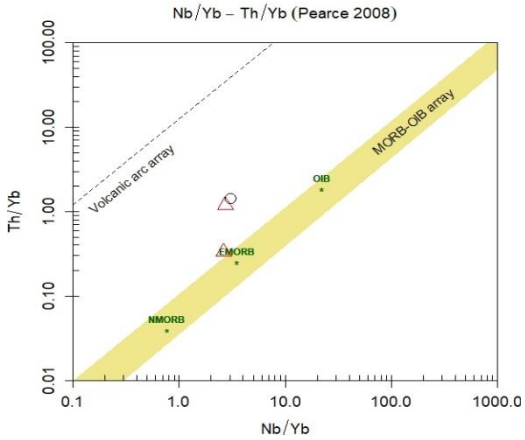

Figure 4.21 Th/Yb vs Nb/Yb plot by (Pearce 2008) of the meta volcanic rocks of the Lampinsaari region. LEGENDS represents rock types as in Figure 4.20.

primitive mantle, with negative anomalies of Ba, and Sr to lesser degree Ti and Zr. These weakly enriched LREE mafic metavolcanic rocks resemble E-MORB type rocks.

4.2.3. Intermediate Meta Volcanic Rocks

Intermediate meta-volcanic rocks (8 samples) are further considered and classified to slightly mineralized to non-mineralized rock samples. Major and trace elemental classification of the intermediate metavolcanic rocks is described in Figure 4.11 and Figure 4.12 together with other meta-volcanic rock samples. However, classification was done separately (Figure 4.22 and Figure 4.23) to demonstrate the behaviour of samples in more detail. In Figure 4.23 most samples plot in the field of rhyolite/dacite except two lying in andesite basaltic andesite field. In Zr/TiO_2 vs Nb/Y Figure 4.22, all the samples are strictly restricted to the andesitic field.

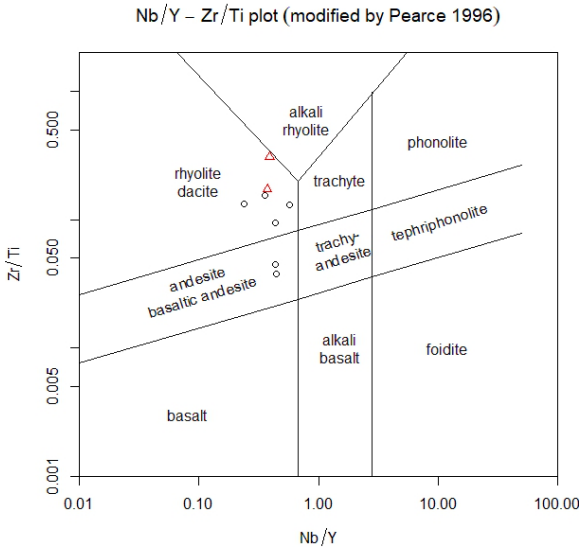

Figure 4.23 Nb/Y vs Zr/Ti plot modified by Pearce 1996 of the meta volcanic rocks of the intermediate composition of the Lampinsaari region. Legends: Red triangles= slightly mineralized, Black circles= not mineralized.

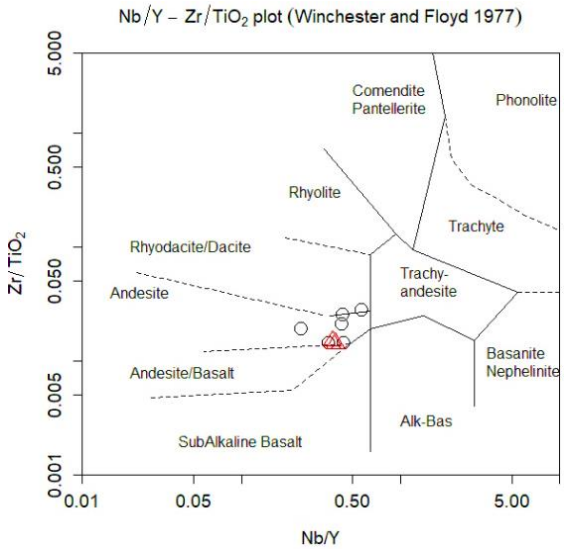

Figure 4.22 Zr/TiO2 vs Nb/Y plot by Winchester and Floyd 1977 of the meta volcanic intermediate rocks of the Lampinsaari region. Legends: Red triangles= slightly mineralized and Black circles= not mineralized.

LREE relative to HREE's enriched in the chondrite normalized plot of intermediate metavolcanic rocks behaved similarly in trend for both slightly mineralized (two lowermost samples) and not mineralized samples (Figure 4.28). A slightly negative anomaly of Eu in between Sm and Gd represents plagioclase fractionations and results in more evolved composition. The trend in chondrite normalized trace elements is no different in behaviour to other two distinct groups discussed having enriched LREEs to low HREEs indicating the island arc setting. The primitive mantle normalized trace elements behaviour is interesting in that Ba, Sr and Ti are depleted enormously while U and Pb show high spikes. In primitive mantle

normalized spider plot Nb is not depleted but less than U, representing the concentrations similar to MORB type rocks (Figure 4.28). Ce, P and Sm are mostly transported by partial

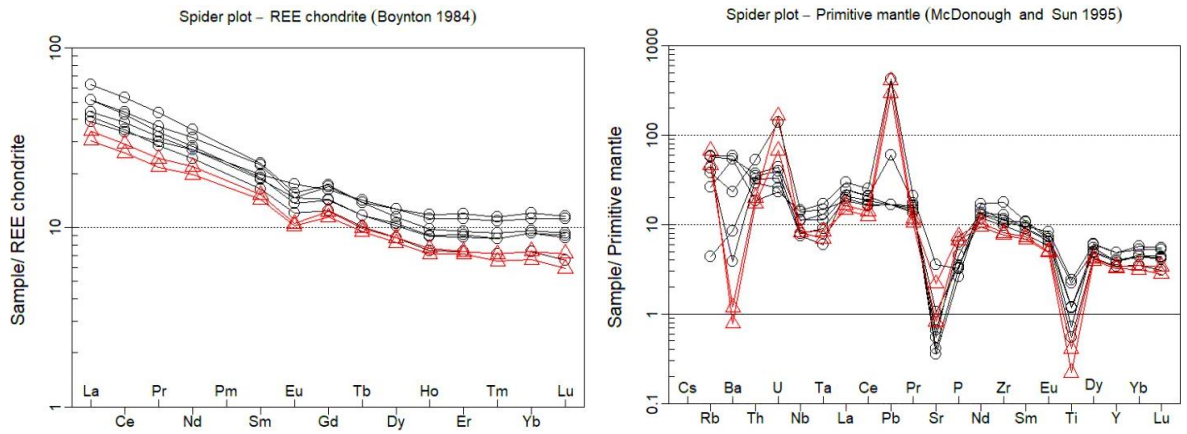

Figure 4.24 chondrite and primitive mantle normalized trace elements patterns of intermediate metavolcanics rocks of the Lampinsaari region.

melts than the aqueous fluids. Ba is depleted only in the two slightly mineralized samples while it is in higher concentrations in the rest of the samples. Its derivation is mainly considered to be from the subducted oceanic sediments.

4.2.4. Geochemistry of Sedimentary Carbonates and Volcanic Sedimentary Rocks

Both groups comprise 12 rock samples' whole-rock data. Sedimentary carbonates (7 samples) have all the Serpentinite-dolomite rock types, while volcanic sedimentary (5 samples) group

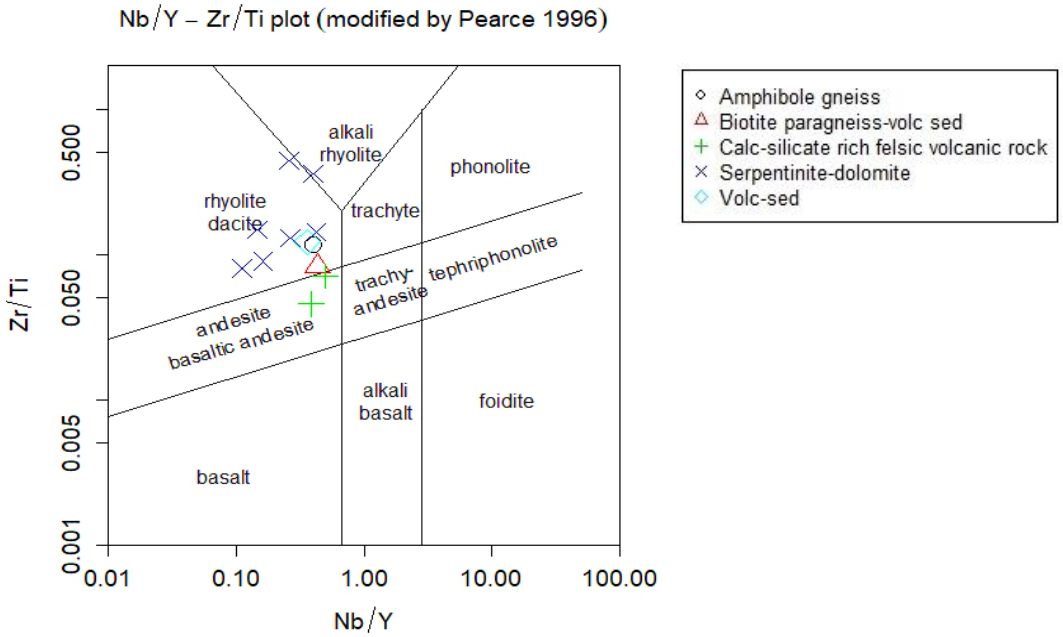

Figure 4.25 Harker diagram for the rock types classification by using trace elemenets plot of Nb/Y vs Zr/Ti (modified by Pearce 1996). 12 Samples are from the Lampinsaari area of both carbonatic sedimentary and volcanic sedimentary rock groups. Legends as rock types.

have amphibole gneiss, biotite paragneiss and calc-silicate rich felsic volcanic rocks. By using Nb/Y-Zr/Ti plot (modified by Pearce 1996) majority of the rock types plot in the Rhyolite/dacite field except the two calc-silicate rich felsic volcanic rocks lying in the andesite-basaltic andesite field area (Figure 4.25).

Only the sedimentary carbonate group with the rock types of serpentinite-dolomites are bearing mineralization in them. All the serpentinite-dolomite samples are slightly mineralized, except three of the samples are mineralized with the one bearing Zn ore and other two as cupreous sulphides. However, volcanic sedimentary rock types are not showing any mineralization at all.

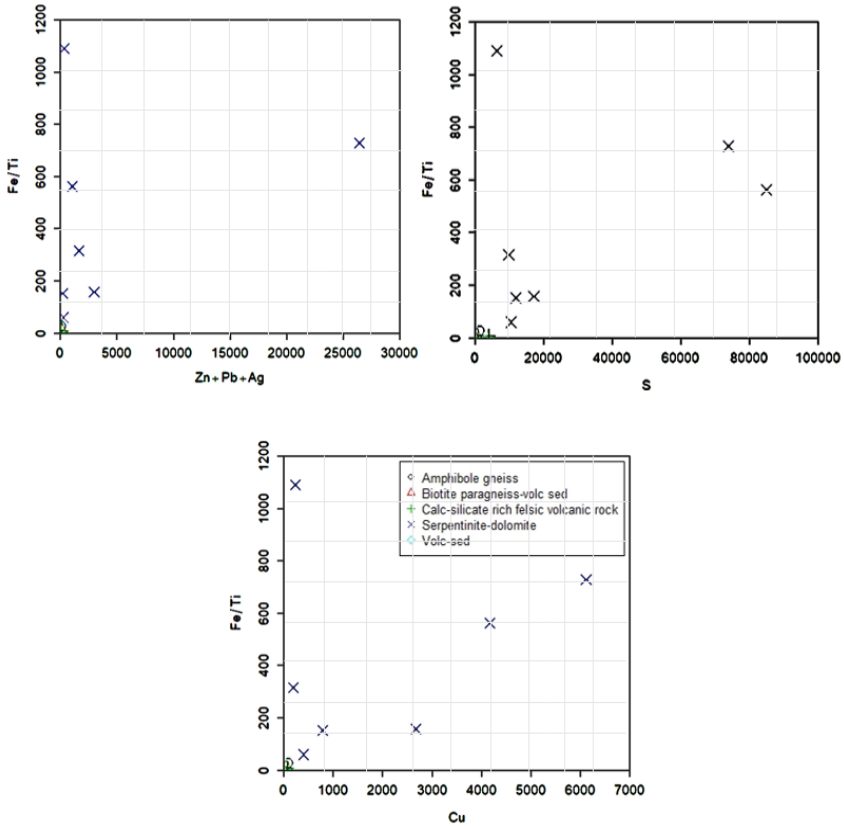

Figure 4.26 Harker diagrams of Fe/Ti vs Zn+Pb+Ag, S and Cu for discrimination of the concentration of mineralization types in both rock groups of Carbonate sedimentary & Volcanic sedimentary. Legends as rock types.

Two distinct groups can easily be identified in the Silica vs major elements Harker diagrams (Figure 4.27). Sedimentary carbonates comprising serpentinite-dolomite rock types have MgO ranging from 14-31 wt%, SiO_2 10-32 wt%, FeO^t 5-48 wt% and CaO 18-41 wt% as the main components of minerals in dolomite and serpentinite. Sample R644 (2.6-2.85 meters) have the lowest SiO_2 content of 14.8 wt% with highest CaO of 41.1 wt% and Carbonates as 7.60 wt%

analysed by +811L and 816 L methods. Two samples (R768 4.75-4.95 & R768 51.25-51.45) are classified as mineralized due to the high concentrations of FeO with sulfur and to some extents Copper with carbonate wt% of 3.76 to 2.34 respectively. Sample R768 (29.35-29.55)

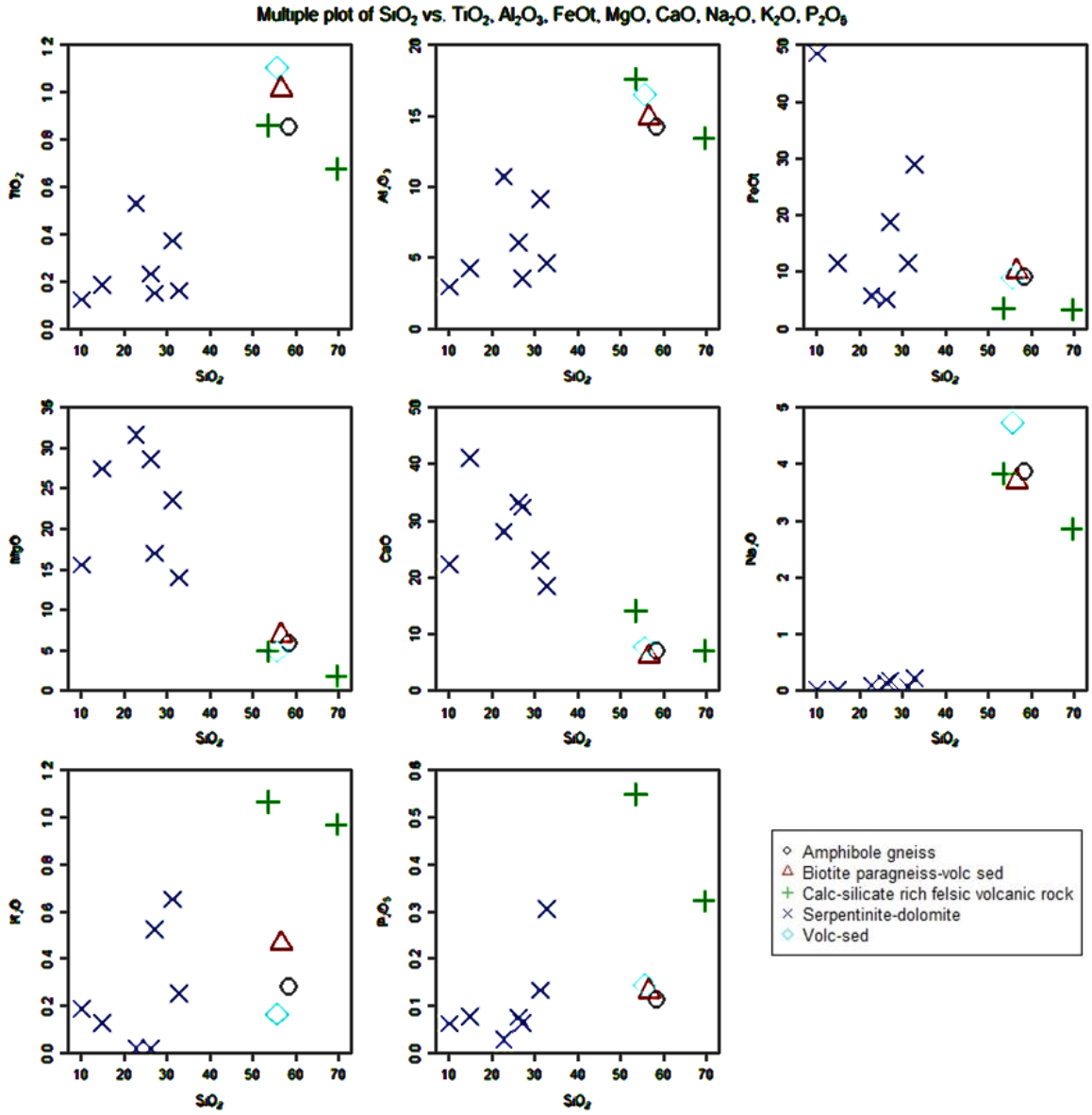

Figure 4.27 Multiple Harker diagrams SiO_2 vs major elements TiO_2, Al_2O_3, FeO^t, MgO, CaO, Na_2O, K_2O and P_2O_5. WR data comprise two major groups carbonate sedimentary & Volcanic sedimentary. Legends as rock types.

is considered as the Zn ore with SiO_2 32 wt%, FeO^t 29 Wt%, MgO 13.9 Wt% and CaO 18.4 wt%. Sample R768 (29.35-29.55) is the only sample with a Zinc content of 26300 ppm, higher than the rest of the samples from the same group.

The comparatively volcanic sedimentary group with different rock types (legends in Figure 4.30) have less ranges of above-mentioned major elements except the TiO_2 ranging from 0.67-1.1 wt%, Al_2O_3 13-14.9 wt%, Na_2O 2.85-4.72 wt% and P_2O_5 0.11-0.54 wt%.

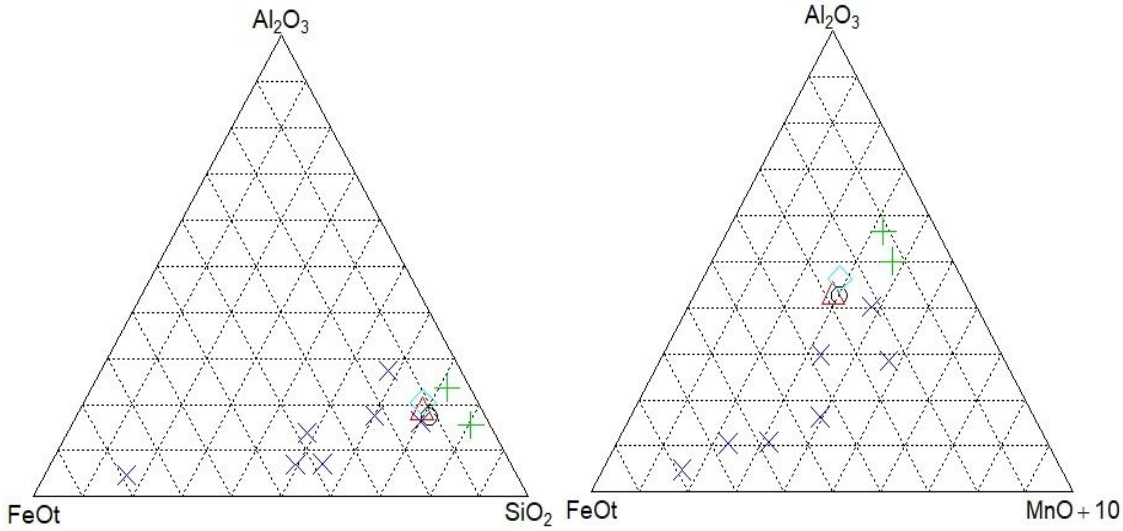

Figure 4.28 Ternary Diagrams of Fe_2O_3-Al_2O3-SiO_2 & MnO+10 discriminating plot for the Sed.-Carbonates and Vol-Sedimentary group of rocks. Legends as in Figure 4.31.

In Figure 4.28 the ternary diagram of Fe_2O_3-Al_2O_3-SiO_2 which shows Volcanic sedimentary rocks being more silica and Aluminium rich than the carbonate sedimentary rocks afterwards. Volcanic sedimentary group of rocks have higher concentrations of Al_2O_3, TiO_2, Sc, Zr, Th, Nb and RB relative to Carbonate sedimentary rocks Table. Higher concentrations of these elements reflect the presence of detrital components (Kalogeropoulos and Scott 1983, Spry et al. 2000 and Slack et al. 2009). A ternary plot of Fe-Al-Mn+10 is used to distinguish

Rock type	Group	TiO_2	Al_2O_3	Nb	Rb	Sc	Th	Zr
Serpentinite-dolomite	Sedimentary carbonate	0.184	4.262	1.11	3.32	2.12	<0.5	20.6
Serpentinite-dolomite	Sedimentary carbonate	0.122	2.938	2.17	5.66	5.31	0.91	42.0
Serpentinite-dolomite	Sedimentary carbonate	0.161	4.620	1.96	5.05	3.58	0.72	43.1
Serpentinite-dolomite	Sedimentary carbonate	0.372	9.171	4.71	13.0	15.8	1.38	73.2
Serpentinite-dolomite	Sedimentary carbonate	0.232	6.081	2.16	0.44	4.00	0.88	53.5
Serpentinite-dolomite	Sedimentary carbonate	0.150	3.529	1.73	10.9	2.84	0.66	26.7
Serpentinite-dolomite	Sedimentary carbonate	0.529	10.734	4.88	0.76	10.3	1.40	66
Amphibole gneiss	Volcsed	0.853	14.216	5.64	3.45	27.0	1.32	83.9
Biotite paragneiss-volc sed	Volcsed	1.014	14.909	6.85	6.56	32.8	0.50	86.9
Volc-sed	Volcsed	1.106	16.534	6.19	3.37	23.6	1.00	88.2
Calc-silicate rich felsic volcanic rock	Volcsed	0.862	17.645	9.15	17.7	28.4	2.13	112
Calc-silicate rich felsic volcanic rock	Volcsed	0.676	13.423	10.8	22.0	13.0	6.32	130

between hydrothermal and detrital inputs to these two sedimentary groups.

Fe and Mn chiefly due to the hydrothermal origin, while Al is essential of detrital origin. Volcanic sedimentary group of rocks are strictly close to one another with the same higher

concentrations of Al_2O_3. While Sedimentary carbonate rocks (serpentinite-Dolomites) have less Al_2O_3 comparatively higher MnO+10 and enriched FeO^t representing the presence of hydrothermal alterations in the sediments.

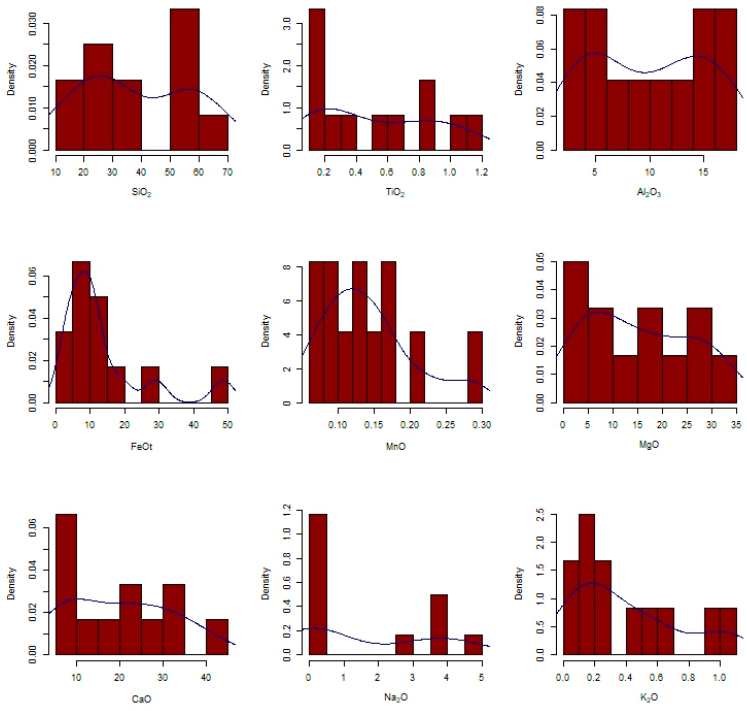

Figure 4.29 Histogram of the major elements of all the samples of both groups (carbonate sedimentary & Volcanic sedimentary) from the Vihanti Lampinsaari area.

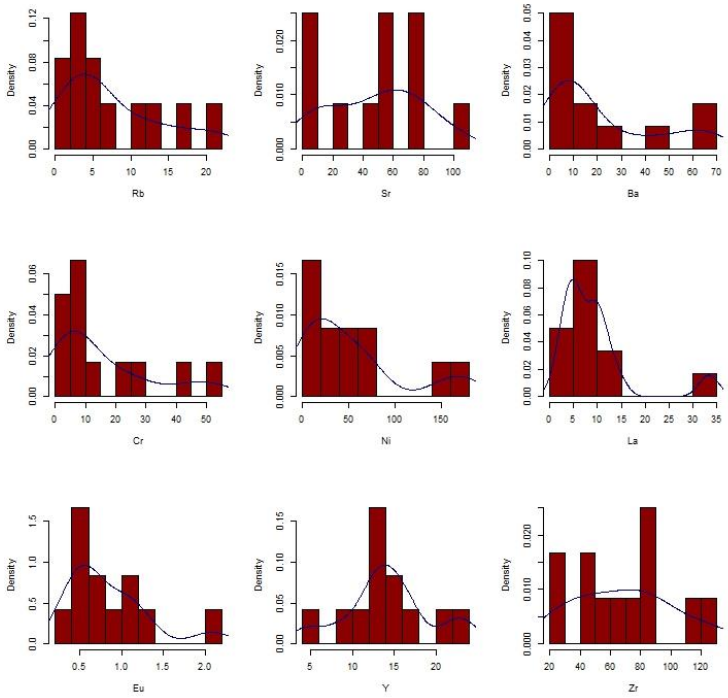

Figure 4.30 Histogram of the trace elements of all the samples of both groups (carbonate sedimentary & Volcanic sedimentary) from the Vihanti Lampinsaari area.

The reduction in the SiO_2 content with increasing CaO content tells the fact that rock has distinct silicate and carbonate fractions with variations in compositions. Carbonates fractions increases at the expense of silicates and vice versa. Positive relations between MgO and SiO_2 confirms MgO being part of the silicate fractions. Positive relations of SiO_2 and Al_2O_3 together with TiO_2, Fe_2O_3 and K_2O suggests the non-carbonates or silicate fractions are mainly aluminosilicates. In samples where Al_2O_3 is extremely low as in few samples Al_2O_3 = 2.9 and 3.5, (Table 1) clearly the SiO_2 cannot be introduced into the original sediment in aluminosilicate phases and was probably therefore in the traces of detrital quartz. All the carbonate sedimentary rocks are enriched in Pb, Sr and Ni due to the consistency these elements have with CaO, which is an important component of the Carbonate rocks. The enrichment of Sr in carbonates is due to the fact that Sr^2 substitutes for Ca^2 in calcium-bearing structures.

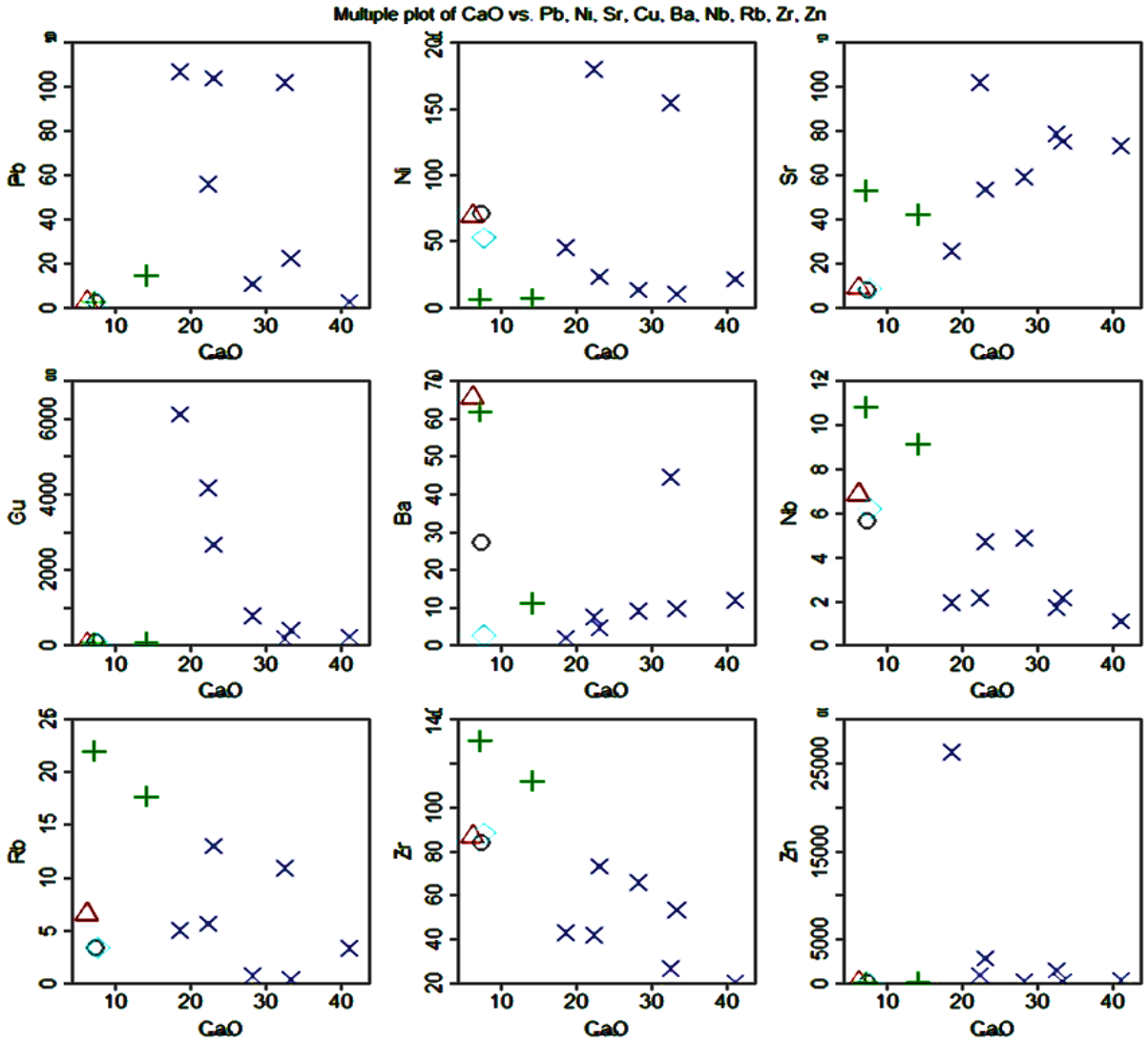

Figure 4.31 Degree of correspondence of Trace elements with CaO of the Vihanti Lampinsaari area. Legends as in Figure 4.27.

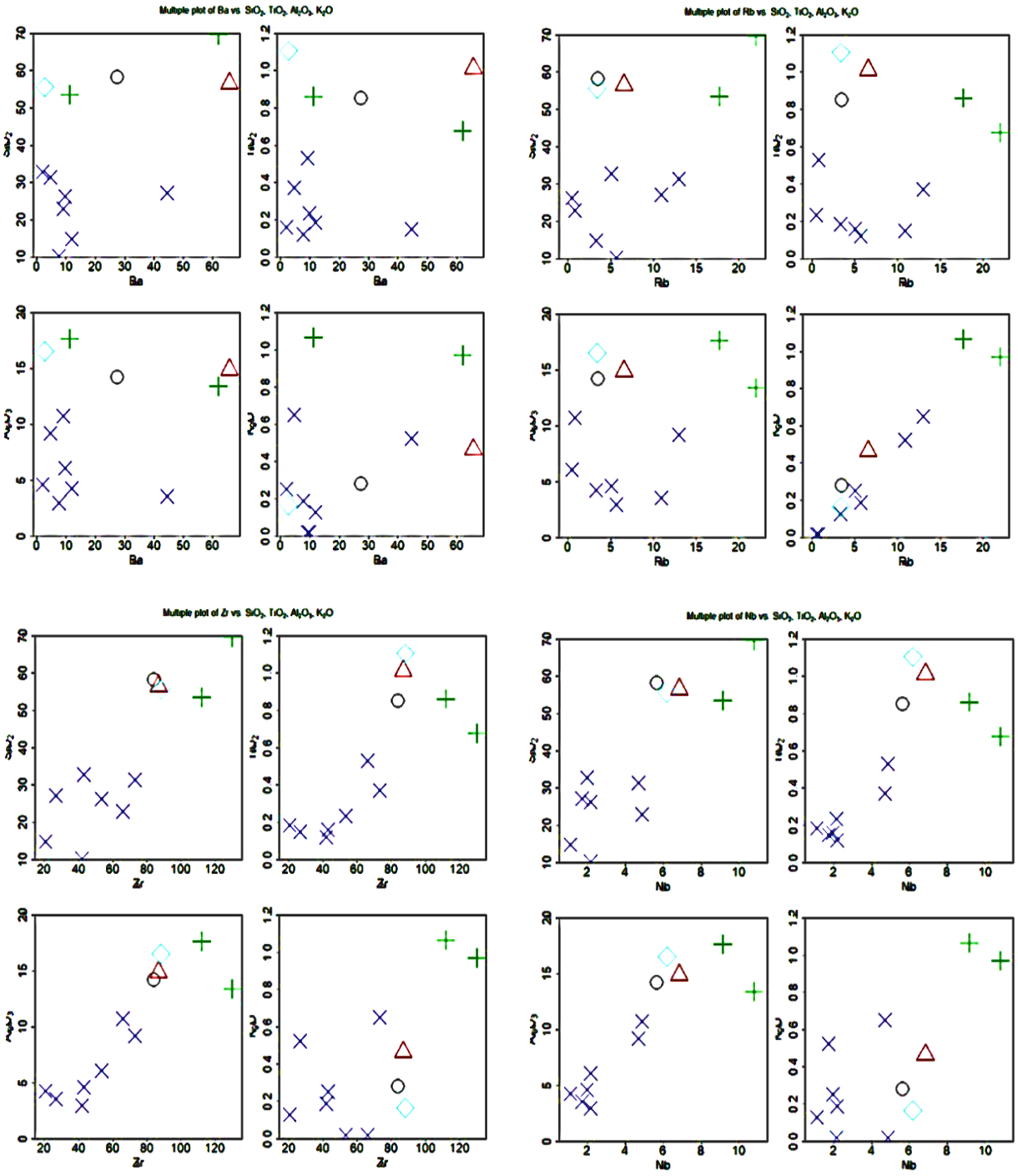

Figure 4.32 Binary plot showing degrees of positive inter-relationships displayed between various trace elements and the insoluble components of the Vihanti Lampinsaari metamorphosed Sed.Carbonates and Volcanic sedimentary rocks.

Other trace elements very notable Ba (dispersed), Nb and Rb tend to concentrate in the silicate fraction as analysed from the negative correlation with CaO (Figure 4.35) and have a positive relation with major insoluble residue component of the rock (Figure 4.35). The marked correlation between Zr and Al_2O_3 (Figure 4.36) seems reasonable to suggest much of the rock's Zr was not as a detrital component but may be formed parts of the rock's silicate fraction.

The strong positive relation between the trace elements and major elements shows the relevance of the minor aluminosilicate phase controlling both of their distributions. The positive correlation among Al_2O_3, TiO_2, Nb, Rb and Zr (Figure 4.36) taken to imply that all these elements are contained in different proportions of aluminosilicate phases. Positive inter-relationship amongst Ba, Rb and K_2O (Figure 4.36) shows the presence of K-bearing minerals in the aluminosilicate phases. Its already known that Ba and Rb retain in K-bearing minerals, while common K-bearing minerals are feldspars. However non-linear inter-relationship of Al_2O_3, Na_2O and CaO show that feldspar does not constitute a significant phase in the mineralogy of the rock rather quartz, talc, phlogopite or muscovite are the main aluminosilicate phases in the rock.

4.2.5. Geochemistry of sedimentary carbonates

Sedimentary carbonates are serpentinite-dolomites (7 samples) are further analysed with chondritic and primitive mantle normalized spider grams. Serpentinite-dolomite rock types are further categorized into mineralized to slightly mineralized types for differentiating the REE's behaviour in each one of the rock types.

All the samples of sedimentary carbonates (Figure 4.37) chondrite normalized rare earth elements (REE) plot show that all samples exhibit moderate to strong fractionation of light rare earth elements (LREE) over heavy REE (HREE) and slightly negative Eu anomaly in only two

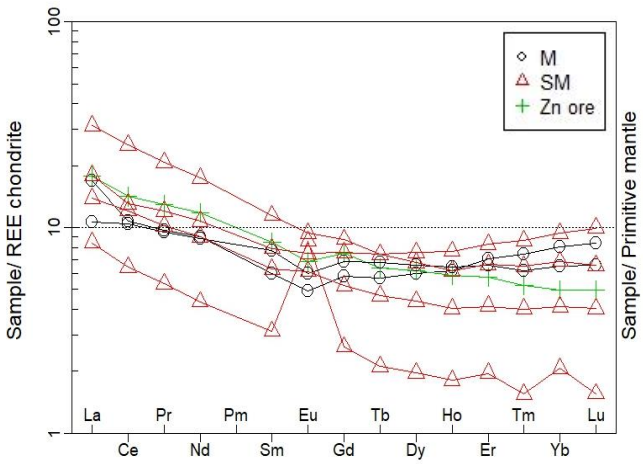

Figure 4.34 REE chondrite normalized (Boynton 1984) of the 7 rock samples of the Serpentinite-dolomite rock types of the Vihanti-Lampinsaari area. Legends as M=mineralized, SM= slightly mineralized and Zn ore.

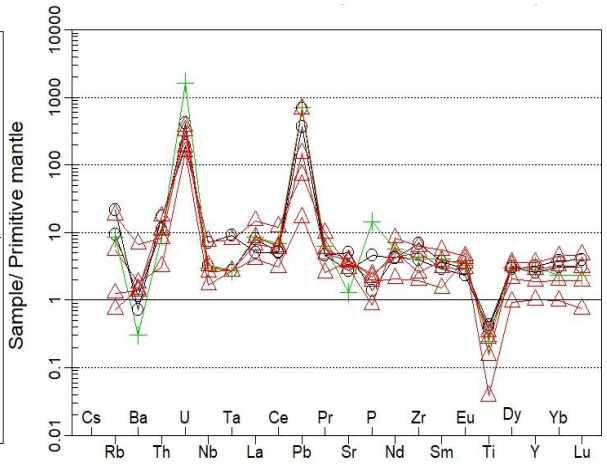

Figure 4.33 Sedimentary carbonates (serpentinite-dolomite rock types) normalized to Primitive mantle (McDonough and Sun 1995) values. Rock samples are from the Vihanti-Lampinsaari area. Legends as in Figure 4.38.

mineralized and one Zn ore sample. One slightly mineralized (SM) sample shows extreme positive Eu anomaly. Lowermost slightly mineralized sample bearing very low concentrations of LREE as well as HREE (Lu= below detection limit) with strong positive Eu anomaly suggests an abundance of calcium-rich clay minerals in the rock. Primitive mantle normalized sedimentary carbonates (Figure 4.38) shows a typical trend for Subduction related environments with Nb and Ta being immobile and Ti depletion and U and Pb enrichment due to crustal contaminations. Ba is mobile, however, depleted and it is controlled by the presence of K-feldspars and Micas.

4.2.6. Geochemistry of volcanic sedimentary rocks

Volcanic sedimentary rocks further analysed by subcategorizing them into their rock types. A distinct group with amphibole gneiss, biotite paragneiss and calc-silicate felsic volcanic rock types analysed in the chondritic and primitive mantle normalized spider plots.

All rock types have higher light rare earth elements relative to heavy rare earth elements (Figure 4.39). Two calc-silicate rock types are enriched in LREE's with minor negative Eu anomaly, while rest of the rock types behave much similar way in chondritic normalized plot. However, in the primitive mantle normalized spidergram these rocks being highly evolved in their composition, shows depletion in Ba and Ti, including Sr (Figure 4.39).

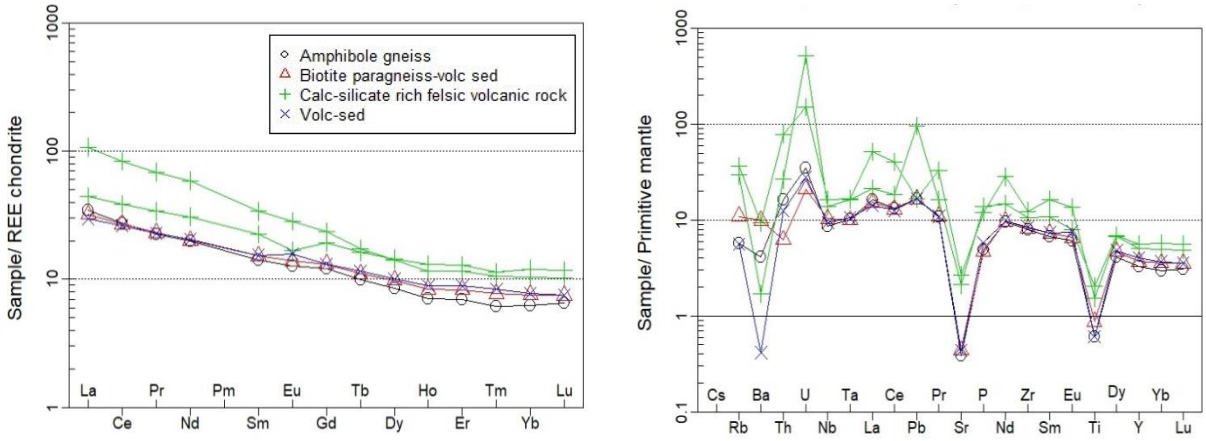

Figure 4.35 Volcanic sedimentary group normalized with Chondritic and Primitive mantle values. Rock types with legends described.

4.3. Geochemistry of Ore Deposits of Vihanti-Lampinsaari

Results of the 12 VMS ore samples have high Zn, Fe and Pb with minor Cu and Au consistent with sphalerite, pyrite, pyrrhotite and galena are seen in the whole rock data.

Table 4 Major constituents of the 12 rock samples of the ore deposits of Vihanti Lampinsaari area. All trace elements= ppm, except Au & Te =µg/kg

SAMPLE	Rock type	Group	Co	Cu	Zn	Ag	Au	Te	Cr	Fe	Mn	P	Pb	S
R1475 68,50-68,7	Pyrrhotite-pyrite	Sulphide ore	9.46	1330	48.0	2.08	66.2	265	26.5	272000	81.7	511	114	43600
R917 208-208,3	Pyrite-bearing quartzite	Sulphide ore	21.8	5770	258	2.35	5.00	902	6.26	99500	270	198	26.8	71500
R1457 139,35-139,55	Pyrrhotite-pyrite	Sulphide ore	64.0	1820	87.1	1.49	<1	61.7	10.0	196000	18.3	<50	42.6	72400
R1095 68,70-68,95	Pyrite ore	Sulphide ore	7.06	8350	968	10.1	35.7	440	5.43	*174000*	9.72	502	22.5	*170000*
R917 110,7-111,45	Zn-ore+dolomite	Zn ore	15.2	2590	65000	5.02	251	333	4.06	74400	550	770	762	2680
R1457 158,9-159,3	Skarn associated Zn ore	Zn ore	4.54	3520	25900	10.7	172	110	5.74	54700	1130	4900	745	24000
R2061 109,4-109,55	Calc-silicates + ore	Zn ore	7.54	2760	91600	9.34	30.9	57.3	5.21	58700	530	2680	584	29500
R2061 112-112,2	Calc-silicates + ore	Zn ore	3.25	437	12600	47.7	217	689	2.64	8530	341	453	10900	10100
R667 35,2-35,45	Zn ore	Zn ore	18.6	2200	263000	2.38	80.4	190	7.00	80800	985	333	366	24600
R1640 52,25-52,5	Skanr+Pb ore	Pb ore	44.8	3030	226	38.4	1460	12600	15.9	19600	31.1	320	11500	6760
R1095 64,3-64,5	Anthophyllite skarn+ore	Zn Cu ore	1.86	13200	16800	14.1	455	2660	11.1	42100	214	318	241	14100
R1457 145,5-146,1	Granite+mobilized Cu+Au	Mobilized	0.64	22500	794	32.4	4840	39.7	6.80	41800	452	191	79.1	28700

Silver (Ag) is negligible with an average of 14.6 ppm as analysed from the 12 samples (Table 1) so does the Pb and Co (average = 16). However, Pb is high in two samples R2061 112-112.2 & R1640 52.25-52.5 with Pb concentrations of 10900 and 11500 ppm respectively (Table 4).

The ore samples exhibit sub-parallel patterns while absolute concentrations vary significantly. All REE are slightly enriched relative to chondrite and LREE are higher than those for HREE, except the Fe ore samples which have a flat trend in LREEs and HREEs. Scattered trends of the chondrite-normalized REE patterns may have resulted from the high fluid/rock ratios and/or diverse REE behaviour, consistent with secondary mineral assemblages that contain highly deformed and metamorphosed calc-silicates, dolomites and quartzites. Samples exhibiting scattered trends are more likely to have lost primary textures than the samples with sub-parallel tendency due to higher fluid/rock ratios.

Zinc bearing ore samples and one lowermost Fe-ore have positive Eu anomaly (Figure 4.40) while rest of the samples referred to as Fe ore, mobilized ore, Pb and Zn-Cu ores have negative Eu anomalies. Eu depletion may result from the dissolution of Eu-rich mineral phases by hydrothermal fluids (J. Lewis et al. 1997). Eu anomalies occur parallel to depletion in Na_2O and CaO, which is due to partially in response to weathering of plagioclase, where most of the

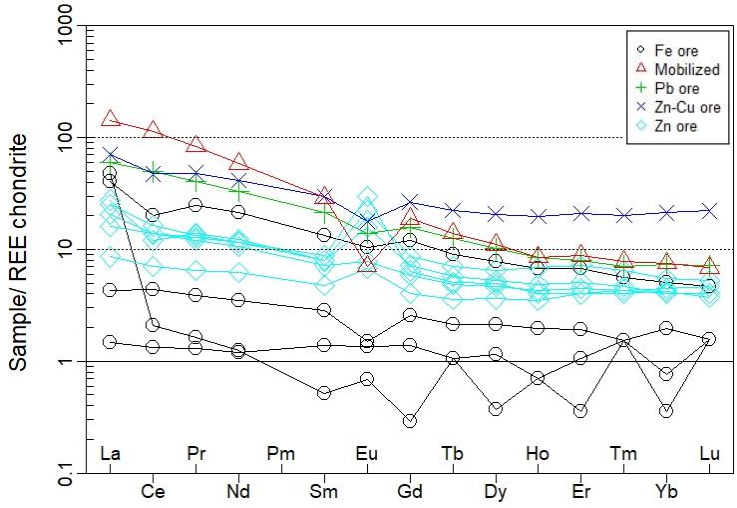

Figure 4.36 Chondrite normalized (Boynton 1984) 12 ore samples of the Vihanti Lampinsaari area.

Eu is hosted and indicating felsic source rocks (Grant et al. 2018). The positive Eu* anomaly of Zn-bearing host rocks of calc-silicates and dolomitic samples may be explained by the alteration of plagioclase in the parent rock. Moreover, the Zn-bearing host rocks having higher concentrations of Sr^{+2} content indicate that Eu^{+2} was possessed by hydrothermal albite or taken up by the suitable hosts in the altered rock (Kamineni 1986). Eu is also divalent under reducing conditions and very reducing water contains Eu^{+2}. These conditions are also perfect for the occurrence of calcite in the altered samples formed from parent rock. The positive and nearly positive Eu anomalies sometimes related to ore mineralization while strongly negative Eu indicates late-stage mineralization processes. Therefore positive anomalies may act as good indicators of ore bearing rocks (Grant et al. 2018).

Almost all the samples show no Ce anomaly except for few samples which have weak positive anomalies (Figure 4.41). Ce is only fractionated from other rare earth elements owing to the formation of Ce^{+4} under highly oxidizing conditions: the other REE remain trivalent (Braun et al. 1990, Class and Le Roex 2008). These conditions only occur in the surficial conditions under oxidizing seawater and not present in the deep mantle. Oxidized seawater is depleted in Ce while oxic-sediments are enriched with respect to Ce. While in less oxidized seawater, Ce

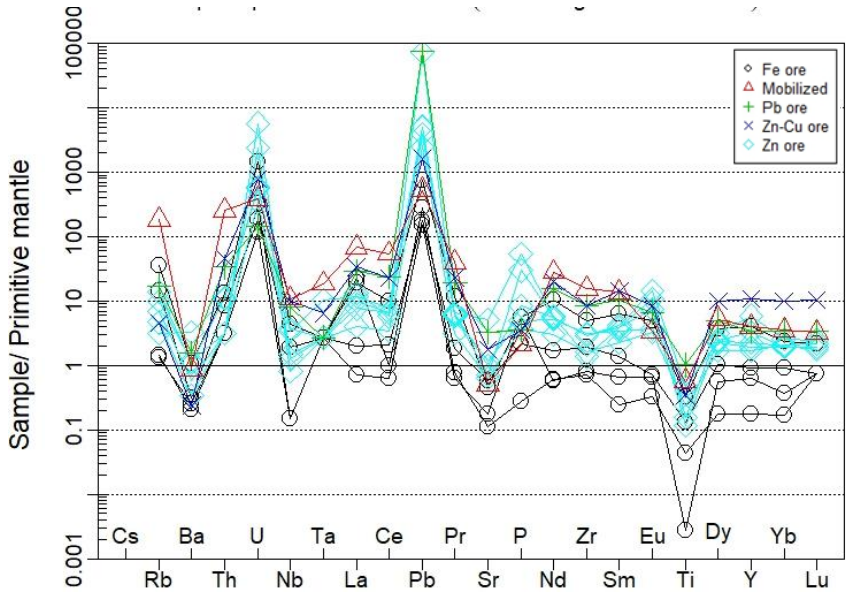

Figure 4.37 Primitive mantle normalized Spider plot (McDonough and Sun 1995) of the 12 ore samples' trace elements behaviour of Vihanti-Lampinsaari area.

in sediments gets mobilized and Ce releases in the water column and results in less negative to a positive anomaly in seawater (Çelik Karakaya et al. 2012).

High field strength elements (HFSE) mobility results due to the number of factors, including P-T conditions. The solubility of HFSE enhances by increasing pressure and temperature as well as highly alkaline (8-12) or acidic (<4) pH conditions (Barnes and O'neil 1969, Van Baalen 1993, Veyland et al. 2000). Under eclogite conditions, Ti mobility is probably limited due to restricted fluid flow in low-permeability rocks (Van Baalen 1993). HFSE shows mobile

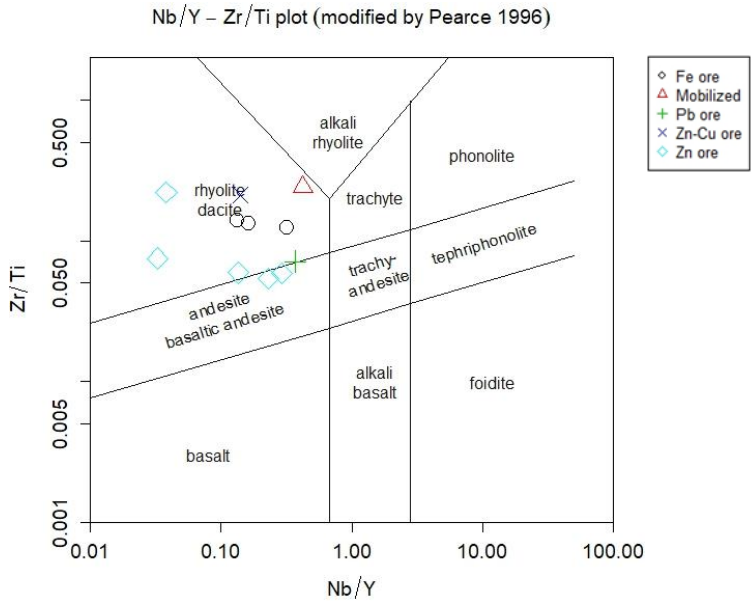

Figure 4.38 Nb/Y vs Zr/Ti plot (modified by Pearce 1996) of the 12 ore-bearing samples from the Vihanti-Lampinsaari area. Legends as mentioned.

behaviour except for Ti (Figure 4.41), which is due to the reason of high-grade metamorphic rocks in Vihanti.

HFSE contents of all the samples are either depleted or enriched relative to the primitive mantle, exhibiting slightly different patterns suggesting that they are all not originating from the same source rock. HFSE contents of the Fe-ore bearing rock samples are the most depleted ones compared to the other ore bearing rock samples.

The high Y/Ho ratios are interpreted to imply the contribution of seawater (Bau 1996). The Y/Ho ratios of all studied samples scatter between the chondrite and seawater field indicating the significant role by hydrothermal fluids originating through seawater during ore genesis (Figure 4.43). Seawater which is naturally low-temperature aqueous solution, characterized by Y/Ho ratios between 44 and 74. The Y/Ho ratios of seawater are significantly higher than those of chondrites or shales (Bau 1996). These samples show huge variation in their Y/Ho ratios comparatively to the sedimentary rock samples discussed previously having chondritic characteristics and interpreted to lack the seawater contribution.

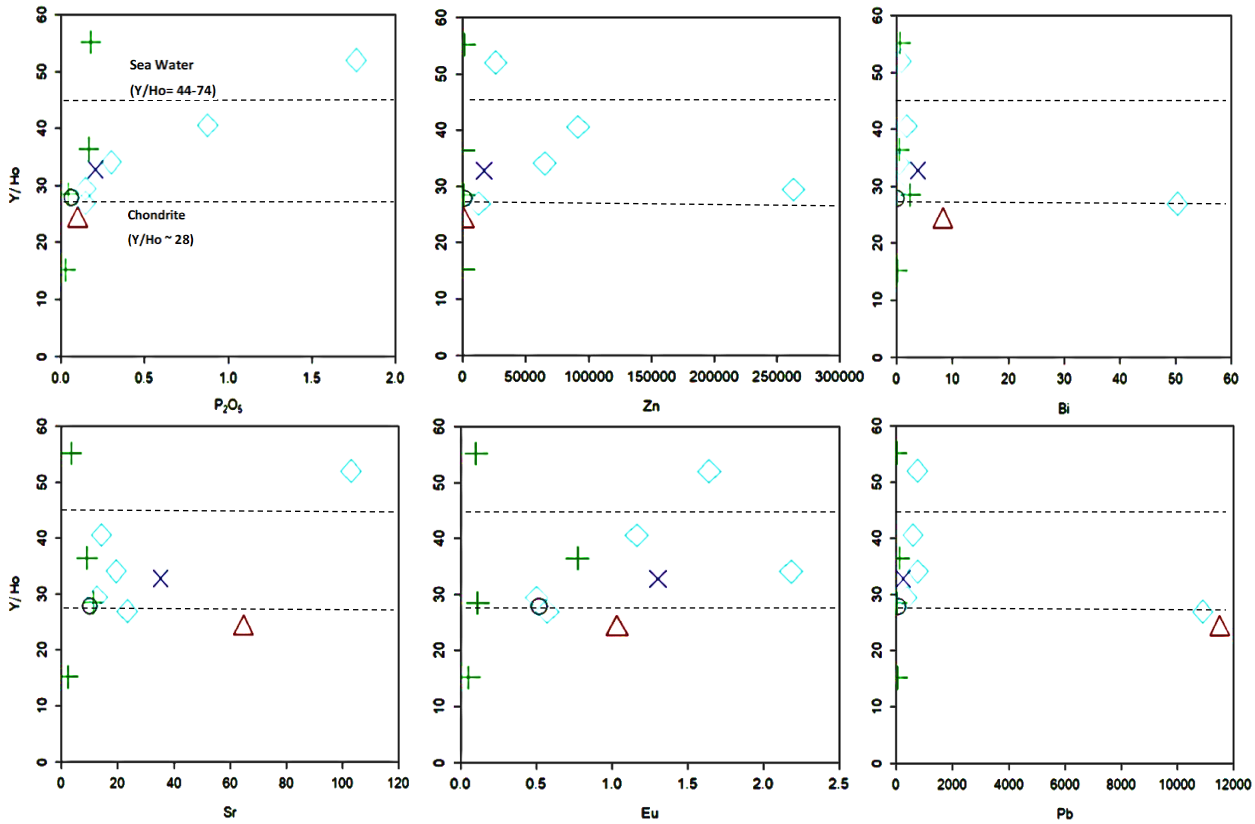

Figure 4.39 Bivariate plots of Y/Ho versus selected trace elements in the ore-samples from the Lampinsaari region. Legends as in Figure 4.38.

5. PETROGRAPHY

In total 25 thin sections were selected from the two drill cores R851 and R1457 of the two profile logs PL106 and PL130 respectively (Figure 3 and 4). Thin sections discussed in groups of Sedimentary, felsic metavolcanic rocks, sedimentary carbonates and volcanic sedimentary rock types and ore bodies, which are further subcategorized into rock types presented in each group.

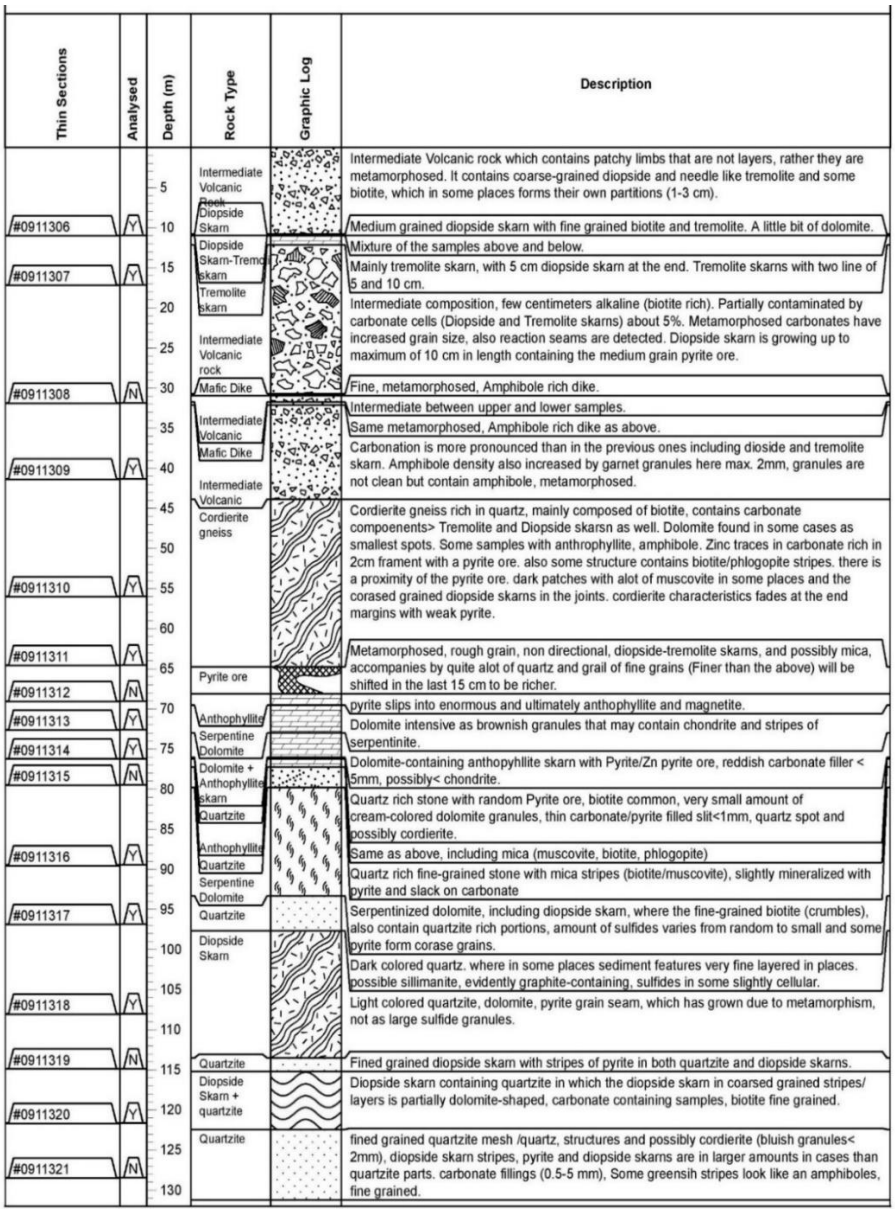

Figure 3 Drill hole R851 with a description of rock types at various depths along with thin sections analysed.

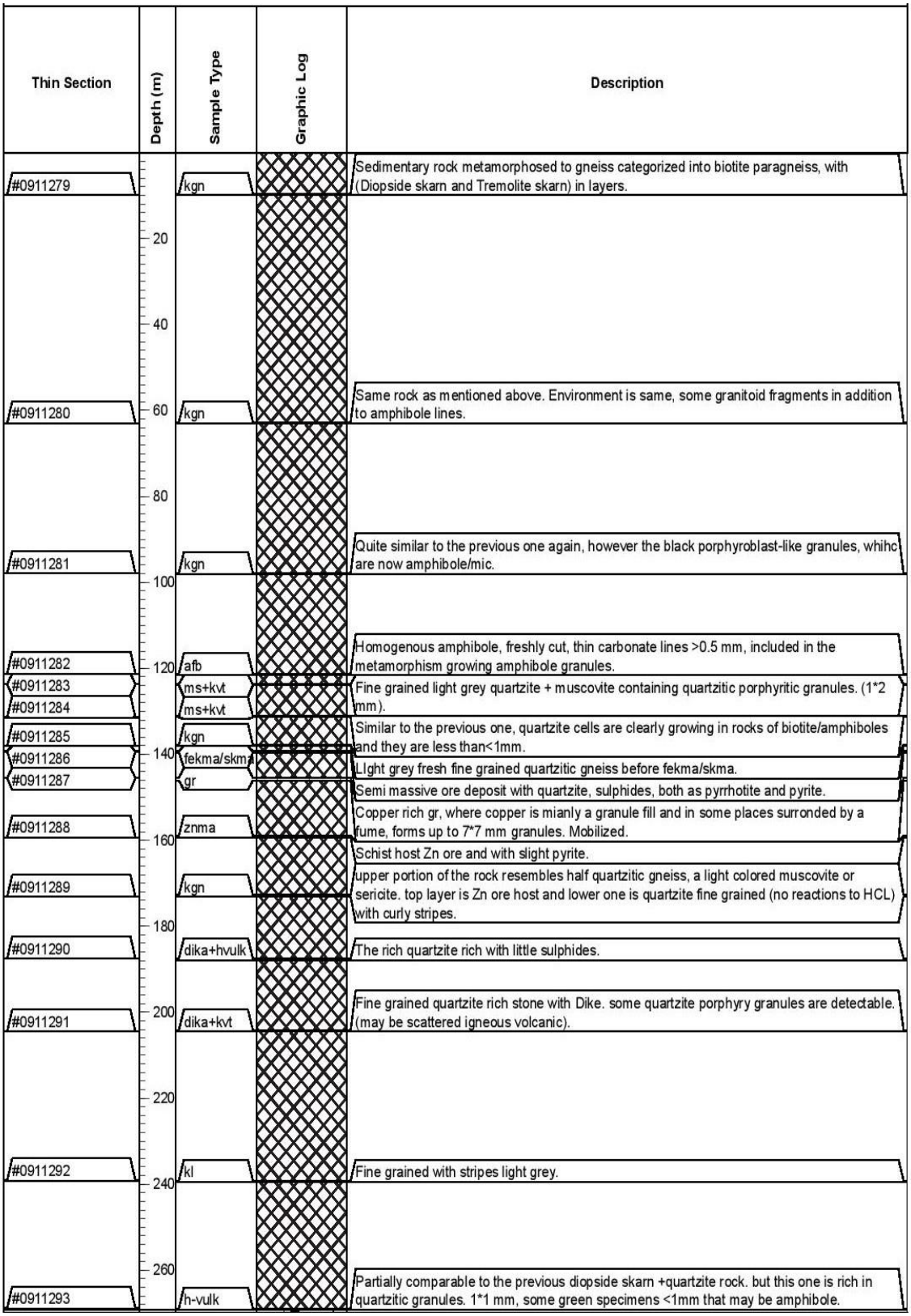

Figure 4 Drill hole R1457 with a description of rock types at various depths along with thin sections analysed.

PROFILE	DRILL HOLE	NUMBER OF THIN SECTIONS WITH THEIR GROUPS AND ROCK TYPES										
		SEDIMENTARY		FELSIC META-VOLCANIC		SED.CARBONATE & VOLCANIC SED.				ORE BODIES		
		THIN SECTION (S)	ROCK TYPE	THIN SECTION (S)	ROCK TYPE	SEDIMENTARY CARBONATES		VOLCANIC SEDIMENTARY		THIN SECTION (S)	DEPOSIT	
						THIN SECTION (S)	ROCK TYPE	THIN SECTION (S)	ROCK TYPE			
PL 106	R 851	*911306*	*Calc-Silicate Paragneiss*	*911307*	*Qtz-Feldspar schist*	*911313*	*Serpentinite-Dolomite*					10
		911318	*Calc-Silicate Paragneiss*	*911309*	*Qtz-Feldspar schist*	*911316*	*Serpentinite-Dolomite*					
		911320	*Calc-Silicate Paragneiss*	*911310*	*Cordierite Gneiss*							
		911317	*Quartz + Sulfides*	*911311*	*Cordierite Gneiss*							
PL 130	R 1457	*911279*	*Biotite Paragneiss*	*911283*	*Qtz-Feldspar schist*			*911290*	*Calc-Silcate-Felsic Vol.*	*911288*	*Skarn Associated Zn-ore*	15
		911280	*Biotite Paragneiss*	*911284*	*Qtz-Feldspar schist*			*911291*	*Calc-Silcate-Felsic Vol.*	*911286*	*Pyrrhotite-Pyrite*	
		911285	*Biotite Paragneiss*	*911293*	*Qtz-Feldspar schist*			*911281*	*Biotite-Paragneiss*	*911287*	*Granite + Cu&Au Mobilized*	
		911289	*Biotite Paragneiss*					*911282*	*Volcanic Sedimentary*			
		911292	*Biotite Paragneiss*									
Total thin sections		9		7		2		4		3		25

Table 5 Classification of thin sections into groups and rock types.

5.1. Sedimentary Rocks

In total nine thin sections of sedimentary rocks from drill holes R851 and R1457, including distinct rock types of calc-silicate paragneiss, sulphide-bearing quartzites and biotite paragneiss were examined. Each rock type is discussed separately by using both transmitted and reflected light microscopy.

5.1.1. Calc-Silicate Paragneiss:

Three thin sections of calc-silicates from the drill hole R851 and one rich in quartz and sulphides were examined (Table 5). The main minerals in the calc-silicate paragneiss are diopside, hornblende, amphibole, quartz and plagioclase with variable amounts of feldspars,

tremolites, biotite and chlorite. Chlorite is the alteration of the hornblende. Large quartz veins are observed in one thin section (#0911320) Figure 6 C&D. Sericitization of the feldspars is commonly observed and distinguishing feature of K-feldspars from the quartz minerals. Accessory minerals are zircon, apatite, carbonate, titanite, tremolite and in some cases diopside. The rocks are almost non mineralized to slightly mineralized pyrrhotite, chalcopyrite and pyrite present as sulfide minerals. Some of the samples exhibit strong orientation representing paragneissic nature of the rocks.

Thin section #0911317 is quartzite enriched in sulfide minerals. Figure 6 E&F. Main minerals besides quartz are abundant plagioclase, phlogopite and mica minerals. Quartz is anhedral and very small in size.

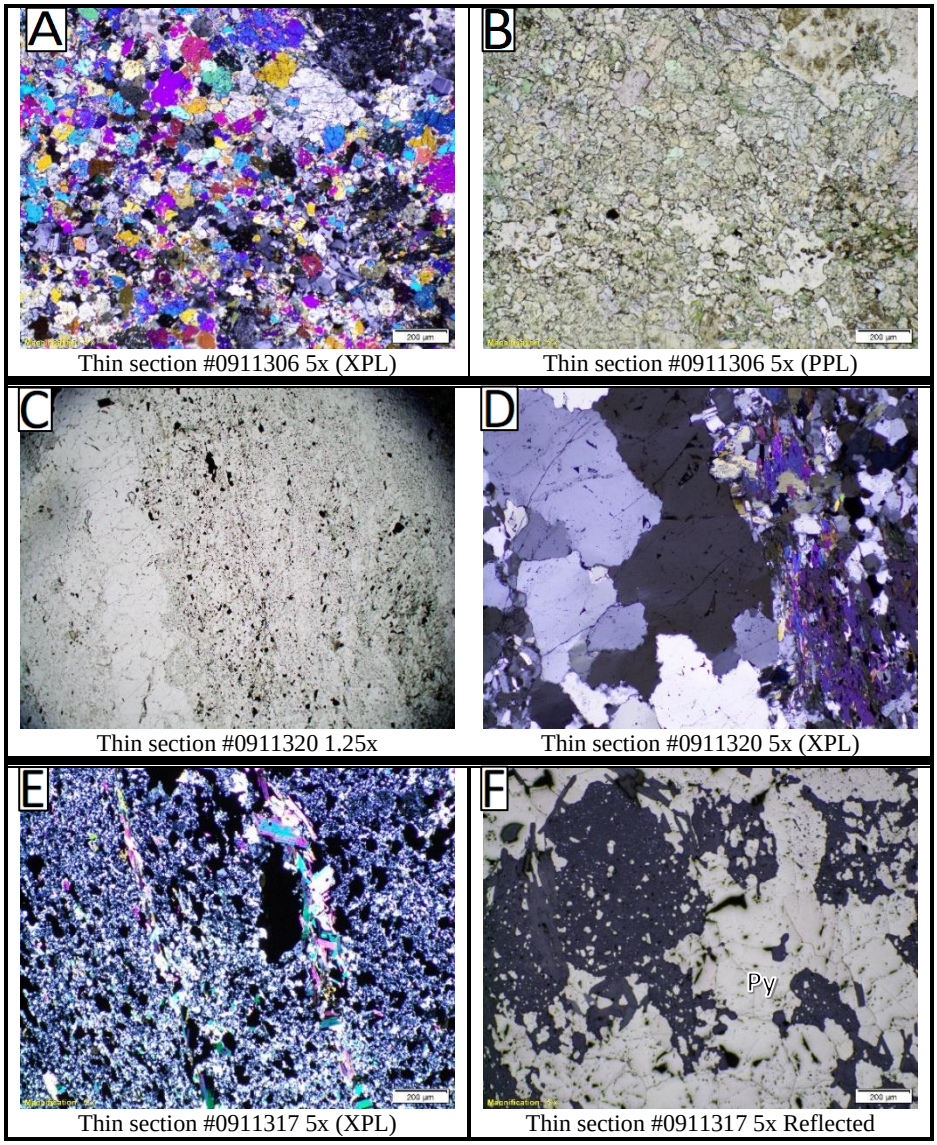

Thin section #0911306 5x (XPL) | Thin section #0911306 5x (PPL)

Thin section #0911320 1.25x | Thin section #0911320 5x (XPL)

Thin section #0911317 5x (XPL) | Thin section #0911317 5x Reflected

Figure 6 A, B) Photomicrographs of the typical calc-silicate paragneiss in the study area. C) A calc-silicate paragneiss with quartz veins at the left margin. D) The same thin section as "C" at the borders of quartz veins. E, F) Mainly enriched in quartz (E) and sulphides in the reflected microscope(F). All calc-silicate thin sections including quartz with sulphides Pyrite (Py) are taken from drill hole R851.

5.1.2. Biotite Paragneiss:

Five thin sections categorized into biotite paragneiss rock types under the sedimentary group of rocks were taken from drill hole R1457. Main minerals in biotite paragneiss are quartz, plagioclase and biotite and in some cases tremolite. Accessory minerals are K-feldspars, apatite, epidote, diopside, titanite and carbonates. Quartz percentage varies and occur as small anhedral grains or phenocrysts in some samples. A distinct feature of paragneiss is the presence of biotite in layers. Chlorite and sericite are the alteration products of biotite and feldspars respectively.

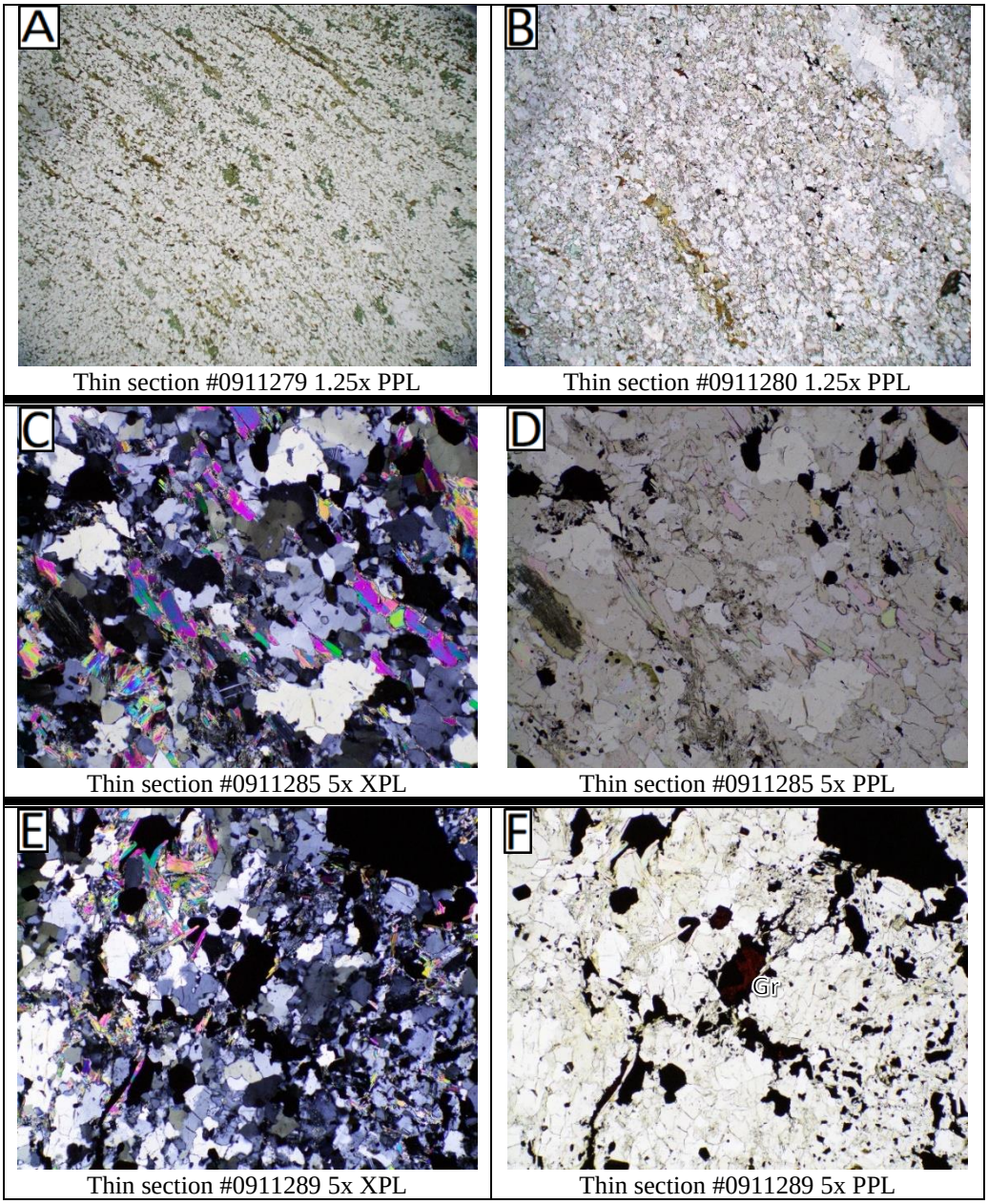

Figure 7 Photomicrographs of the typical biotite paragneiss in the study area. First two images represent the biotite paragneiss nature of the rock (A, B). Thin section #0911285 is observed in both plane-polarised (PPL) and crossed-polarised microscope (XPL) and shows strained quartz along with biotite and amphiboles (C, D). Thin section #0911289 a biotite paragneiss also observed in both PPL and XPL representing in the centre a garnet (Grt) mineral with isotropic nature.

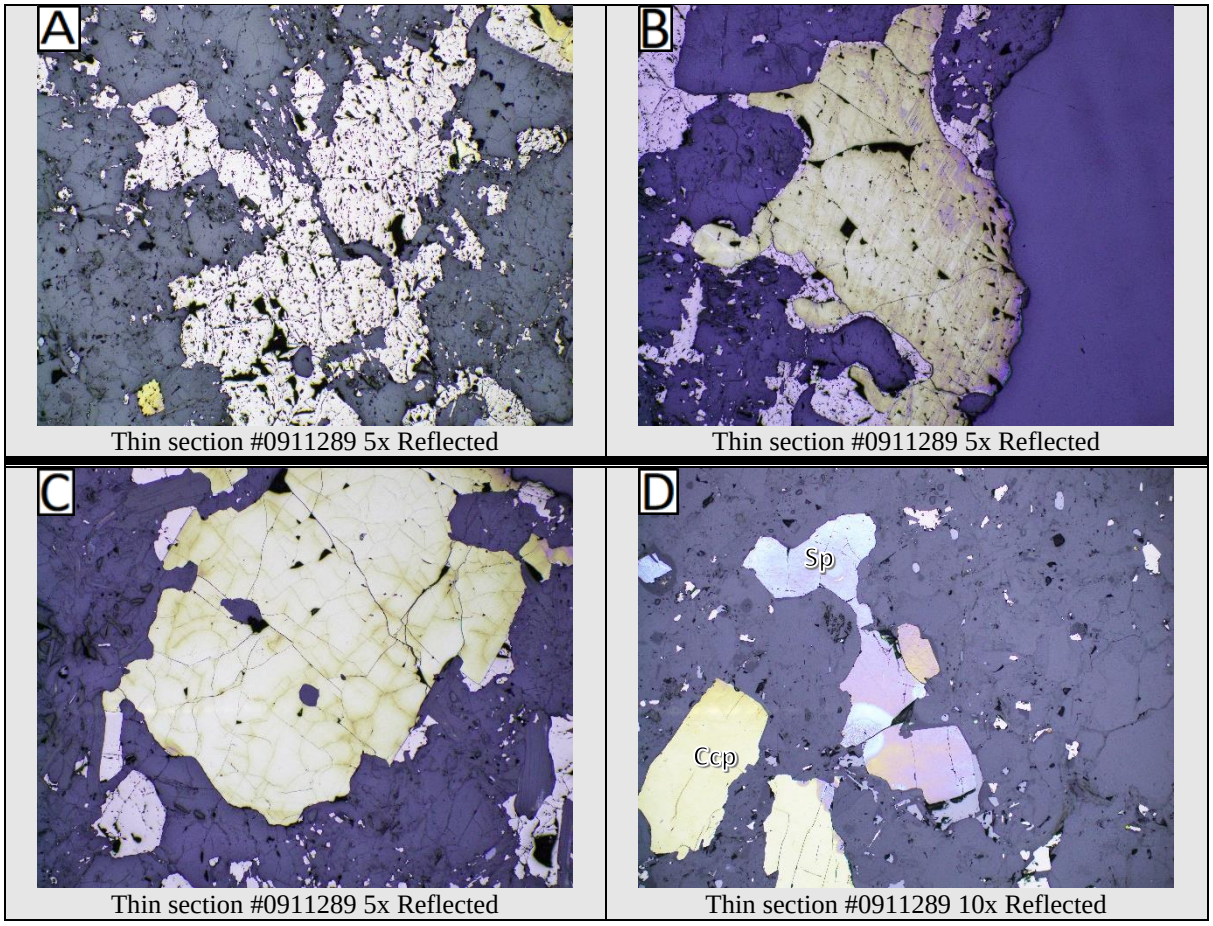

Figure 8 Photomicrographs of the mineralized thin section #0911289 classified as biotite paragneiss rock in the sedimentary group of rocks in the reflected microscope. All images are at 5x magnification in reflected microscope except one (D) which is at 10x magnification. Common minerals are iron sulphides and minor Sphalerite (Sp) and-Chalcopyrite (Ccp).

These biotite paragneiss rocks are bordered either by quarzitic or calc-silicate rocks. In the contact zones, there are more garnet, quartz or calc-silicate minerals than elsewhere. Ore minerals are mostly iron sulphides and, in some cases, sphalerite and chalcopyrite were observed in thin section #0911289-R1457 (Figure 8).

5.2. Felsic Meta Volcanic Rocks

Felsic metavolcanic rocks from the drill holes R851 and R1457 were examined (Table 1). Quartz-feldspar schist (5 thin sections) and cordierite gneiss (2 thin sections) samples were examined in detail.

5.2.1. Quartz-Feldspar Schist

All thin sections in this rock type composed of quartz and feldspars as major constituents along with varying amounts of phlogopite/biotite and sericite in well-developed layers.

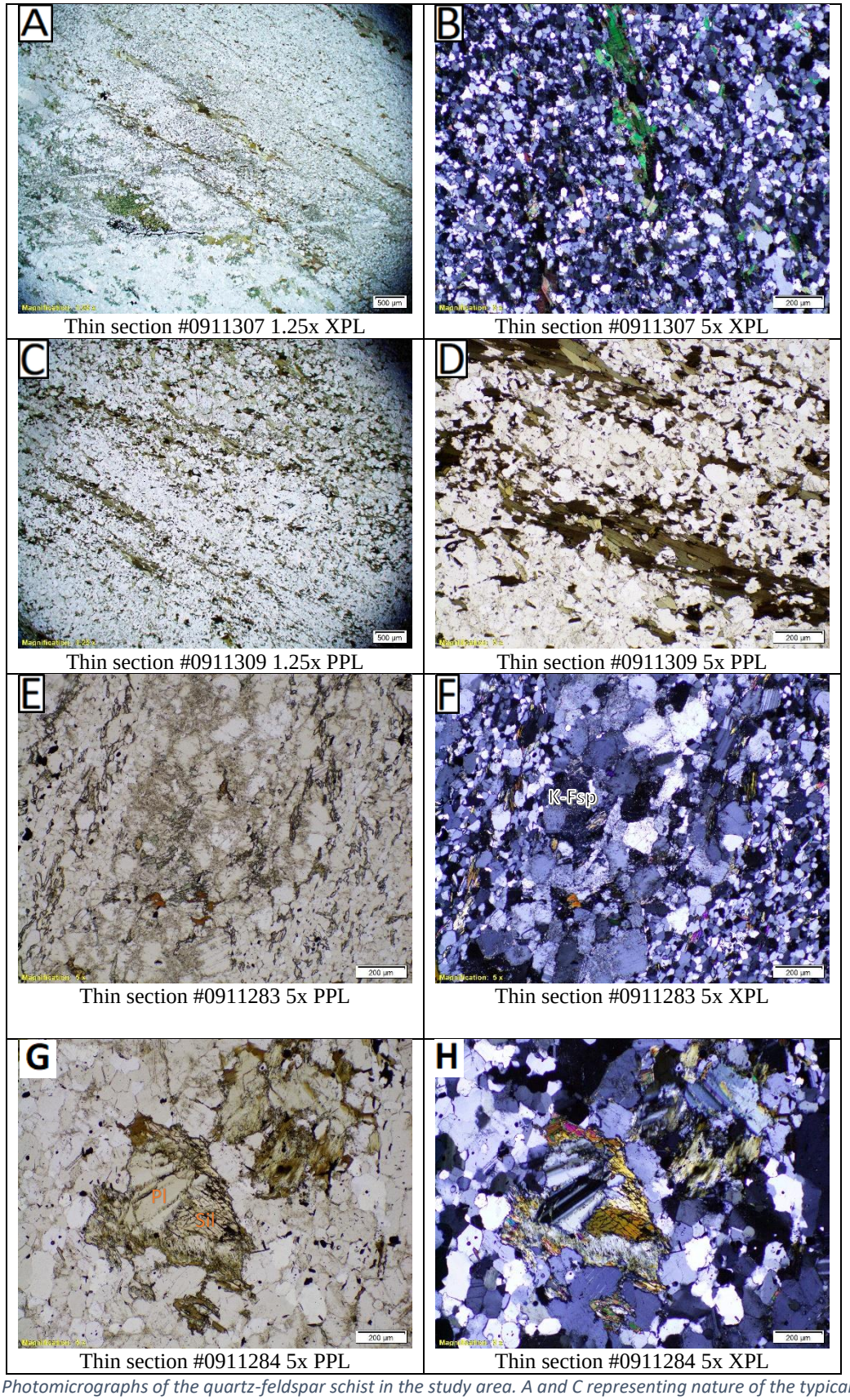

Thin section #0911307 1.25x XPL | Thin section #0911307 5x XPL

Thin section #0911309 1.25x PPL | Thin section #0911309 5x PPL

Thin section #0911283 5x PPL | Thin section #0911283 5x XPL

Thin section #0911284 5x PPL | Thin section #0911284 5x XPL

Figure 8 Photomicrographs of the quartz-feldspar schist in the study area. A and C representing nature of the typical quartz-feldspar schist. B and D show the cross-polarized and plane-polarized light microscopic images of quartz grain and phlogopite along with biotite minerals respectively. In E and F, K-feldspar (K-Fsp) is easily identified with its cloudy nature and alterations inside the mineral. G and H, in the centre sillimanite-needle like fibrolite (Sil), plagioclase (Pl) with twinning inside and diopside-simple and lamellar twinning together are noticeable in both PPL and XPL. Ore minerals are not present in any of the thin section in this category.

Diverse quantities of sillimanite, diopside/tremolite, titanite, rutile and minor iron sulphides encountered. Accessory minerals are zircon and apatite. The amount of plagioclase differs in each thin section however the amount of quartz is mostly under 60 vol%. K-feldspars are in minor amount however they are easily distinguished from quartz due to alterations at the margins. These rocks are not mineralized.

5.2.2. Cordierite Gneiss

Along with cordierite, thin sections contain quartz, plagioclase, mica and small amounts of potassium feldspars, sillimanite, apatite, zircon, rutile and titanite. Phlogopite is the most common of the micas. However, the presence of muscovite, biotite, chlorite and talc is also noticeable. One thin section of cordierite gneiss is mineralized, and another slightly mineralized with iron sulphides (Figure 9. E & F).

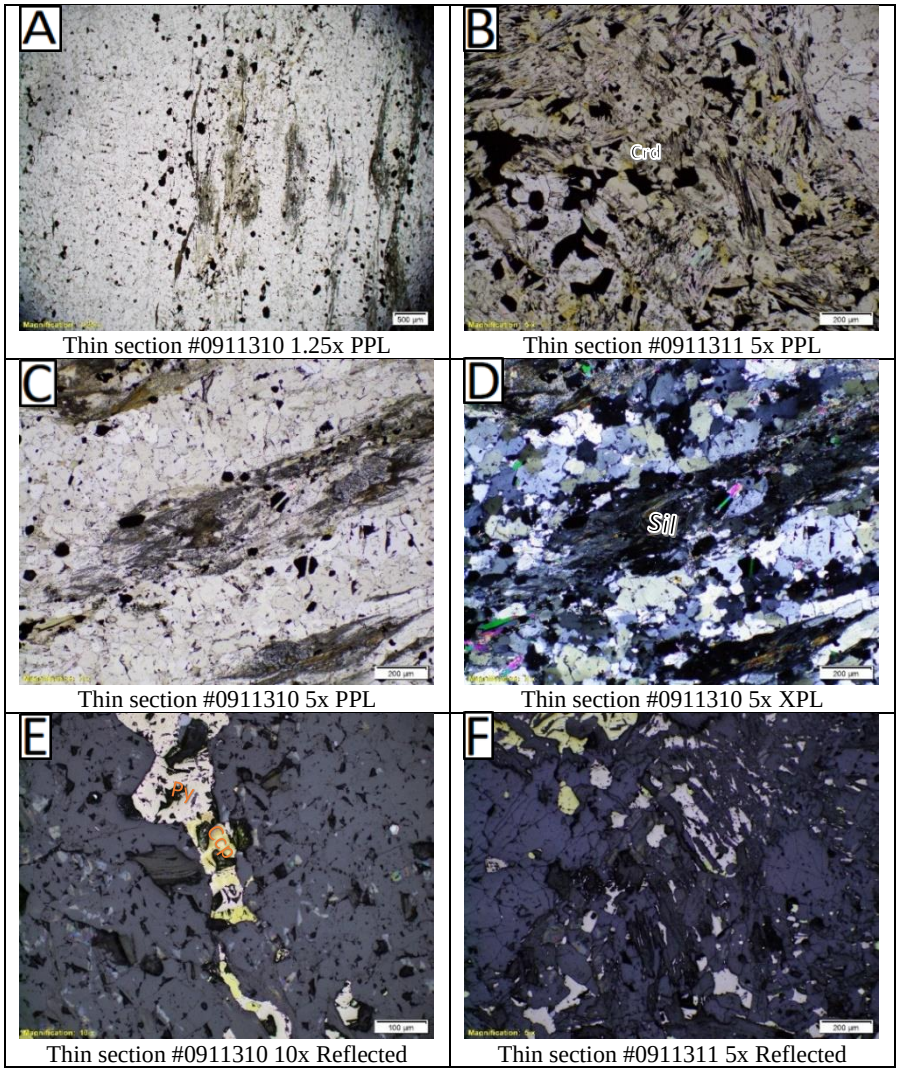

Thin section #0911310 1.25x PPL | Thin section #0911311 5x PPL

Thin section #0911310 5x PPL | Thin section #0911310 5x XPL

Thin section #0911310 10x Reflected | Thin section #0911311 5x Reflected

Figure 9 Photomicrographs of the cordierite gneiss in the study area. A) Representing typical major minerals concentrations in cordierite gneiss. B) Plane polarized light-yellow coloured cordierite (Crd) is noticeable due to magnesium enrichment, however, it stays colourless in iron-rich varieties. No good crystal face edges present, and alteration is common. C) and D) Masses of high-relief fibrous sillimanite (Sil) with clear crystals of quartz present in both PPL and XPL respectively. In reflected light microscopy both thin section E & F examined and have main minerals of chalcopyrite (Ccp) and pyrite (Py).

5.3. Sedimentary Carbonates and Volcanic Sedimentary

It is quite noticeable under the petrographic study of these rock types, that they have excessive carbonates and volcanic fragments, respectively. They both are also clearly sedimentary rocks by texture, hence the category names *sedimentary carbonates* and *volcanic sedimentary rocks*. In total 6 thin sections (drill holes R851 and R1457) consisting of sedimentary carbonates (2-thin sections) and volcanic sedimentary (4-thin sections) were examined in detail.

5.3.1. Sedimentary Carbonates

Two thin sections under this category comprise excessive dolomite and serpentine which is the altered end-product of olivine hence the name given is serpentinite-dolomite. Along with carbonate minerals, varying amounts of diopside, tremolite, olivine and garnet are present. Chlorite and apatite occur sporadically. Both thin sections are slightly mineralized and pyrrhotite occurs as dissemination throughout the rock.

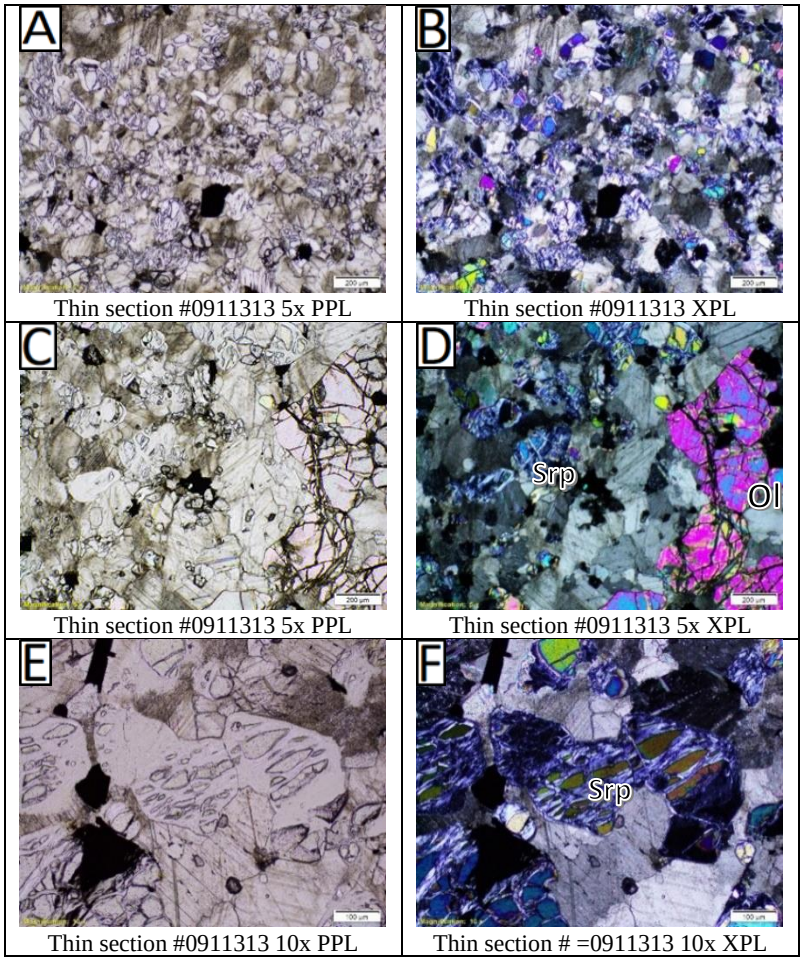

Thin section #0911313 5x PPL | Thin section #0911313 XPL

Thin section #0911313 5x PPL | Thin section #0911313 5x XPL

Thin section #0911313 10x PPL | Thin section # =0911313 10x XPL

Figure 10 photomicrograph of the serpentinite-dolomite in the study area. A) and B) representing major elements of serpentinite along with dolomitic crystals in both PPL (A) and XPL (B). C) and D) represents carbonates, olivine (Ol) and serpentinite (Srp) all together in both PPL and XPL. E) and F) serpentinite at 10x magnification in the centre with olivine fragments inside.

5.3.2. Volcanic Sedimentary

Since the volcanic material in these rocks is sedimentary in origin. they are included in this category. Major rock types are biotite paragneiss (2 thin sections) and calc-silicate rich felsic volcanic sedimentary (2 thin sections) (Table 1).

Two thin sections of the volcanic sedimentary group being in biotite paragneiss rock type comprise major minerals like quartz, plagioclase feldspars along with orthoclase as minors and biotite. Accessory minerals are apatite, diopside, titanite. These thin sections are not mineralized at all.

Two other thin sections in the volcanic sedimentary group represent calc-silicate rich felsic volcanic rock types. Main minerals identified in these thin sections are diopside, amphibole, quartz and plagioclase, and some variable amounts of feldspars, tremolites and biotite and chlorite. Feldspar sericitization is observed in one thin section #0911281. Rocks are not mineralized at all.

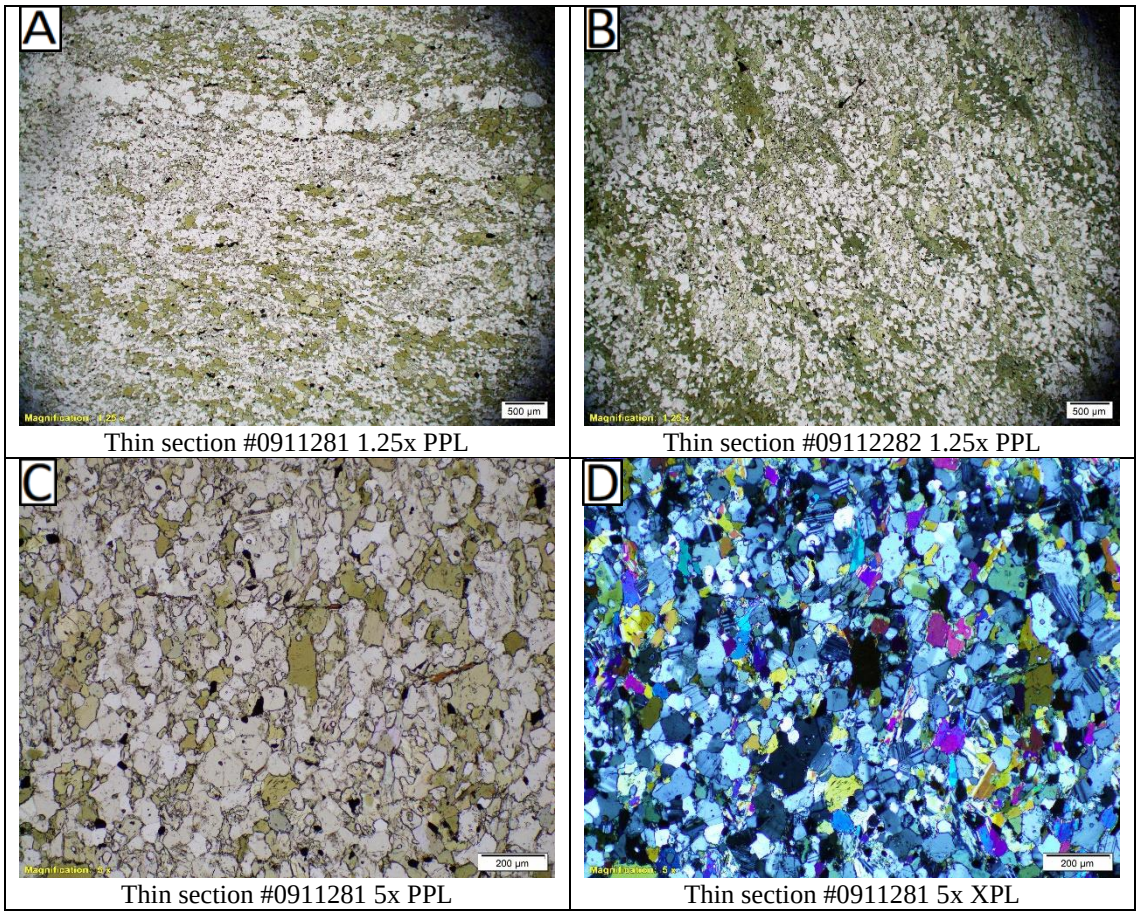

Thin section #0911281 1.25x PPL | Thin section #09112282 1.25x PPL

Thin section #0911281 5x PPL | Thin section #0911281 5x XPL

Figure 11 Photomicrographs of the biotite-paragneiss in the study area. A) and B) are at 1.25x magnification for both thin sections in this category of rock type. C) and D) at 5x magnification of typical biotite paragneiss at both PPL and XPL.

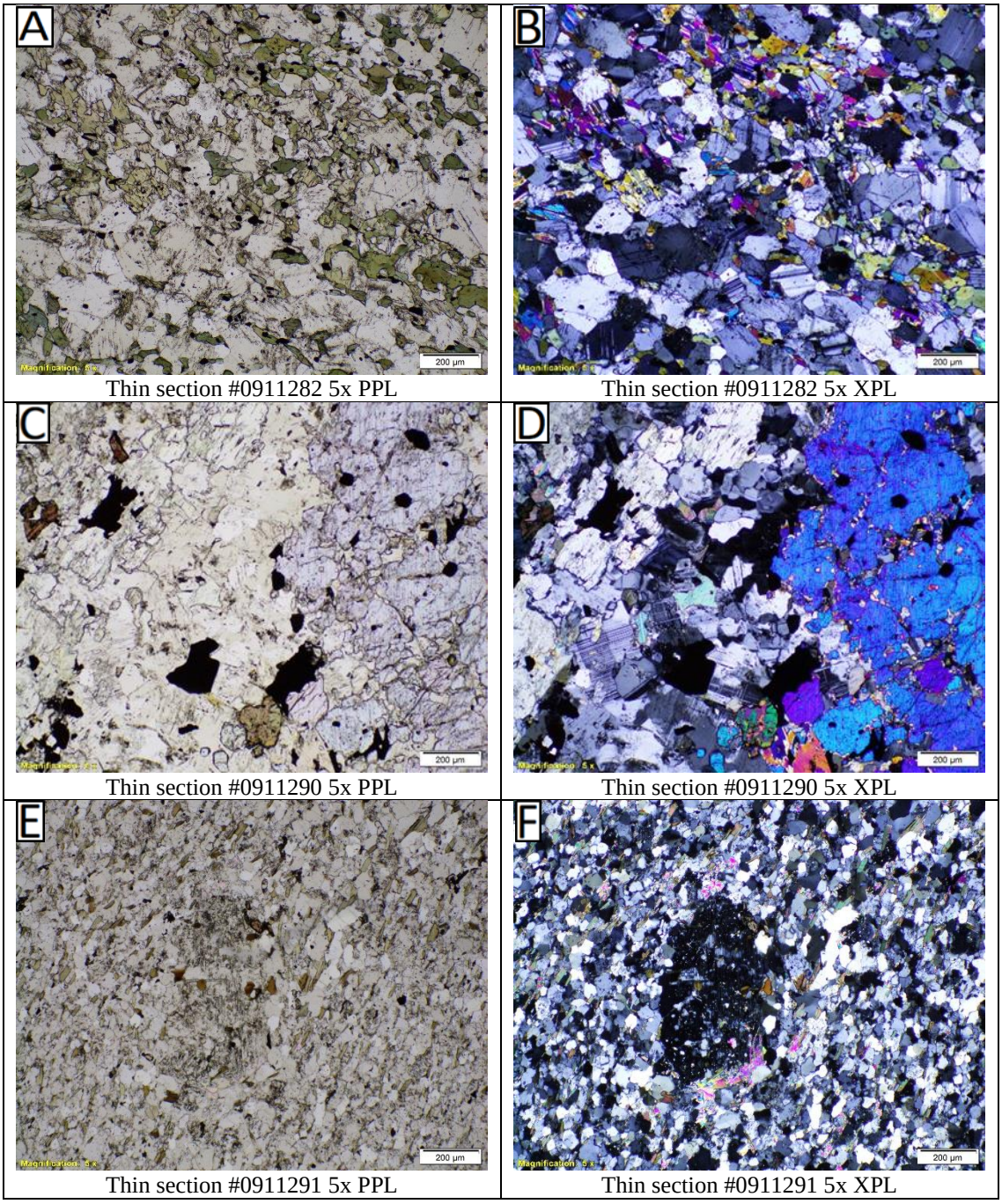

Thin section #0911282 5x PPL | Thin section #0911282 5x XPL

Thin section #0911290 5x PPL | Thin section #0911290 5x XPL

Thin section #0911291 5x PPL | Thin section #0911291 5x XPL

Figure 12 Photomicrograph of the biotite paragneiss (A) and (B) In both PPL and XPL and calc-silicate rich felsic volcanic sedimentary rocks in the rest of the thin section images. C) and D) represent typical nature of calc-silicate rich rock types with plagioclase feldspars as distinct black and white twinning in the lower-left corner, blue coloured diopside in the right corner and some quartz minerals in the upper left corner.

5.4. Sulfide-rich samples

Out of two drill holes understudy R851 and R1457, former has three highly mineralized intervals at depth from 139.30 – 159.30 meters having skarn-associated Zn ore, Fe ore (Pyrrhotite-Pyrite) and mobilized ore in veins include Cu and Au. Main minerals identified in these thin sections are sphalerite, chalcopyrite, pyrite-pyrrhotite and minor native gold.

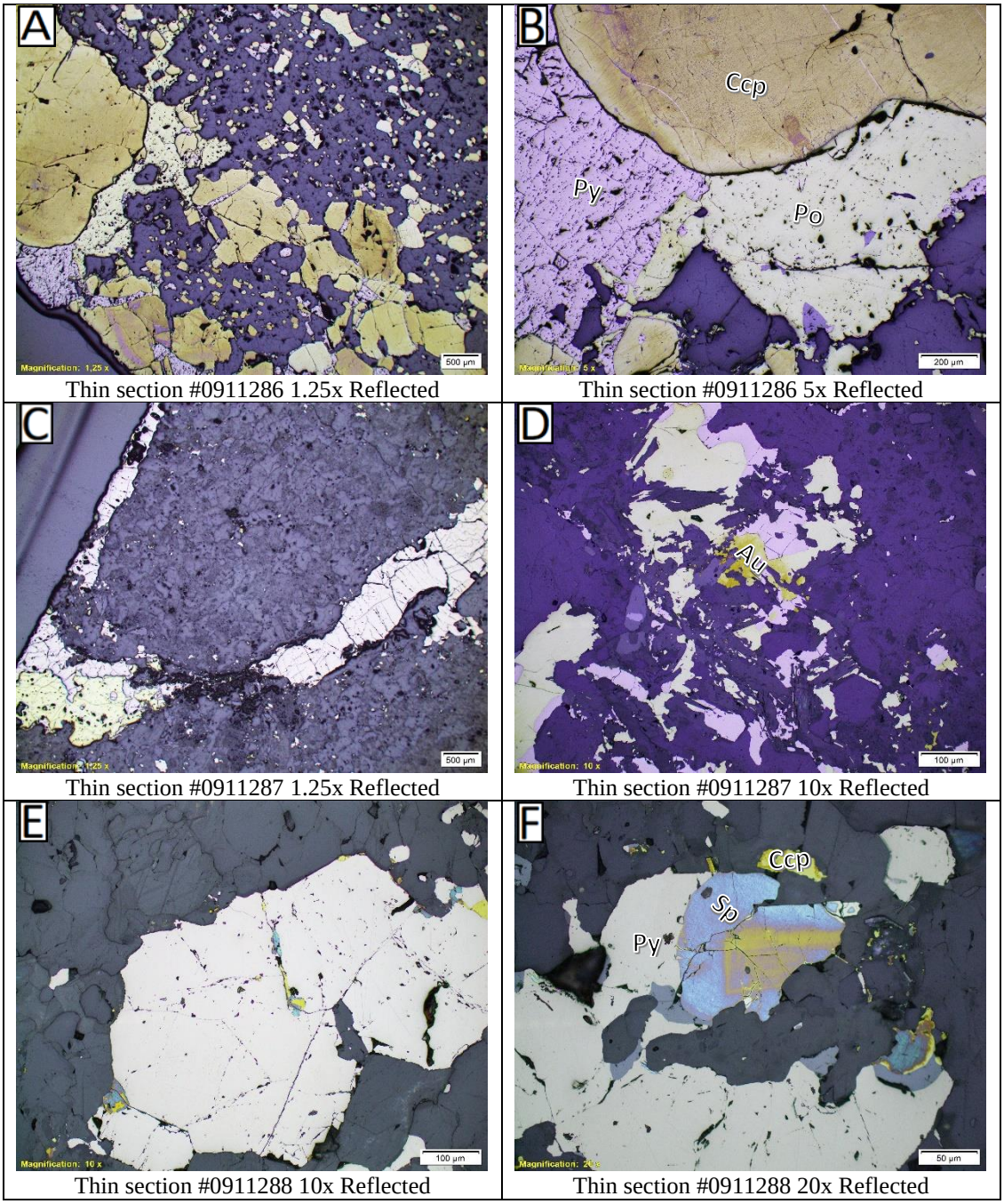

Thin section #0911286 1.25x Reflected | Thin section #0911286 5x Reflected

Thin section #0911287 1.25x Reflected | Thin section #0911287 10x Reflected

Thin section #0911288 10x Reflected | Thin section #0911288 20x Reflected

Figure 13 Photomicrographs of the ore samples under the reflected light microscope of the study area. A) and B) Common Iron sulfides, i.e. Pyrite (Py) and Pyrrhotite (Po) along with Chalcopyrite (Ccp) in the upper right corner of (B). C) and D) thin section under reflected light microscope along with mobilized Au (D- in centre-bright yellow) and chalcopyrite in veins. E) and F) Pyrite with inclusions of chalcopyrite and sphalerite.

6. DISCUSSION

6.1. Overview of data on Vihanti-Pyhäsalmi Belt

Supracrustal rocks along the Raahe Ladoga Zone (RLZ) are mainly turbiditic metasedimentary rocks. The sequence of these rocks was defined by (Laajoki 1988) as the Näläntöjärvi suite, while it is considered a depositional basement for volcanic rocks of the island arc by (Kousa et al. 1997). There are several arc-related rocks of the Vihanti-Pyhäsalmi belt with separate volcanic centres which happened to be in narrow and discontinuous belts in the western part of the Näläntöjärvi suite (Mäki et al. 2015). The metavolcanic rocks of the Pyhäsalmi group represent a bimodal type of volcanism which is different litho-geochemically from 1.89-1.88 Ga Ylivieska-type metavolcanic rocks in the west (Kojonen et al. 1989, Kousa et al. 1994). Regional metamorphic grade in the Vihanti-Pyhäsalmi belt ranges from lower amphibolite facies to upper amphibolite facies. While locally, in the Kiuruvesi area, it reaches much higher grades of granulite facies (Korsman et al. 1997).

The volcanic belt is separated into two blocks by major trending faults. Due to distinct lithological features of these two blocks, Vihanti and Pyhäsalmi are defined. Vihanti block has intermediate and felsic metavolcanic rocks as dominant protolith with calc-silicate and graphite tuffite interlayers. In Pyhäsalmi block bimodal felsic-mafic metavolcanics association being the most characteristic. Both the groups are categorized into different lithological associations which indicates two different volcanic environments despite having broadly similar ages of 1.93-1.92 Ga.

6.2. Overview of the volcanogenic massive sulfide deposits of the Vihanti Area

Lampinsaari-Alpua area is considered as the area where Vihanti Zn-Pb-Ag deposits are situated. Sulfide mineralizations mainly occur in felsic metavolcanic rocks, dolomites, calc-silicate rocks and graphite bearing metatuffs. Mineralized calcareous rocks and massive sulfide ore lenses have been intensely folded (Figure 3.1). Five different ore types are identified in the Vihanti deposit and almost 20 ore bodies which are mined out. Different bodies had variable sizes and metal content in them (Rouhunkoski 1968). In Vihanti area one of the most important ore types is Zn ore. Zn- ore from the three largest bodies namely Ristonaho, Välisaari and Lampinsaari contained 75% of the total mined ore (Autere et al. 1991). Zn ores occur typically

in the upper levels of the mine in calc-silicate-dolomite-serpentinite beds. Along with Zn-ores normally there are some Ag and Au ore types. Second ore type, Pb-Ag ores, occurs in close connection to the Zn-ores. Third ore type which is pyrite or pyrrhotite-rich ores named as pyrite ore is to be found in the upper parts of the mineralized horizon hosted by felsic metavolcanics and calc-silicate rocks. Fourth ore type is the Cu ore, which has a very close connection with pyrite ores. The fifth unexploited ore type U-P horizon is hosted by banded calc-silicate bearing felsic metavolcanic rocks.

6.3. Discussion on the obtained data

The whole rock data obtained from systematic drill core sampling allowed geochemical classification and identification of the protoliths of the altered rocks. The intense destruction of primary textures due to metamorphism and alteration has made it difficult to correlate original lithologies. Identification of the protoliths based on their chemical composition is important to improve our understanding of the stratigraphy of the mine area. Vihanti-Lampinsaari massive sulfide deposits and hydrothermally altered rocks are formed within volcano-sedimentary environment with dominantly intermediate-felsic magma composition together with minor mafic intercalates.

Turbiditic metasedimentary rocks do not have detrital zircons pointing to a zircon-poor source (volcanic) whereas the Näläntöjärvi suite has abundant detrital zircons. There is no significant ore deposit accumulation in sedimentary rocks of Vihanti-Lampinsaari area. Most important components of metasediments are Si, Fe and Ca occurring in quartz, pyrrhotite-pyrite and calc-silicate minerals respectively. Meta-sedimentary rocks in Vihanti group are largely silica-rich and consist of, detrital material and amount of hydrothermal material in the sediments is almost negligible. Three distinct samples with high P_2O_5 with high Mn content represent phosphate minerals-bearing samples. Enriched LREE relative to HREE is an indication of evolved source areas. Using Nb/Y vs Zr/Ti classification rocks ranges from rhyolitic to basaltic in nature.

All the intermediate-felsic and mafic rock types laid in the category of andesite/basaltic-andesite to rhyolitic dacite. According to the classification of (Barrie and Hammington 1999 Franklin et al 2005), igneous rocks of Vihanti-Lampinsaari indicates a felsic-siliciclastic or bimodal-felsic group. (Ross and Bedard 2009) Zr vs Y (Figure 4.19) agree with major elements classification by Miyashiro 1974 (Figure 4.16) and associates all inter-mafic and felsic rock

types into calc-alkaline magmatic affinity. In mafic meta-volcanic rock types, there is no distinct Eu anomaly, reflecting the absence of plagioclase fractionation process. The trend in chondrite normalized patterns of all group of rocks discussed has enrich LREE to depleted HREE indicating island arc settings. In intermediate meta-volcanic rock samples, Nb is not depleted but less than U represents concentrations similar to mid-oceanic ridge basalt (MORB) type of setting. Ce, P and Sm abundances are mostly controlled by magmatic processes rather than hydrothermal activity. Barium is depleted only in two slightly mineralized samples in intermediate metavolcanic rocks and it is considered to be derived from the subducted oceanic sediments.

In Nb/Y-Zr/Ti plot (modified by Pearce 1990) majority of rock types lie in the rhyolite-dacite field except two calc-silicate rich felsic volcanic rocks plotting in the field of andesite-basaltic-andesite. Under the category of sedimentary carbonates, only serpentinite-dolomite rock types are mineralized, with one hosting Zn ore and other two Cu rich sulphides. Two distinct groups can easily be identified in the silica vs major elements Harker diagrams (Figure 4.31), sedimentary carbonates and volcanic sedimentary rocks. Sedimentary carbonates have less SiO_2 than the volcanic sedimentary rock types. In Fe_2O_3-Al_2O_3-SiO_2 volcanic sedimentary rocks are silica-rich and aluminium rich compared to the carbonate-sedimentary rocks. Volcanic sedimentary rocks are rich in Al_2O_3, TiO_2, Sc, Zr, Th, Nb and Rb relative to carbonate sedimentary rocks reflecting the presence of detrital component (Figure 4.32). Sedimentary carbonates contain less Al_2O_3 comparatively and higher MnO+10 and enriched with FeO^t representing hydrothermal alterations in the sediments. All the sedimentary carbonates are rich in Pb, Sr and Ni, due CaO, which is an important component of carbonate rocks. Enrichment of Sr is due to the reason that Sr^{+2} substitutes for Ca^{+2} in calcium bearing minerals. Non-liner inter-relationship of Al_2O_3, Na_2O and CaO show feldspar have no significant role in the mineralogy of rocks rather quartz, talc, phlogopite or muscovite are the main alumino-silicate phases in the rock. In the primitive mantle normalized spidergram, rocks of the volcanic sedimentary are highly evolved ones in composition with depletion in Ba and Ti, including Sr unlike sedimentary carbonates (serpentinite-dolomite).

Investigated sulfide ore deposits of Vihanti-Lampinsaari shows sub-parallel behaviours (Figure 4.40). One of the factors resulting in dissimilar trends of chondrite normalized REE patterns and/or diverse REE behaviour in the secondary minerals of highly deformed and metamorphosed calc-silicates, dolomites and quartzites are high fluid/rock ratios. It is more

likely to lose parent-texture for the rocks having dissimilar trends than the one with subparallel, and it is due to the higher fluid/rock ratios. Eu anomalies either positive or negative, are indicative of ore mineralization or late-stage mineralization processes respectively. If Eu-anomalies are positive, better chances of ore-bearing rocks. HFSE of all samples of sulfides have slightly different patterns from one another suggesting they are not originating from the same source rock. All sulfide bearing rock samples have huge variation comparatively to sedimentary rock samples analysed previously, having chondritic characteristics and are interpreted as to have a lack of seawater contribution.

7. CONCLUSION

1) Almost no hydrothermal alteration in metasedimentary rocks of the Vihanti-Lampinsaari area. Presence of detrital material and REE indicate evolved source areas for the sediments.
2) Igneous (intermediate-felsic-mafic) metavolcanic rocks have all calc-alkaline magmatic affinity.
3) Trace elements trends in chondritic normalized patterns having enriched LREE's relative to HREE imply island arc-setting for all igneous meta-volcanic rocks.
4) Sedimentary carbonates have relatively high MnO and enriched in FeO^t indicating a hydrothermal alteration in the sediments.
5) Sulfide rich samples have slightly different chondritic and primitive mantle normalized patterns of REEs relative to their host rocks. Variable trends of chondrite normalized REE patterns of mineralized samples indicate high fluid/rock ratios.

8. ACKNOWLEDGEMENTS

Sincere thanks to my supervisor Dr Petri Peltonen, the professor of Practice the economic geology of the University of Helsinki, Faculty of Geosciences and Geography. I am also grateful to Dr. Raimo Lahtinen from the Geological Survey of Finland for his constructive suggestions during the development of my Master's thesis. This project was done in collaboration with the Geological Survey of Finland.

9. REFERENCES

Barnes, I, & O'Neil, J. R. 1969. The Relationship between Fluids in Some Fresh Alpine-Type Ultramafics and Possible Modern Serpentinization, Western United States. GSA Bulletin 80(10), 1947-1960.

Bau, M. 1996. Controls on the fractionation of isovalent trace elements in magmatic and aqueous systems: Evidence from Y/Ho, Zr/Hf, and lanthanide tetrad effect. Contribution to Mineralogy and Petrology 123, 323-333.

Braun, J.-J., Pagel, M., Muller, J.-P., Bilong, P., Michard, A. & Guillet, B. 1990. Cerium anomalies in lateritic profiles. Geochimica et Cosmochimica Acta 54 (3), 781-795.

Çelik Karakaya, M., Karakaya, N., Küpeli, Ş. & Yavuz, F. 2012. Mineralogy and geochemical behaviour of trace elements of hydrothermal alteration types in the volcanogenic massive sulfide deposits, NE Turkey. Ore Geology Reviews 48, 197-224.

Class, C., & Le Roex, A. 2008. Ce anomalies in Gough Island lavas. Trace element characteristics of a recycled sediment component. Earth and Planetary Science Letters 265 (3), 475-486.

Grant, H. L. J., Hannington, M. D., Petersen, S., Frische, M. & Fuchs, S. H. 2018. Constraints on the behaviour of trace elements in the actively forming TAG deposit, Mid-Atlantic Ridge, based on LA-ICP-MS analyses of pyrite. Chemical Geology 498, 45-71.

J. Lewis, A., Palmer, M., Sturchio, N., & J. Kemp, A. 1997. The rare earth element geochemistry of acid-sulphate and acid-sulphate-chloride geothermal systems from Yellowstone National Park, Wyoming, USA. Geochimica et Cosmochimica Acta 61, 695-706.

Janousek, V., Farrow, C. M., & Erban, V. 2006. Interpretation of whole-rock geochemical data in igneous geochemistry: Introducing Geochemical Data Toolkit (GCDkit). Journal of Petrology 47(6), 1255-1259.

Kahma, A. 1973. The main metallogenic features of Finland. Second printing 1979. Geological Survey of Finland, Bulletin - Bulletin de la Commission Géologique de Finlande 265.

Kamineni, D. 1986. Distribution of uranium, thorium and rare-earth elements in the Eye-Dashwa Lakes pluton. A study of some analogue elements. Chemical Geology 55(3-4), 361-373.

Kärki, A., Laajoki, K., & Luukas, J. 1993. Major Palaeoproterozoic shear zones of the central Fennoscandian Shield 64(1-4), 207-223.

Kojonen, K., Johanson, B., & Västi, K. 1989. Ore mineralogy of the Rauhala Zn-Cu-Pb sulphide deposit, western Finland. Autio, S. (Eds.) Geological Survey of Finland, Special Paper 10, 67-70.

Korsman K., Koistinen T., et al. (Eds) 1997. Bedrock Map of Finland 1:1000000. Geological Survey of Finland, Espoo.

Kousa, J., et al. 1997. Geology and mineral deposits of the central Ostrobothnia. Geological Survey of Finland. Guide 41, 43-67

Kousa, J., Marttila, E., & Vaasjoki, M. 1994. Petrology, geochemistry and dating of Paleoproterozoic metavolcanic rocks in the Pyhäjärvi area, central Finland. Geological Survey of Finland, Special paper 19, 7-27.

Laajoki, K., & J. Luukas 1988. Early Proterozoic stratigraphy of the Salahmi-Pyhäntä area, central Finland, with an emphasis on applying the principles of lithodemic stratigraphy to a complexly deformed and metamorphosed bedrock. Bulletin of the Geological Society of Finland 60.2, 79—106.

Luukas, J., Nikander, J., Kousa, J., & Ruotsalainen, A. 2004. Kallioperä- ja sinkkimalmitutkimukset Keiteleen Kangasjärven alueella Keski-Suomessa. 58 s., 1 liitekartta. Geologian tutkimuskeskus, arkisttoraportti, M 10.4/2004/1.

MacLean, W. H. & Barrett, T. J. 1993. Lithogeochemical techniques using immobile elements. Journal of Geochemical Exploration 48(2), 109-133.

Mäki, T., Imaña, M., Kousa, J., & Luukas, J. 2015. The Vihanti-Pyhäsalmi VMS belt. In: Maier, W.D., Lahtinen, R. & O'Brien, H. (Eds.), Mineral Deposits of Finland, Elsevier, pp. 507-530.

Makkonen, H., & Luukas, J. 2014. Modeling VMS and Structures. Geologian tutkimuskeskus, Tieteelliset posterit 365.
Rehtijarvi, P., Aikas, O., & Makela, M. 1979. A middle Precambrian uranium-and apatite-bearing horizon associated with the Vihanti zinc ore deposit, western Finland. Economic Geology 74(5), 1102-1117.
Rouhunkoski, P. 1968. On the geology and geochemistry of the Vihanti zinc-ore deposit, Finland. Geological Survey of Finland, Bulletin de la Commission Géologique de Finlande N:o 236.
Van Baalen, M. R. 1993. Titanium mobility in metamorphic systems: A review. Chemical Geology, 110(1), 233-249.
Västi, K. 2008. Chemical composition of metamorphosed black shale and carbonaceous metasedimentary rocks at selected targets in the Vihanti area, western Finland. Tutkimusraportti - Report of Investigation 173.
Veyland, A., Dupont, L., Rimbault, J., Pierrard, J.-C., & Aplincourt, M. 2000. Aqueous Chemistry of Zirconium (IV) in Carbonate Media. Helvetica Chimica Acta 83(2), 414-427.
Weihed, P., & Eilu, P. 2005. Fennoscandian Shield - Proterozoic VMS deposits. Ore Geology Reviews 27(1), 324-325.

10. APPENDIX

The tables that were too large to fit in among the text are included in the appendix. The appendix contains full sample lists.

Table 5 List of all samples with major elements.

SAMPLE	Rock type	Group	Classification	SiO_2	TiO_2	Al_2O_3	FeO^t	MnO	MgO	CaO	Na_2O	K_2O	P_2O_5
R1475 68,50-68,7	Pyrrhotite-pyrite	Sulphideore	Fe ore	40.669	0.211	6.953	46.896	0.014	0.883	1.622	1.050	1.538	0.165
R1475 85,65-85,8	Graphite-pyrrhotite bearing paragneiss	Sedimentary	NM	64.949	0.510	17.152	5.647	0.015	3.441	3.744	1.600	2.803	0.138
R1475 91.00-91.25	Quartzite	Sedimentary	SM	86.359	0.207	5.369	1.598	0.024	1.725	3.481	0.551	0.602	0.082
R644 2,6-2,85	Serpentinite-dolomite	Sedimentarycarbonate	SM	14.885	0.184	4.262	11.600	0.282	27.440	41.114	0.026	0.129	0.078
R644 48,15-48,45	Graphite-pyrrhotite bearing paragneiss	Sedimentary	SM	64.983	0.546	11.795	13.365	0.020	2.228	2.577	1.988	2.272	0.226
R644 67,3-67,6	Graphite-pyrrhotite bearing paragneiss	Sedimentary	SM	63.212	0.519	12.415	15.475	0.010	1.595	1.982	2.255	2.415	0.123
R644 90-90,15	Graphite-pyrrhotite bearing paragneiss	Sedimentary	SM	60.544	0.810	17.052	10.779	0.004	1.230	4.004	3.605	1.770	0.203
R644 115,10-115,3	Graphite-pyrrhotite bearing paragneiss	Sedimentary	SM	56.438	0.651	14.811	17.668	0.018	0.943	4.297	3.108	1.885	0.181
R917 18,45-18,65	Pyrrhotite-bearing para gneiss	Sedimentary	SM	56.237	0.823	16.251	13.757	0.036	2.983	4.704	3.838	1.091	0.280
R917 31,25-31,55	Calc-silicate bearing paragneiss	Sedimentary	SM	59.298	0.783	16.599	8.182	0.043	3.090	7.527	3.623	0.668	0.187
R917 51,05-51,45	Calc-silicate bearing paragneiss	Sedimentary	M	53.120	0.677	14.920	9.455	0.086	6.635	12.137	1.630	1.153	0.186
R917 65,15-65,4	Calc-silicate bearing paragneiss	Sedimentary	SM	60.125	0.775	15.398	8.652	0.061	3.582	8.987	1.372	0.838	0.208
R917 78,9-79,05	Biotite paragneiss	Sedimentary	SM	65.073	0.830	13.937	8.502	0.111	3.320	2.224	3.412	2.470	0.122
R917 106,05-106,25	Quartz-feldspar gneiss	Sedimentary	SM	75.935	0.546	11.437	3.838	0.004	1.391	2.957	2.802	0.989	0.101
R917 110,7-111,45	Zn-ore+dolomite	Znore	Zn ore	42.442	0.257	7.327	12.440	0.166	13.673	23.281	0.023	0.090	0.301
R917 116,15-116,35	Calc-silicate paragneiss	Sedimentary	SM	60.041	0.752	16.052	4.040	0.072	5.212	10.535	2.489	0.640	0.167
R917 208-208,3	Pyrite-bearing quartzite	Sulphideore	Fe ore	66.167	0.109	4.005	24.240	0.056	4.206	0.559	0.143	0.474	0.041
R917 246,05-246,25	Graphite- bearing paragneiss	Sedimentary	NM	64.934	0.639	15.958	6.556	0.042	3.995	3.489	1.508	2.729	0.150
R917 248,95-249,15	Biotite paragneiss	Sedimentary	NM	71.258	0.476	14.211	4.018	0.077	2.066	2.973	3.104	1.734	0.084
R1589 24,95-25,10	Biotite paragneiss	Sedimentary	NM	63.398	0.794	16.078	6.941	0.084	5.699	3.562	1.710	1.587	0.148
R1589 39,55-39,8	Magnetite-bearing biotite paragneiss	Sedimentary	NM	64.778	1.014	14.902	7.662	0.108	1.044	3.335	2.889	3.832	0.436
R1589 69,8-69,95	Amphibole gneiss	Volcsed	NM	58.285	0.853	14.216	9.137	0.136	5.930	7.179	3.869	0.282	0.113
R1589 75,05-75,15	Biotite paragneiss	Sedimentary	NM	63.579	0.739	15.490	7.497	0.119	2.774	3.371	6.085	0.166	0.179
R1457 9,55-9,8	Biotite paragneiss	Sedimentary	NM	65.674	0.637	14.953	5.382	0.149	1.859	7.204	2.930	1.000	0.212
R1457 62,7-62,95	Biotite paragneiss	Sedimentary	NM	64.133	0.768	15.958	6.598	0.077	2.707	4.121	4.444	1.010	0.186
R1457 97,85-98,05	Biotite paragneiss-volc sed	Volcsed	NM	56.592	1.014	14.909	10.038	0.167	6.886	6.095	3.702	0.465	0.131
R1457 121,25-121,55	Volc-sed	Volcsed	NM	55.588	1.106	16.534	9.018	0.169	4.879	7.669	4.727	0.166	0.143
R1457 123,7-123,95	Quartz-feldspar schist	Felsicvolcanic	NM	71.436	0.460	14.509	3.536	0.053	1.118	1.864	6.751	0.153	0.120
R1457 131,1-131,4	Quartz-feldspar schist	Felsicvolcanic	NM	72.584	0.386	14.315	3.157	0.043	1.069	1.462	6.553	0.340	0.092
R1457 137,8-138	Biotite paragneiss	Sedimentary	SM	70.762	0.587	12.978	6.775	0.028	2.884	1.967	1.473	2.400	0.146
R1457 139,35-139,55	Pyrrhotite-pyrite	Sulphideore	Fe ore	47.374	0.003	0.378	51.736	0.005	0.301	0.097	0.023	0.058	0.026
R1457 145,5-146,1	Granite+mobilized Cu+Au	Mobilized	Mobilized	71.007	0.250	12.638	6.302	0.101	0.407	1.478	3.084	4.670	0.063

R1457 158,9-159,3	Skarn associated Zn ore	Znore	Zn ore	35.412	0.076	2.018	12.505	0.353	17.506	30.067	0.023	0.277	1.764
R1457 172,7-173,1	Biotite paragneiss	Sedimentary	M	70.231	0.374	10.341	11.402	0.009	1.740	2.524	1.117	2.116	0.147
R1457 187,5-187,9	Calc-silicate rich felsic volcanic rock	Volcsed	NM	53.545	0.862	17.645	3.458	0.060	4.898	14.086	3.833	1.065	0.548
R1457 204,15-204,45	Calc-silicate rich felsic volcanic rock	Volcsed	NM	69.539	0.676	13.423	3.324	0.069	1.797	7.025	2.856	0.969	0.322
R1457 239,15-239,4	Biotite paragneiss	Sedimentary	SM	56.812	0.838	16.868	9.498	0.095	4.874	7.627	1.738	1.428	0.222
R1457 268,9-269,15	Quarts-feldspar schist	Felsicvolcanic	NM	77.996	0.431	12.061	1.121	0.008	0.965	2.623	4.051	0.633	0.110
R2061 40,25-40,45	?	Intermediatevolcanic	NM	64.885	0.770	15.487	6.685	0.072	1.579	5.355	3.259	1.731	0.177
R2061 68,05-68,25	Amphibolite	Maficvolcanic	NM	53.078	1.302	14.642	10.979	0.155	6.081	8.673	4.759	0.228	0.105
R2061 78,10-78,35	Amphibolite	Maficvolcanic	SM	53.518	0.981	15.962	8.833	0.118	7.146	8.596	3.098	1.534	0.214
R2061 102,25-102,45	Altered mafic volcanic?	Maficvolcanic	M	41.028	1.056	20.899	10.986	0.139	11.439	11.187	0.979	1.947	0.340
R2061 109,4-109,55	Calc-silicates + ore	Znore	Zn ore	46.438	0.056	1.923	13.065	0.241	16.090	21.231	0.022	0.058	0.876
R2061 112-112,2	Calc-silicates + ore	Znore	Zn ore	50.621	0.165	4.731	3.682	0.255	17.535	22.586	0.060	0.219	0.146
R2061 119,4-119,55	Pyrite-pyrrhotiite paragneiss	Sedimentary	M	51.950	0.632	17.598	12.231	0.043	4.594	7.482	3.667	1.686	0.116
R2061 138-138,15	Quartz-feldsparporphyry	Felsicvolcanic	NM	72.473	0.698	13.241	3.374	0.035	0.799	3.902	3.568	1.587	0.323
R768 4,75,4,95	Serpentinite-dolomite	Sedimentarycarbonate	M	10.151	0.122	2.938	48.548	0.097	15.561	22.309	0.025	0.188	0.063
R768 29,35-29,55	Serpentinite-dolomite	Sedimentarycarbonate	Zn ore	32.859	0.161	4.620	29.000	0.110	13.975	18.494	0.223	0.252	0.306
R768 51,25-51,45	Serpentinite-dolomite	Sedimentarycarbonate	M	31.320	0.372	9.171	11.611	0.100	23.553	23.027	0.061	0.651	0.133
R768 60,60-60,75	Calc-silicate paragneiss	Sedimentary	M	44.463	0.416	10.527	18.803	0.167	16.451	8.303	0.333	0.452	0.084
R851 10.80-10.95	Calc-silicate paragneiss	Sedimentary	NM	47.694	0.911	11.380	9.095	0.245	9.084	17.650	1.293	1.283	1.366
R851 11.00-11.15	Calc-silicate paragneiss	Sedimentary	NM	47.386	0.797	10.589	13.395	0.240	8.974	15.076	1.520	0.933	1.090
R851 16.80-17.15	Quarts-feldspar schist	Felsicvolcanic	NM	71.066	0.465	14.334	3.715	0.059	1.474	4.310	2.281	2.180	0.115
R851 31.90-32.10	Mafic dyke	Dyke	NM	53.264	0.935	18.094	9.604	0.146	4.615	8.020	4.290	0.762	0.269
R851 41.05-41.30	Quarts-feldspar schist	Felsicvolcanic	NM	69.984	0.499	14.441	4.244	0.080	2.141	4.433	2.313	1.777	0.088
R851 56-56.25	Cordierite gneiss	Felsicvolcanic	M	75.298	0.492	9.852	6.925	0.017	2.322	2.729	0.312	1.760	0.293
R851 64.35-64.55	Cordierite gneiss	Felsicvolcanic	SM	75.613	0.405	10.699	5.100	0.020	5.658	1.625	0.116	0.689	0.073
R851 69.05-69.20	Anthophyllite skarn	Unknown	M	44.767	0.772	18.146	13.101	0.093	18.689	3.097	0.804	0.424	0.106
R851 72.45-72.60	Serpentinite-dolomite	Sedimentarycarbonate	SM	26.232	0.232	6.081	5.126	0.123	28.617	33.347	0.147	0.020	0.076
R851 76.05-76.20	Quartz-dolomite rock	Unknown	SM	64.763	0.687	16.481	8.404	0.023	6.212	1.891	0.468	0.909	0.162
R851 79,50-79,8	Quartz-dolomite rock	Unknown	SM	61.435	0.989	15.990	10.791	0.019	2.893	4.671	2.009	0.978	0.225
R851 89,15-89,45	Serpentinite-dolomite	Sedimentarycarbonate	SM	27.084	0.150	3.529	18.831	0.220	16.962	32.460	0.175	0.524	0.064
R851 96,90-97,1	Quartzite+sulphides	Sedimentary	SM	56.452	0.544	12.040	21.667	0.024	1.976	3.851	2.397	0.931	0.117
R851 107,75-108	Calc-silicate paragneiss	Sedimentary	SM	51.486	0.499	10.937	6.592	0.076	9.554	17.767	2.806	0.137	0.144
R851 114,9-115,1	Quartzite/(felsic volcanic rock?)	Unknown	SM	77.046	0.518	10.978	2.835	0.004	1.850	2.704	3.456	0.508	0.101
R851 121,7-121,9	Calc-silicate paragneiss	Sedimentary	SM	66.181	0.415	12.928	5.475	0.032	2.822	7.603	3.930	0.509	0.106
R851 128,5-128,7	Quartzite/(felsic volcanic rock?)	Unknown	NM	73.335	0.431	14.084	2.055	0.010	1.408	2.937	4.638	0.946	0.157
R1095 6,45-6,7	Intermediate volcanic	Intermediatevolcanic	NM	70.028	0.525	14.833	4.086	0.057	1.503	2.422	5.731	0.727	0.089
R1095 28,05-28,2	Intermediate volcanic	Intermediatevolcanic	NM	68.849	0.575	14.919	4.562	0.091	2.520	3.548	2.984	1.814	0.137
R1095 37,5-37,75	Intermediate volcanic	Intermediatevolcanic	NM	62.358	0.724	12.736	7.848	0.121	5.655	7.540	2.731	0.193	0.095
R1095 44,65-44,95	Intermediate volcanic	Intermediatevolcanic	NM	70.692	0.609	14.706	4.682	0.060	6.146	0.482	0.700	1.836	0.088
R1095 54,8-55,05	Intermediate volcanic	Intermediatevolcanic	SM	73.316	0.568	11.669	6.039	0.017	1.859	2.705	0.713	2.922	0.192

R1095 63,6-63,8	Intermediate volcanic	Intermediatevolcanic	SM	69.068	0.571	12.463	7.635	0.049	4.487	3.874	0.200	1.444	0.209
R1095 64,3-64,5	Anthophyllite skarn+ore	ZnCuore	Zn-Cu ore	56.976	0.551	11.682	11.205	0.068	8.012	11.043	0.127	0.130	0.206
R1095 68,70-68,95	Pyrite ore	Sulphideore	Fe ore	23.377	0.003	0.360	73.107	0.006	1.275	1.651	0.028	0.016	0.177
R1095 74,05-74,3	Anthophyllite skarn	Unknown	SM	32.418	0.995	21.239	13.378	0.099	27.947	3.398	0.255	0.041	0.229
R1095 77,35-77,55	Anthophyllite skarn+quartzite	Unknown	SM	35.837	0.957	20.227	11.573	0.100	27.922	2.781	0.346	0.173	0.085
R1095 83,6-83,8	Serpentinite-dolomite	Sedimentarycarbonate	SM	22.850	0.529	10.734	5.810	0.147	31.619	28.164	0.097	0.020	0.029
R1095 95,4-95,65	Quartz+calc-silicates	Unknown	NM	40.153	0.136	3.174	13.429	0.123	15.753	26.543	0.428	0.192	0.069
R1095 99,2-99,45	Quartz+calc-silicates	Unknown	SM	44.575	0.466	11.004	16.084	0.087	10.434	15.797	0.726	0.704	0.123
R667 2,85-3,05	Biotite paragneiss	Sedimentary	SM	70.080	0.663	14.485	5.186	0.120	3.550	2.917	1.285	1.540	0.172
R667 11-11,25	Biotite paragneiss	Sedimentary	SM	64.759	0.515	11.957	11.426	0.050	5.323	2.719	1.048	2.032	0.171
R667 35,2-35,45	Zn ore	Znore	Zn ore	55.834	0.160	3.285	18.739	0.244	9.066	12.226	0.030	0.268	0.147
R911 135,5-135,7	Biotite paragneiss	Sedimentary	M	62.896	0.652	13.135	13.644	0.079	6.226	1.548	0.259	1.335	0.226
R911 136,9-137,05	Anthophyllite skarn	Unknown	M	36.856	0.421	11.330	25.691	0.222	18.542	5.369	0.359	1.126	0.083
R911 167,95-168,25	Anthophyllite skarn	Unknown	SM	43.015	0.450	13.760	11.602	0.140	21.020	7.942	0.439	1.506	0.127
R911 182,5-182,7	Quartz+calc-silicates	Unknown	SM	66.372	0.413	12.909	3.183	0.042	4.686	10.896	1.149	0.231	0.121
R1640 8,25-8,6	Quarts-feldspar schist	Felsicvolcanic	NM	78.301	0.389	12.178	0.969	0.004	0.654	2.999	3.019	1.389	0.099
R1640 24,3-24,5	Calc-silicate paragneiss	Sedimentary	NM	60.120	0.545	15.131	3.948	0.073	5.558	10.521	3.288	0.716	0.100
R1640 31,3-31,45	Mafic dyke	Dyke	NM	52.474	1.131	13.653	10.543	0.165	9.252	10.128	2.293	0.128	0.233
R1640 37,35-37,5	Quartz-fedspar schist+calc-silicates	Unknown	NM	53.438	0.567	14.776	5.009	0.090	7.813	16.102	1.407	0.719	0.079
R1640 52,25-52,5	Skanr+Pb ore	Pbore	Pb ore	53.073	0.478	12.152	6.532	0.125	8.589	16.805	1.631	0.518	0.098
R1640 63-63,2	Intermediate volcanic	Intermediatevolcanic	NM	59.026	0.667	17.384	4.611	0.045	5.266	9.430	2.456	1.031	0.084
R1640 76,25-76,5	Mafic dyke	Dyke	NM	53.301	0.923	16.298	10.238	0.157	6.335	8.866	3.301	0.366	0.217
R1640 78,8-79	Quartz-feldspar schist	Felsicvolcanic	NM	72.520	0.647	14.544	1.972	0.021	1.040	3.778	3.707	1.586	0.185

Table 6 Major elements ratio of sedimentary group of rocks.

SAMPLE	Rock type	Group	Classification	SiO_2	TiO_2	Al_2O_3	FeO^t	MnO	MgO	CaO	Na_2O	K_2O	P_2O_5
R1475 85,65-85,8	Graphite pyrrhotite bearing paragneiss	Sedimentary	NM	64.949	0.510	17.152	5.647	0.015	3.441	3.744	1.600	2.803	0.138
R1475 91.00-91.25	Quartzite	Sedimentary	SM	86.359	0.207	5.369	1.598	0.024	1.725	3.481	0.551	0.602	0.082
R644 48,15-48,45	Graphite pyrrhotite bearing paragneiss	Sedimentary	SM	64.983	0.546	11.795	13.365	0.020	2.228	2.577	1.988	2.272	0.226
R644 67,3-67,6	Graphite pyrrhotite bearing paragneiss	Sedimentary	SM	63.212	0.519	12.415	15.475	0.010	1.595	1.982	2.255	2.415	0.123
R644 90-90,15	Graphite pyrrhotite bearing paragneiss	Sedimentary	SM	60.544	0.810	17.052	10.779	0.004	1.230	4.004	3.605	1.770	0.203
R644 115,10-115,3	Graphite pyrrhotite bearing paragneiss	Sedimentary	SM	56.438	0.651	14.811	17.668	0.018	0.943	4.297	3.108	1.885	0.181
R917 18,45-18,65	Pyrrhotite bearing paragneiss	Sedimentary	SM	56.237	0.823	16.251	13.757	0.036	2.983	4.704	3.838	1.091	0.280
R917 31,25-31,55	Calc-silicate paragneiss	Sedimentary	SM	59.298	0.783	16.599	8.182	0.043	3.090	7.527	3.623	0.668	0.187
R917 51,05-51,45	Calc-silicate paragneiss	Sedimentary	M	53.120	0.677	14.920	9.455	0.086	6.635	12.137	1.630	1.153	0.186
R917 65,15-65,4	Calc-silicate paragneiss	Sedimentary	SM	60.125	0.775	15.398	8.652	0.061	3.582	8.987	1.372	0.838	0.208
R917 78,9-79,05	Biotite paragneiss	Sedimentary	SM	65.073	0.830	13.937	8.502	0.111	3.320	2.224	3.412	2.470	0.122
R917 106,05-106,25	Quartz feldspar gneiss	Sedimentary	SM	75.935	0.546	11.437	3.838	0.004	1.391	2.957	2.802	0.989	0.101
R917 116,15-116,35	Calc-silicate paragneiss	Sedimentary	SM	60.041	0.752	16.052	4.040	0.072	5.212	10.535	2.489	0.640	0.167
R917 246,05-246,25	Graphite bearing paragneiss	Sedimentary	NM	64.934	0.639	15.958	6.556	0.042	3.995	3.489	1.508	2.729	0.150
R917 248,95-249,15	Biotite paragneiss	Sedimentary	NM	71.258	0.476	14.211	4.018	0.077	2.066	2.973	3.104	1.734	0.084
R1589 24,95-25,10	Biotite paragneiss	Sedimentary	NM	63.398	0.794	16.078	6.941	0.084	5.699	3.562	1.710	1.587	0.148
R1589 39,55-39,8	Magnetite bearing Biotite paragneiss	Sedimentary	NM	64.778	1.014	14.902	7.662	0.108	1.044	3.335	2.889	3.832	0.436
R1589 75,05-75,15	Biotite paragneiss	Sedimentary	NM	63.579	0.739	15.490	7.497	0.119	2.774	3.371	6.085	0.166	0.179
R1457 9,55-9,8	Biotite paragneiss	Sedimentary	NM	65.674	0.637	14.953	5.382	0.149	1.859	7.204	2.930	1.000	0.212
R1457 62,7-62,95	Biotite paragneiss	Sedimentary	NM	64.133	0.768	15.958	6.598	0.077	2.707	4.121	4.444	1.010	0.186
R1457 137,8-138	Biotite paragneiss	Sedimentary	SM	70.762	0.587	12.978	6.775	0.028	2.884	1.967	1.473	2.400	0.146
R1457 172,7-173,1	Biotite paragneiss	Sedimentary	M	70.231	0.374	10.341	11.402	0.009	1.740	2.524	1.117	2.116	0.147
R1457 239,15-239,4	Biotite paragneiss	Sedimentary	SM	56.812	0.838	16.868	9.498	0.095	4.874	7.627	1.738	1.428	0.222
R2061 119,4-119,55	Pyrite-pyrrhotiite paragneiss	Sedimentary	M	51.950	0.632	17.598	12.231	0.043	4.594	7.482	3.667	1.686	0.116
R768 60,60-60,75	Calc-silicate paragneiss	Sedimentary	M	44.463	0.416	10.527	18.803	0.167	16.451	8.303	0.333	0.452	0.084
R851 10.80-10.95	Calc-silicate paragneiss	Sedimentary	NM	47.694	0.911	11.380	9.095	0.245	9.084	17.650	1.293	1.283	1.366
R851 11.00-11.15	Calc-silicate paragneiss	Sedimentary	NM	47.386	0.797	10.589	13.395	0.240	8.974	15.076	1.520	0.933	1.090
R851 96,90-97,1	Quartzite sulphides	Sedimentary	SM	56.452	0.544	12.040	21.667	0.024	1.976	3.851	2.397	0.931	0.117
R851 107,75-108	Calc-silicate paragneiss	Sedimentary	SM	51.486	0.499	10.937	6.592	0.076	9.554	17.767	2.806	0.137	0.144
R851 121,7-121,9	Calc-silicate paragneiss	Sedimentary	SM	66.181	0.415	12.928	5.475	0.032	2.822	7.603	3.930	0.509	0.106
R667 2,85-3,05	Biotite paragneiss	Sedimentary	SM	70.080	0.663	14.485	5.186	0.120	3.550	2.917	1.285	1.540	0.172
R667 11-11,25	Biotite paragneiss	Sedimentary	SM	64.759	0.515	11.957	11.426	0.050	5.323	2.719	1.048	2.032	0.171
R911 135,5-135,7	Biotite paragneiss	Sedimentary	M	62.896	0.652	13.135	13.644	0.079	6.226	1.548	0.259	1.335	0.226
R1640 24,3-24,5	Calc-silicate paragneiss	Sedimentary	NM	60.120	0.545	15.131	3.948	0.073	5.558	10.521	3.288	0.716	0.100

Table 7 Mineralized samples of sedimentary group of rocks.

SAMPLE	R917 51,05-51,45	R1457 172,7-173,1	R2061 119,4-119,55	R768 60,60-60,75	R911 135,5-135,7
Rock type	Calcsilicateparagneiss	Biotiteparagneiss	Pyritepyrrhotiiteparagneiss	Calcsilicateparagneiss	Biotiteparagneiss
Group	Sedimentary	Sedimentary	Sedimentary	Sedimentary	Sedimentary
Cu (*ppm*)	1610	443	3750	3690	2570
FeO^t (*wt%*)	9.455	11.402	12.231	18.803	13.644
Mn (*wt%)*	201	89.1	136	342	298
Zn (*ppm*)	4860	2150	376	1570	857
Cd (*ppm*)	33.4	6.22	1.18	0.71	2.67
Sn (*ppm*)	1.12	3.63	1.07	0.23	1.01
As (*ppm*)	13.9	35.0	11.0	2.66	15.1
S (*ppm*)	10600	41500	18600	17900	22800
Se (*ppm*)	6.56	5.31	4.61	7.84	1.96
Te (*ppm*)	1280	109	137	217	727

Table 8 Major elements composition of the Volcanic and carbonate sedimentary rocks.

SAMPLE	Rock type	Group	Classification	SiO_2	TiO_2	Al_2O_3	FeO^t	MnO	MgO	CaO	Na_2O	K_2O	P_2O_5
R644 2,6-2,85	Serpentinite-dolomite	Sedimentarycarbonate	SM	14.885	0.184	4.262	11.600	0.282	27.440	41.114	0.026	0.129	0.078
R768 4,75,4,95	Serpentinite-dolomite	Sedimentarycarbonate	M	10.151	0.122	2.938	48.548	0.097	15.561	22.309	0.025	0.188	0.063
R768 29,35-29,55	Serpentinite-dolomite	Sedimentarycarbonate	Zn ore	32.859	0.161	4.620	29.000	0.110	13.975	18.494	0.223	0.252	0.306
R768 51,25-51,45	Serpentinite-dolomite	Sedimentarycarbonate	M	31.320	0.372	9.171	11.611	0.100	23.553	23.027	0.061	0.651	0.133
R851 72.45-72.60	Serpentinite-dolomite	Sedimentarycarbonate	SM	26.232	0.232	6.081	5.126	0.123	28.617	33.347	0.147	0.020	0.076
R851 89,15-89,45	Serpentinite-dolomite	Sedimentarycarbonate	SM	27.084	0.150	3.529	18.831	0.220	16.962	32.460	0.175	0.524	0.064
R1095 83,6-83,8	Serpentinite-dolomite	Sedimentarycarbonate	SM	22.850	0.529	10.734	5.810	0.147	31.619	28.164	0.097	0.020	0.029
R1589 69,8-69,95	Amphibole gneiss	Volcsed	NM	58.285	0.853	14.216	9.137	0.136	5.930	7.179	3.869	0.282	0.113
R1457 97,85-98,05	Biotite paragneiss-volc sed	Volcsed	NM	56.592	1.014	14.909	10.038	0.167	6.886	6.095	3.702	0.465	0.131
R1457 121,25-121,55	Volc-sed	Volcsed	NM	55.588	1.106	16.534	9.018	0.169	4.879	7.669	4.727	0.166	0.143
R1457 187,5-187,9	Calc-silicate rich felsic volcanic rock	Volcsed	NM	53.545	0.862	17.645	3.458	0.060	4.898	14.086	3.833	1.065	0.548
R1457 204,15-204,45	Calc-silicate rich felsic volcanic rock	Volcsed	NM	69.539	0.676	13.423	3.324	0.069	1.797	7.025	2.856	0.969	0.322

Table 9 Major elements composition of ore samples.

SAMPLE	Rock type	Group	Classification	SiO_2	TiO_2	Al_2O_3	FeO^t	MnO	MgO	CaO	Na_2O	K_2O	P_2O_5
R1475 68,50-68,7	Pyrrhotite-pyrite	Sulphideore	Fe ore	40.669	0.211	6.953	46.896	0.014	0.883	1.622	1.050	1.538	0.165
R917 208-208,3	Pyrite-bearing quartzite	Sulphideore	Fe ore	66.167	0.109	4.005	24.240	0.056	4.206	0.559	0.143	0.474	0.041
R1457 139,35-139,55	Pyrrhotite-pyrite	Sulphideore	Fe ore	47.374	0.003	0.378	51.736	0.005	0.301	0.097	0.023	0.058	0.026
R1095 68,70-68,95	Pyrite ore	Sulphideore	Fe ore	23.377	0.003	0.360	73.107	0.006	1.275	1.651	0.028	0.016	0.177
R917 110,7-111,45	Zn-ore+dolomite	Znore	Zn ore	42.442	0.257	7.327	12.440	0.166	13.673	23.281	0.023	0.090	0.301
R1457 158,9-159,3	Skarn associated Zn ore	Znore	Zn ore	35.412	0.076	2.018	12.505	0.353	17.506	30.067	0.023	0.277	1.764
R2061 109,4-109,55	Calc-silicates + ore	Znore	Zn ore	46.438	0.056	1.923	13.065	0.241	16.090	21.231	0.022	0.058	0.876
R2061 112-112,2	Calc-silicates + ore	Znore	Zn ore	50.621	0.165	4.731	3.682	0.255	17.535	22.586	0.060	0.219	0.146
R667 35,2-35,45	Zn ore	Znore	Zn ore	55.834	0.160	3.285	18.739	0.244	9.066	12.226	0.030	0.268	0.147
R1640 52,25-52,5	Skanr+Pb ore	Pbore	Pb ore	53.073	0.478	12.152	6.532	0.125	8.589	16.805	1.631	0.518	0.098
R1095 64,3-64,5	Anthophyllite skarn+ore	ZnCuore	Zn-Cu ore	56.976	0.551	11.682	11.205	0.068	8.012	11.043	0.127	0.130	0.206
R1457 145,5-146,1	Granite+mobilized Cu+Au	Mobilized	Mobilized	71.007	0.250	12.638	6.302	0.101	0.407	1.478	3.084	4.670	0.063

Table 10 Major elements of Felsic, intermediate and mafic metavolcanic rock samples.

SAMPLE	Rock type	Group	Classification	SiO	TiO2	Al2O3	FeOt	MnO	MgO	CaO	Na_2O	K_2O	P_2O_5
R1457 123,7-123,95	Quartz-feldspar schist	Felsicvolcanic	NM	71.436	0.460	14.509	3.536	0.053	1.118	1.864	6.751	0.153	0.120
R1457 131,1-131,4	Quartz-feldspar schist	Felsicvolcanic	NM	72.584	0.386	14.315	3.157	0.043	1.069	1.462	6.553	0.340	0.092
R1457 268,9-269,15	Quartz-feldspar schist	Felsicvolcanic	NM	77.996	0.431	12.061	1.121	0.008	0.965	2.623	4.051	0.633	0.110
R2061 138-138,15	Quartz-feldsparporphyry	Felsicvolcanic	NM	72.473	0.698	13.241	3.374	0.035	0.799	3.902	3.568	1.587	0.323
R851 16.80-17.15	Quartz-feldspar schist	Felsicvolcanic	NM	71.066	0.465	14.334	3.715	0.059	1.474	4.310	2.281	2.180	0.115
R851 41.05-41.30	Quartz-feldspar schist	Felsicvolcanic	NM	69.984	0.499	14.441	4.244	0.080	2.141	4.433	2.313	1.777	0.088
R851 56-56.25	Cordierite gneiss	Felsicvolcanic	M	75.298	0.492	9.852	6.925	0.017	2.322	2.729	0.312	1.760	0.293
R851 64.35-64.55	Cordierite gneiss	Felsicvolcanic	SM	75.613	0.405	10.699	5.100	0.020	5.658	1.625	0.116	0.689	0.073
R1640 8,25-8,6	Quartz-feldspar schist	Felsicvolcanic	NM	78.301	0.389	12.178	0.969	0.004	0.654	2.999	3.019	1.389	0.099
R1640 78,8-79	Quartz-feldspar schist	Felsicvolcanic	NM	72.520	0.647	14.544	1.972	0.021	1.040	3.778	3.707	1.586	0.185
R2061 68,05-68,25	Amphibolite	Maficvolcanic	NM	53.078	1.302	14.642	10.979	0.155	6.081	8.673	4.759	0.228	0.105
R2061 78,10-78,35	Amphibolite	Maficvolcanic	SM	53.518	0.981	15.962	8.833	0.118	7.146	8.596	3.098	1.534	0.214
R2061 102,25-102,45	Altered mafic volcanic	Maficvolcanic	M	41.028	1.056	20.899	10.986	0.139	11.439	11.187	0.979	1.947	0.340
R2061 40,25-40,45	?	Intermediatevolcanic	NM	64.885	0.770	15.487	6.685	0.072	1.579	5.355	3.259	1.731	0.177
R1095 6,45-6,7	Intermediate volcanic	Intermediatevolcanic	NM	70.028	0.525	14.833	4.086	0.057	1.503	2.422	5.731	0.727	0.089
R1095 28,05-28,2	Intermediate volcanic	Intermediatevolcanic	NM	68.849	0.575	14.919	4.562	0.091	2.520	3.548	2.984	1.814	0.137
R1095 37,5-37,75	Intermediate volcanic	Intermediatevolcanic	NM	62.358	0.724	12.736	7.848	0.121	5.655	7.540	2.731	0.193	0.095
R1095 44,65-44,95	Intermediate volcanic	Intermediatevolcanic	NM	70.692	0.609	14.706	4.682	0.060	6.146	0.482	0.700	1.836	0.088
R1095 54,8-55,05	Intermediate volcanic	Intermediatevolcanic	SM	73.316	0.568	11.669	6.039	0.017	1.859	2.705	0.713	2.922	0.192
R1095 63,6-63,8	Intermediate volcanic	Intermediatevolcanic	SM	69.068	0.571	12.463	7.635	0.049	4.487	3.874	0.200	1.444	0.209
R1640 63-63,2	Intermediate volcanic	Intermediatevolcanic	NM	59.026	0.667	17.384	4.611	0.045	5.266	9.430	2.456	1.031	0.084

Table 11 Some samples of Dyke and unknown samples left in this study for further examination.

SAMPLE	Rock type	Group	Classification	SiO_2	TiO_2	Al_2O_3	FeO^t	MnO	MgO	CaO	Na_2O	K_2O	P_2O_5
R851 69.05-69.20	Anthophyllite skarn	Unknown	M	44.767	0.772	18.146	13.101	0.093	18.689	3.097	0.804	0.424	0.106
R851 76.05-76.20	Quartz-dolomite rock	Unknown	SM	64.763	0.687	16.481	8.404	0.023	6.212	1.891	0.468	0.909	0.162
R851 79,50-79,8	Quartz-dolomite rock	Unknown	SM	61.435	0.989	15.990	10.791	0.019	2.893	4.671	2.009	0.978	0.225
R851 114,9-115,1	Quartzite/(felsic volcanic rock?)	Unknown	SM	77.046	0.518	10.978	2.835	0.004	1.850	2.704	3.456	0.508	0.101
R851 128,5-128,7	Quartzite/(felsic volcanic rock?)	Unknown	NM	73.335	0.431	14.084	2.055	0.010	1.408	2.937	4.638	0.946	0.157
R1095 74,05-74,3	Anthophyllite skarn	Unknown	SM	32.418	0.995	21.239	13.378	0.099	27.947	3.398	0.255	0.041	0.229
R1095 77,35-77,55	Anthophyllite skarn+quartzite	Unknown	SM	35.837	0.957	20.227	11.573	0.100	27.922	2.781	0.346	0.173	0.085
R1095 95,4-95,65	Quartz+calc-silicates	Unknown	NM	40.153	0.136	3.174	13.429	0.123	15.753	26.543	0.428	0.192	0.069
R1095 99,2-99,45	Quartz+calc-silicates	Unknown	SM	44.575	0.466	11.004	16.084	0.087	10.434	15.797	0.726	0.704	0.123
R911 136,9-137,05	Anthophyllite skarn	Unknown	M	36.856	0.421	11.330	25.691	0.222	18.542	5.369	0.359	1.126	0.083
R911 167,95-168,25	Anthophyllite skarn	Unknown	SM	43.015	0.450	13.760	11.602	0.140	21.020	7.942	0.439	1.506	0.127
R911 182,5-182,7	Quartz+calc-silicates	Unknown	SM	66.372	0.413	12.909	3.183	0.042	4.686	10.896	1.149	0.231	0.121
R1640 37,35-37,5	Quartz-fedspar schist+calc-silicates	Unknown	NM	53.438	0.567	14.776	5.009	0.090	7.813	16.102	1.407	0.719	0.079
R851 31.90-32.10	Mafic dyke	Dyke	NM	53.264	0.935	18.094	9.604	0.146	4.615	8.020	4.290	0.762	0.269
R1640 31,3-31,45	Mafic dyke	Dyke	NM	52.474	1.131	13.653	10.543	0.165	9.252	10.128	2.293	0.128	0.233
R1640 76,25-76,5	Mafic dyke	Dyke	NM	53.301	0.923	16.298	10.238	0.157	6.335	8.866	3.301	0.366	0.217

Table 12 Samples taken from the drill hole R851 with description in Finnish.

FROM	TO	ROCKTYPE	KUVAUS
0	10,8	IVULK	ivulk,joka sisältää laikkumaisia karsi osueita,jotka eivät kerroksia, vaan ennemminkin metamorfoosin aiheuttamaa. Karsi sisältää karkearakeista diopsidia sekä neulasmaista tremoliittia ja jonkin verran biotiittia, joka muodostaa paikoin omia osueitaan (1-3cm).
10,8	10,95	dika	keskirakeinen dika, jossa mukana hienorakeista biotiittia sekä tremoliittia. Hieman myös dolomiittia.
10,95	11	dika-treka	ylläolevan ja allaolevan näytteen välistä.
11	11,15	treka	pääosin treka, jossa lopussa 5cm dika, kokomatkalta trekan seassa dikaraitoja sekä "laikkuja".
11,15	12,15	treka	treka,jossa kaksi pg-juonta (5 ja 10cm),
12,15	16,8	ivulk	emäksisiä muutaman sentin osuieta (biotiittirikkaampia)
16,8	17,15	ivulk	ivulk,joka osin karbonaattiluirakkeiden (dika+treka) saastuttama noin 5%,
17,15	24,8	ivulk	sama kuin edellä,muttei pg-juonia kaksi näytettä (hie/analyysi->niksu) 23.80 asti noin 5% saastutettu karrella ja tästä eteenpäin 10%, ivulkissa lapillimaisia piirteitä,
24,8	30,7	ivulk	metamorfoosissa karbonaatti osueiden raekoko kasvanut, myös reaktiosaumoja havaitaan, dika pahkut kasvavat ollen suurimmillaan 10 cm pituisiksi dika sisältää keskirakeista skii,
30,7	30,95	e-juoni	meta e-juoni amfibolirikas, hienorak.
30,95	31,7	ivulk	karsiosueinen
31,7	31,9	e-juoni	kuin edellä oleva e-juoni, hie 31,85
31,9	32,1	e-juoni	kuin edellä, näyte
32,1	41,05	ivulk	karbonaattiutuminen voimakkaampaa kuin aiemmin ivulkissa sisältäen dika+treka. Lisäksi 25 cm pg-juoni 36.45 lähtien.
41,05	41,3	ivulk	amfiboliraitaisuus lisääntyy myös granaatti rakeita siellä täällä max.2mm, rakeet eivätr puhtaita vaan sisältävät amfibolia->metamorfoosin tuloksena.
41,3	41,35	ivulk	kuin edellä
41,35	43,85	ivulk	karsiutuminen voimakasta dika+treka, sisältää 8cm pg-juonen (42.10), amf,biot kuten edellä
43,85	53	krdgn	kvartsirikas, jossa krd-rakeita (sinertävät/piniittiytyneet), raitainen, jonka muodostaa lähinnä biotiitti, sisältää karbonaattiosuieta ->treka+dika,
53	54,60	krdgn	hienorakeisempi kuin edellä, sisältäen runsaasti dika+treka, dolomiittia melko runsaasasti pienin laikkuina. Kvartsiutuminen nääkyy vaaleina kvartsi täppinä kuten reiässä 1095,
54,60	55,95	krdgn	saman tyyppinen kuin 43,85-53
55,95	56,25	krdgn	hie sekä näyte, sisältää enemmän kiisuja kuin edellä->skii+fek, näytteessä flogopiittiraitoja sekä mahdollisesti antofylliittä joka tapauksessa amfibolia, sisältää dika raitoja <10%, fek rakeet pienempiä kuin skii rakeet (skii max 3mm ja fek max 1 mm)
56,25	64,35	krdgn	sinkkivälke karbonaattirikkaassa 2 cm pätkässä yhdessä skiin kanssa, sama rakenne kui9n edellä sisältäen biotiitti/flogopiitti raitoja ja karsiosueita
64,35	64,75	krdgn	näyte sekä hie, pyriittimalmin kontaktin läheisyydestä, tummia laikkuja, joissa paikoin runsaasti muskoviittia ja yhteydessä karkearakeisempien dika osueiden yhteydessä, heikko skii pirote ja hienorakeinen, yleisesti melko karsivoittoinen, krdgn ominaisuus häipyvä, loppu "sädekiveen" joka antofylliittiä ja tästä hie
64,75	65,45	skiimalmi	kivi puuttuu, oku analyysi 73,58
65,45	68,10	skiimalmi	metamorfoosoissa karkearakeiseksi kasvanut suuntautumaton, harmeena karsikivi ->dika-treka ja mahdollisesti kiillettä, mukana melko runsaasti kvartsia ja harme kauttaaltaan hienorakeista (hienorakeisempi kuin edellä) vaihettuu viimeisen 15 cm matkalla fek rikkaammaksi, harme ikäänkuin murskaleina, paikoin vähän fek,
68,10	69,00	antofylliittikarsi	skiimalmi vaihettuu fek valtaiseksi ja lopulta pääosin antofylltipitoiseksi ja magnetiittia sisältäväksi, suskis lähtee 2000 ja nousee aina 10000 asti mentäessä näytteeseen alla,
69,00	69,20	antofylliittikarsi	hie sekä näyte, kuvaus edellisen tavoin
69,20	69,55	antofylliittikarsi	viimeiset 25 cm vaihettuu do valtaiseksi,
69,55	72,45	sptdo	melko dolomiitti valtaista ja dolomiittivaltaisissa osissa rusehtavia rakeita, jotka mahdollisesti kondrodiittia, sisältää raitoina serpentiiniytyneitä osueita, mahdollisesti tummat raidat/osa tummista rakeista magnetiittia, do kerman väristä, raontäytteinä karbonaattia (1mm), sisältää reaktiosaumaisia luirakkeita, joissa sisus melkosama kuinh nulkopuolen dolomiitti, reaktiosaumat amfibolia/biotiittia,
72,45	72,65	sptdo	näyte ja hie sama kuin edellä
72,65	73	sptdo	sama kuin edellä
73	76,05	do+antkarsi	dolomiittipitoinen antofylliittikarsi, jossa skii/zn pirote, punertavia karbonaattiraon täytteitä <5mm, runsaasti mahdollisesti< kondrodiittia,
76,05	76,25	kvt	hie/näyte, kvartsirikas kivi, jossa satunnainen skii pirote, biotiitti kiilteenä, erittäin pieniä määriä kermanvärisiä dolomiittirakeita, ohut karbonaatti/skii täytteinen rako <1mm, kvartsi täppiä ja mahdollsesti krd (jukka),
76,25	77,25	antofylliittikarsi	samantyyppinen kuin edellä, myös kiilteitä (muskoviitti/biotiitti/flogopiitti?),
77,25	78,60	kvt	hyvin kvartsipitoinen hienorakeinen kivi, jossa kiille lämpäreitä ja raitoja (biot/muskov), hieman skii ja rakopinnoilla karbonaattia,
78,60	79,45	kvt	vielä edellistäkin hienorakeisempi, tummia raitoja/pieniä "rakeita" jotka sisältävät skii/fek ja näitä ympäröi hienorakeinen kiille (biotiitti) "reaktio"-kehä,
79,45	79,8	kvt	näyte/hie,kivi edellisen kaltainen,
79,8	89,15	sptdo	serpentiinitynyttä dolomiittia, sisältää myös dika osueita, osin sokerimainen do, jossa hienorakeisena biotiitti (murentuu), sisältää myös kvt rikkaampia osueita, sulfidien määrä vaihtelee satunnaisesta vähään ja osa fek/skii muodostaa karkeampia rakeita,

89,15	89,5	sptdo	näyte/hie,kivi edellisen kaltainen,
89,5	93,3	sptdo	kuin edellä,mutta sisältää enemmän kvt rikkaampia osueita
93,3	96,9	kvt	tummahko kvt, jossa paikoin sedimentti piirteitä erittäin hieno kerroksellinen paikoin sed breksia piirteitä paikoin kohtalainen fek, jonka alussa mahdollinen sillimaniitti, ilmeisen grafiittipitoinen, sulfidit paikoin hieman luirakkeisia
96,9	97,1	kvt	hie/näyte kuin edellä, muttei sillimaniittihavaintoa, sisätäen kohtalaisesti fek raitoja/luiroja, myös tummia vieläkin hienorakeisempia kvt linssejä,
97,1	97,7	kvt	kuin edellä
97,7	107,75	dika	vaalea karsipitoinen (dika), dolomiitti,
107,75	108,05	dika	näyte/hie, kivi kuin edellä, näytteessä erityisesti huomioitavaa skii/fek raekasaumat, jotka metamorfoosissa kasvaneet, samat ainekset myös hienorakeisena pirotteena, mukana grafiitti,
108,05	113,50	dika	kuijn edellä,muttei kuitenkaan niin suuria sulfidirakeita kuin näytteessä, sisältää n. 1 m ennen loppua 25 cm pitkän kvt kerroksen,
113,50	114,85	kvt	hienorakainen dika osueita/raitoja sisältävä, fek pirote sekä kvt, että dika osissa
114,85	115,10	kvt	hie/näyte kuin edellä,
115,10	115,2	kvt	kuin edellä
115,2	121,65	dikakvt	dika pitoinen kvt, jossa dika karkearakeisina raitoina/"kerroksina" osin dolomiittiutunut, karbonaatti pitoisia raontäytteitä, kilteistä biotiittia hienorakeisena,
121,65	121,9	dikakvt	hie/näyte sama kuin ed.
121,9	122,40	dikakvt	sama kuin ed.
122,40	128,45	kvt	hienorakeinen kvt, jossa kvt silmiä/kvartsiutumaa, rakenteita ja mahdollisesti krd läsnä (sinertävät rakeet <2mm), dika raitoja/osueita, skii ja fek dika osuieissa isompia kuin kvt osissa, karbonaattiraon täytteitä (0,5-5 mm), osa vihertävistä raidoista näyttävät amfiboliittiutuneilta hienorakeisilta kiilteiltä,
128,45	128,7	kvt	hie/näyte, kivi sama kuin edellä
128,7	131,2	kvt	sama kuin edellä,

Table 13 Samples taken from drill hole R1457 description in Finnish.

FROM	TO	ROCKTYPE	KUVAUS NÄYTE	NÄYTTEEN YMPÄRISTÖ
9,55	9,85	kgn	Tyypillinen kgn, jossa karsi (dika+treka) välikerroksia/raitoja/lunsseja, selvä raitaisuus,	kuin näyte ja poimutusta näkyvillä, afb-juonia siellä täällä leveydeltään 1-10 cm, karsiraidat kauttaaltaan, paikoin aavistuksen vihreä sävy kgn:ssä viittaa mahdollisesti kloriittiutumiseen /amfiboliittiutumiseen,
62,7	63	kgn	sama kuin ed.	ympäristö sama, joitain granitoidisia juonen pätkiä afb-juonien lisäksi,
97,85	98,05	kgn	hieman saman tyyppinen edellsiten kanssa, mutta tässä mustia porpyroblastimaisia rakeita, jotka nyt kiille/afb, osittain näyttää olevan myös kvartsi luiroja,	tämä alapuyolella graiittijuoni 16,5 m paksu,
121,25	121,55	afb	homogeeninen afb, hienorakeinen, raitainen, raitaisuutta leikkaavia ohuita karb juonia >0,5 mm, mukana metamorfoosissa kasvaneiuta afb rakeita? (1x2mm), paikoin häivähdys karsimaisista vaaleista lunsseista,	afb asteeltaan vaihtelevaa saman tyyppistä hienorakeista kiveä granitoidistenjuonien sävyttämänä,
123,7	123,95	ms+kvt	hienorakeinen vaalean harmaa kvt+ms sisältävä kivi, jossa kvt porfyyrimäisiä rakeita (1x2mm)	
131,1	131,4	ms+kvt	verrattuna edelliseen tässä kvt luirakkeet kasvavat selvästi, kivessä b iotiittia/afb sekä bpieniä granaatteja (<1mm),	vaihettuminen edellisestä näytteestä tähän ja välillä joitain afb-juonia (10cm), jälkeen tulee fekma/skma,
137,8	138,05	kgn	vaalean harmaa raitainen hienorakeinen kgn ennen fekma/skma,	samatyyppi ennen ja tämän jälkeen n 1 m päässä alkaa fekma/skma,
139,3	139,55	fekma/skma	semimassiivinen malmi, jossa harmeena kvt, sulfidit sekä pirotteena, että metamorfoosissa kasvaneita, skii omamauotoista ja rakeet 10x10 mm,	yläpuoli kgn ja alapuolelle tulee kvt, joka karkearakeinen (juoni?), se sisältää diopsi kiteitä (jopa 8x8mm),
145,45	146,1	gr	kuparirikas gr, jossa kupari lähinnä raontäytteenä ja paikoin fekman ympäröimänä muodostaa jopa 7x7mm rakeita (mobilaatti?),	analyysissä aiemmin on ollut mukana pätkä fekma/skma ja näin ollen nyt pitäisi cuk pitoisuuden kasvaa, näytteen jälkeen skma/fekma rikasta kvt isäntäistä kiveä, jossa myös cuk ja myös gr juonta ennen cuk rikastuma,
158,9	159,3	znma	karsi isäntäinen znma, jossa mukana fek/skii,	sama kuin näyte
172,7	173,15	kgn	muistuttaa kattopuolen kgn, vaaleana kiilteenä muskoviitti tai serisiitti,	yläpuoli znma karsiisännässä ja alapuolella vaalea massamainen hienorakeinen kvt (ei reagointia hcl) sisältää karsi raitoja,
187,45	187,9	dika+hvulk	karsi laikkuinen kvt rikas hieman sulfideja pääasiassa karsirikkaisiin osueisiin keskittyen,	muuten sama molemmin puolinh,mutta karren määrä vaihtelee,
204,15	204,5	dika+kvt	hienorakeinen kvt rikas kivi, jossa dika lunsseja (budinoituneet), joitakin kvt porf mäisiä rakeita havaittvissa, (mahd karsiutunut h-vulk)	sama kuij näyte
239,15	239,4	kl	hienorakeinen raidallinen vaalean harmaa,	sama kui näyte mutta paikoin karsi välikerroksia
268,9	269,15	h-vulk	verrattavissa osittain edelliseen dika+kvt kiveen, mutta tämä karsi "vapaampi", sisältää runsaasti kvt rakeita keskim. 1x1 mm, joitain vihreitä raontäytteitä (<1mm), jotka mahd amfibolia,	muuten sama kuin näyte, mutta dika lunsseja ja välikerroksia